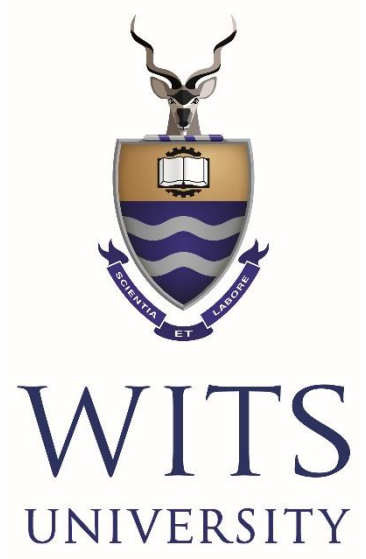

The Petrochemistry of the Arcadia Pegmatites of the Harare Greenstone Belt of Zimbabwe. Implications on genesis and mineral exploration on pegmatites.

BY

Selina Sibanda- 0616723Y

A Research Report submitted to the Faculty of Science, University of the Witwatersrand, Johannesburg, in partial fulfilment of the requirements for the degree of Master of Science.

UNIVERSITY OF THE WITWATERSRAND

2020

Supervisors: Prof. J. Kinnaird and Prof. P. Nex

DECLARATION

I declare that this research report is my own, unaided work. It is being submitted for a degree of Master of Science at the University of the Witwatersrand, Johannesburg. It has not been submitted before for any other degree or examination at any other university.

Selina Sibanda

Signature. 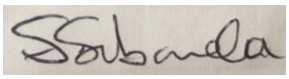

Date.....24 November 2020

DEDICATIONS

I dedicate this research project to my dear husband Lawrence and my family for their love, understanding, encouragement and support while conducting this study and throughout my MSc study programme.

ABSTRACT

The aim of this project was to conduct additional petrographic and geochemical analyses on selected samples to ascertain the mineralogical and geochemical makeup of the stacked pegmatites comprising the Main Pegmatite Zone (MP) and the Lower Main Pegmatite Zone (LMP) at Arcadia. The findings were essential in understanding the following; any similarities or variations within these two major units in terms of the distribution of Li-bearing minerals; the mineralisation phases that characterise the pegmatites so as to come up with a detailed paragenetic sequence and to explain the mineral chemistry of the observed deep pink coloured mineral referred to as petalite. Petrography, XRD (Rietveld) and XRF analyses were conducted on 15 representative samples, 7 from the LMP unit and 8 from the MP unit. The results from the fieldwork and petrographic analyses revealed no significant variations between the two units other than, the following slight variations; the MP unit appeared to have a significant concentration of the lithium minerals petalite and spodumene compared to the LMP unit, while the LMP unit had a significant concentration of secondary minerals. Petrographic analysis also indicated the presence of disseminated accessory garnets, within the LMP zone and this observation concurs with the MSA findings in which accessory garnets were identified within the LMP layer. The observed textural difference between the two units was the abundance of the coarse-grained texture within the MP unit, while the LMP unit appeared dominated by the fine-grained aplitic texture as well as the replacement textures from the hydrothermal alteration of feldspars and petalite. The pit mapping revealed patchy irregular concentric zonations on the exposed MP zone, characterised by both a change in textural and mineralogical assemblage. The only visible zones from the pit were the intermediate and the aplitic zones. The coarse-grained texture defined the intermediate zone which hosts the lithium mineralisation and it comprises the following mineral assemblage; blocky or coarse-grained K - feldspar + quartz + spodumene + petalite + minor albite, while the aplitic zone which is characterised by a fine-grained texture comprising fine-grained quartz+ albite+ muscovite (green) +garnet (pink). The core zone rich in coarse-grained quartz was only visible in some sections of the core. The aplitic and the intermediates zones are demarcated by sharp contacts. The petrographic analysis corroborated by the XRD Rietveld technique revealed that the mineralisation at Arcadia occurred in two phases the first phase comprising the early magmatic crystallisation of primary petalite and spodumene and the second mineralisation phase which is characterised by the alteration of the primary mineral phases petalite and spodumene producing secondary minerals, eucryptite, bikitaite and Spodumene+ Quartz intergrown (SQI). The hydrothermal alteration of plagioclase feldspars to smectite, stilbite and calcite constitutes the second mineralisation phase and the mineral phases were documented in a paragenetic sequence in Chapter 5. The whole rock geochemical analysis on major oxides revealed high silica (SiO_2-88.64wt%) and alumina (Al_2O_3-20.69wt%) contents for this suite of pegmatites, and low concentrations for Na_2O (-0.03-9.21wt%), K_2O (0.05-9.04wt %), CaO (0.08-3.11wt%), Fe_2O_3 (0.30-1.36wt%), MgO (0.01-0.48wt%), MnO (0.02-0.33wt%), P_2O_5 (0.02-0.19wt%), TiO_2 (0.01-0.05wt%) and Cr_2O_3 (0.01wt%). The alumina concentration appeared to be higher than the total alkali of Na_2O+ K_2O+CaO for all the samples, and this coupled with high silica concentrations > 70% and low MgO, CaO and Fe_2O_3, implied that the rocks are both highly evolved and peraluminous. The majority of the binary plots of the above mentioned oxides against SiO_2, revealed a negative correlation with SiO_2, suggesting a non- association with silica, while Fe_2O_3 and TiO_2 revealed a weak positive correlation with silica. The geochemical classification of the samples revealed the majority of the analysed samples from both units as calcic-rich and further classification

revealed the rocks as sub-alkali basalts. The two units did not reveal any significant geochemical variation, other than the significant concentrations of CaO, MgO, P_2O_5 and TiO_2 in the LMP unit as compared to the MP unit. The fact that there are slight variations is an indication that all the samples crystallised from the same magma although the protolith according to geochemical evidence appears to have been from different or mixed sources; igneous/sedimentary source. From the analyses conducted it can therefore be concluded that the MP and the LMP are genetically affiliated seeing they originated from the same magma and they don't exhibit significant mineralogical and geochemical variations. The petrographic analysis also confirmed the deep pink-coloured coarse-grained mineral as secondary petalite and it mostly occurs adjacent to the grey primary petalite in the intermediate zone of the MP unit although it still occurs in minor concentrations in the LMP unit, however without the primary petalite. This version of petalite appears to have distinctive and prominent cleavage planes just like the grey petalite.

ACKNOWLEDGEMENT

I am very grateful to the Almighty God for giving me strength to go through this demanding but rewarding journey. The completion of this study was realised through the will of God and the contribution and support of many people.

Special thanks go to my supervisors, Professor Judith Kinnaird and Professor Paul Nex who patiently and selflessly guided me throughout the entire process. My appreciation goes to the senior management at Prospect Resources namely Mr Roger Tyler, Mr Adam Moodley, the Arcadia technical team as well as the MSA geological services, who assisted me with my research. I also owe much gratitude to my fellow students in the MSc class who either contributed or supported this study in one way or another, as well as Mr Caiphus Majola the school of Geosciences Laboratory Technician for his assistance in the preparation of the thin sections.

LIST OF FIGURES

LIST OF TABLES

ACRONYMS AND ABBREVIATIONS

ALB.....**ALBITE**

ALT.....**ALTERATION**

GNT.....**GARNET**

K-FELD.....**K-FELDSPAR**

LMP.....**LOWER MAIN PEGMATITE**

MC.....**MICROCLINE**

MP.....**MAIN PEGMATITE**

OPQ.....**OPAQUE**

PET.....**PETALITE**

PPL.....**PLANE POLARISED LIGHT**

PLG.....**PLAGIOCLASE**

QTZ.....**QUARTZ**

SP.....**SPODUMENE**

XPL.....**CROSS-POLARISED LIGHT**

XRD.....**X-RAY DIFFRACTION**

XRF.....**X- RAY FLOURESCENCE**

WT%.....**WEIGHT PERCENT**

Table of Contents

CHAPTER 1: INTRODUCTION

1.1. Introduction

Zimbabwe is known to host numerous isolated pegmatite deposits throughout its granite greenstone terranes, with some of the notable world class economic pegmatite deposits occurring at Bikita, Kamativi, Sandawana and Beryl Rose (Cooper, 1964; Mamuse, 1999; Mugumbate et al., 2001). Pegmatites are defined by London (2008), as very coarse-grained rocks, enriched in rare elements, such as lithium (Li), tantalum (Ta), niobium (Nb), and beryllium (Be) and are characterised by extremely coarse-grained crystals, exhibiting graphic, or other strongly directional growth habits. Pegmatites are also a source of rare elements and minerals that include, tin, tungsten and gemstones such as emerald and aquamarine. The recently resuscitated Arcadia hard rock pegmatite deposit, located 38km east of Harare, Zimbabwe (Figure 1.1), has generated a lot of interest prompting researchers to undertake further research to understand the geochemical features of the deposit. The Prospect Resources (Ltd) regional exploration team has described the Arcadia ore deposits located within the Arcturus Formation of the Harare Greenstone Belt (HGB), as highly evolved metal-bearing Lithium-Caesium-Tantalum (LCT), family of pegmatites that were intruded into the country rock greenstones, with the potentially economic lithium mineralisation dominated by petalite and spodumene. Chemically the Arcadia pegmatites are enriched in Li, Ta and Rb, but relatively low in Nb and Cs (MSA, 2017). Beryl levels are also low, surprisingly so given the Main Pegmatite unit's pedigree as originally being a beryl producer. Moderate levels of beryl averaging 125 Ta ppm have been recorded from the area (Prospect Resource, 2017).

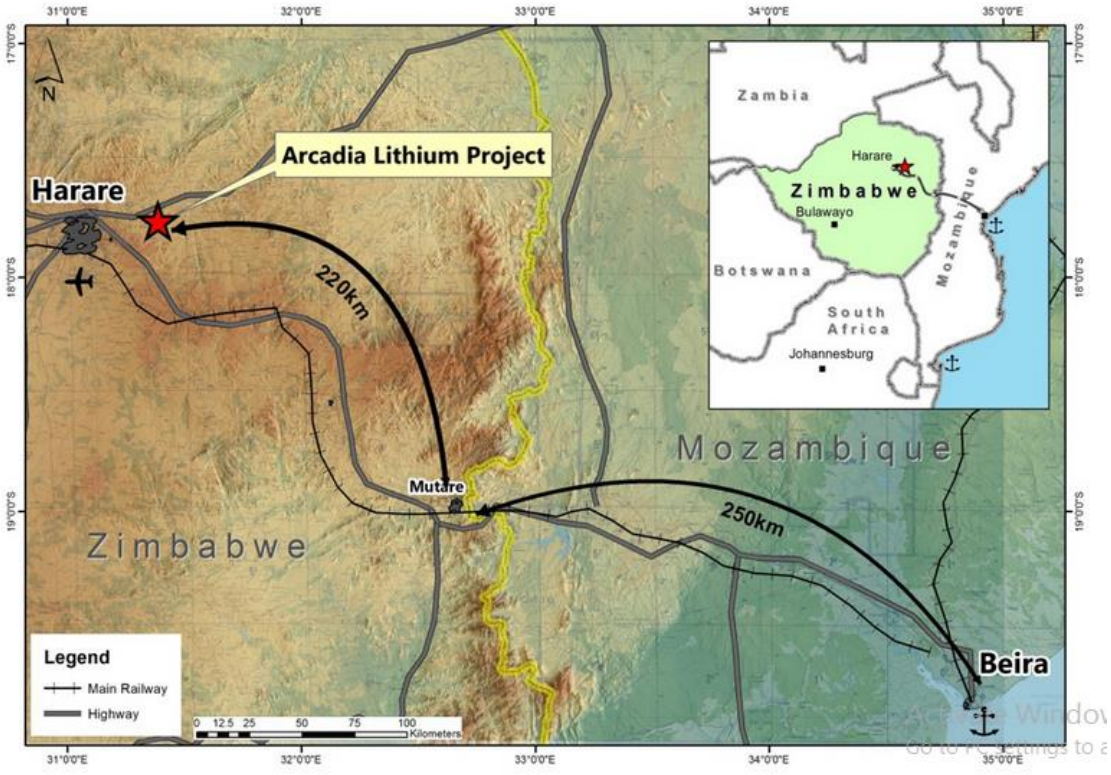

Figure 1. 1: Location of the proposed study area. (Source: Prospect Resources Ltd, 2017)

1.2. Overview of the Lithium Industry

This section will give an overview of the global lithium industry, highlighting the characteristics of Li, its global various uses, its global demand and its various ore types. A brief overview of the common pegmatite fields found in Zimbabwe will also be covered under this section.

1.2.1. Lithium Industry

Lithium is one of the most sought after critical or strategic metals in modern industry. Its peak application in the Li-ion battery industry, that powers modern mobile electronic devices, represents a major and a growing industrial application for this element (Figure 1.2). The various special properties of Li such as high working voltage, high energy density and electrochemical potential, high power to weight ratio, lightweight, energy efficiency and the fact that it's relatively inexpensive has resulted in the drastic growing demand for Li in the battery industry compared to the other battery types (Table 1.1 and Figure 1.3) (Forster, 2011).

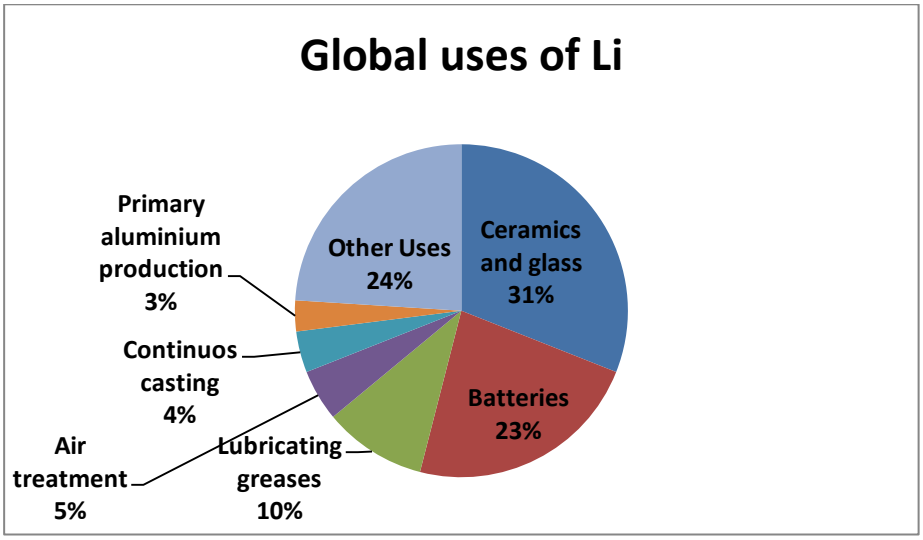

Figure 1. 2: Global uses of lithium (adapted from USGS Lithium, 2010).

Table 1.1: Chart showing an overview of the characteristics of different types of batteries and clearly showing the advantages of Li-ion- batteries (Source: Forster, 2011).

Battery type	Working Voltage (V)	Energy Density (Wh/kg)	Cycle Stability(cycles)	Charge Loss per month (%)	Memory Effect (%)	Energy Efficiency (%)	Weight Ratio	Size Ratio	Environmental Impact
Lithium- Ion	3.7	130-200	500	5%	None	99	1X	1X	Best
Nickel-Metal Hybrid	1.2	60-90	400	30%	40	70	2X	1.8X	Worst
Lead-Acid	2	30-40	300	10%	None	75	4X	3.5	Worst

Best	
Mid	
Worst	

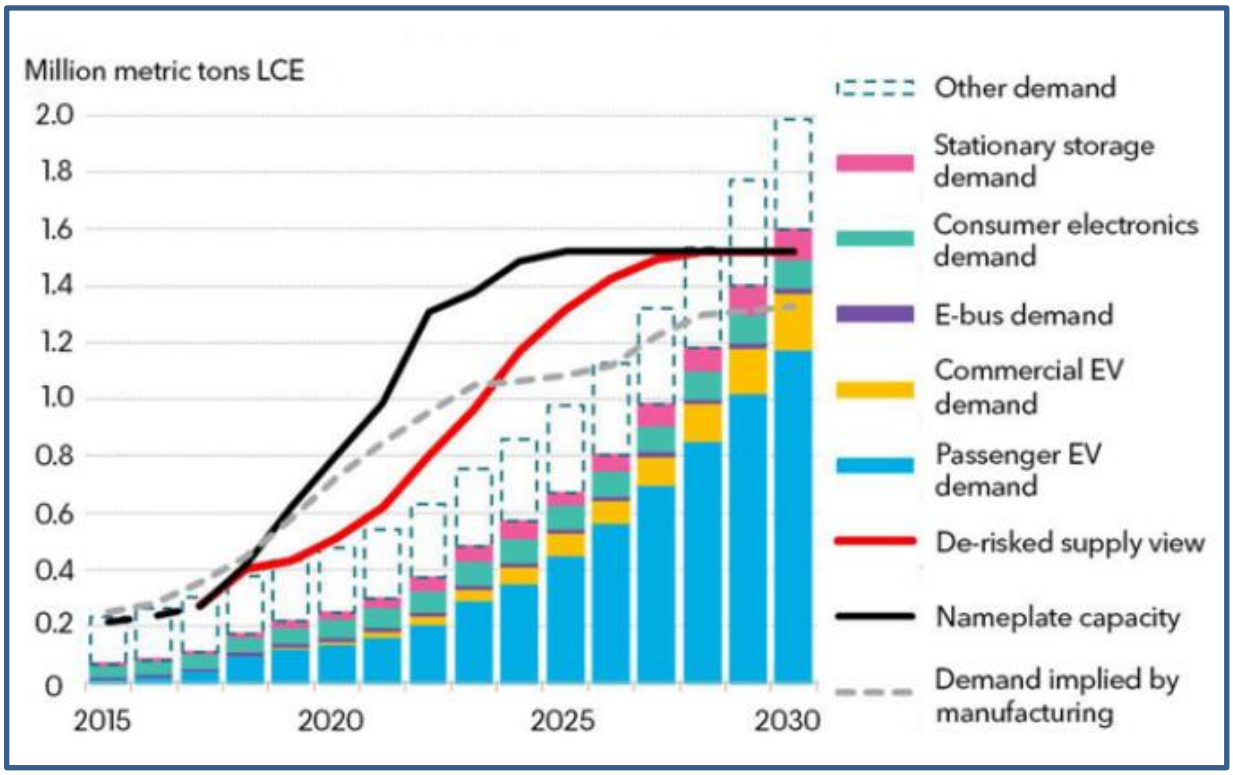

Figure 1. 3: Global Lithium supply and demand forecast (Bohlsen, 2019).

Li is a highly incompatible element which is found in rare-element pegmatites, particularly the complex type known as the Lithium- Caesium- Tantalum (LCT) pegmatites. There are more than 100 known minerals that contain Li, although only a few of these are currently considered economic or principal sources, namely spodumene, petalite and lepidolite. This family of complex pegmatites takes its name LCT from its characteristic enrichment in Lithium-Caesium and Tantalum and is distinguished from other rare element pegmatites by this diagnostic suite of elements. LCT pegmatites account for about 25% of the world's lithium production although they also tend to be enriched in Be, B, F, P, Mn, Ga, Rb, Nb, Sn and Hf (London, 2019).

The scientific study of LCT pegmatites according to Cerny (1991) is confined to a relatively small number of dedicated researchers. This is further supported by Barber (2016), who states that despite the economic importance of pegmatites, the level of understanding of pegmatite mineralisation in the mining sector is relatively low. Little is known in terms of the magmatic sources, mineralogy, geochemistry and structural controls governing pegmatite distribution (Barber, 2016). LCT pegmatites are typical constituents of the Archaean crust or Palaeoproterozoic orogenic belts for most world class deposits, and because of the growing Li market this family of pegmatites has recently become a promising exploration target (Dittrich et al., 2017). Current investment projects in Zimbabwe include the Arcadia Mine in Arcturus by Prospect Resources (Pvt) Ltd and the Zulu Lithium exploration in Fort Rixon by Premier African Minerals. Below is an insight into the various pegmatite deposits found in Zimbabwe.

1.2.2. Pegmatites in Zimbabwe

The pegmatites in Zimbabwe are widespread, with a majority having been mined for cassiterite, mica, beryl, lithium, niobium- tantalum minerals during the past fifty years. Zimbabwe has been one of the major pegmatite mineral producers in the world, with nearly all production coming from the Bikita pegmatite which is regarded as one of the largest Li-bearing pegmatites of the world (Figure 1.4) (von Knorring and Condliffe, 1987). Although the country hosts some of the world class pegmatite deposits, it is worth noting that most of the pegmatite deposits have been poorly explored, with a drastic decline in the production of new geological information (Mugumbate, 2014). Mugumbate (2014), further states that, "much of the country was regionally mapped 40 years ago before the advent of modern mapping technology and a deeper understanding of geological structures and processes". According to Barber (2016), six distinct pegmatite fields can be delineated and documented in Zimbabwe and these include the Kamativi, Miami-Urungwe, Bikita, Bepe hills, Makati Makaha (Benson) and Harare- Shamva (Figure 1.4). The Kamativi and the Miami-Urungwe pegmatite fields were emplaced within the Palaeoproterozic terrane, while the Bikita, Bepe Hills, Harare-Shamva and the Makati Makaha pegmatites were emplaced within the Archaean terrane (Figure 1.4). However, it should be highlighted that there also has been a lot of new mineral discoveries including Li-mineralisation which have not been systematically documented by the Geological Survey of Zimbabwe and these include the Zulu pegmatites located in the southwestern part of the craton (Figure 1.5) (Mugumbate, 2014).

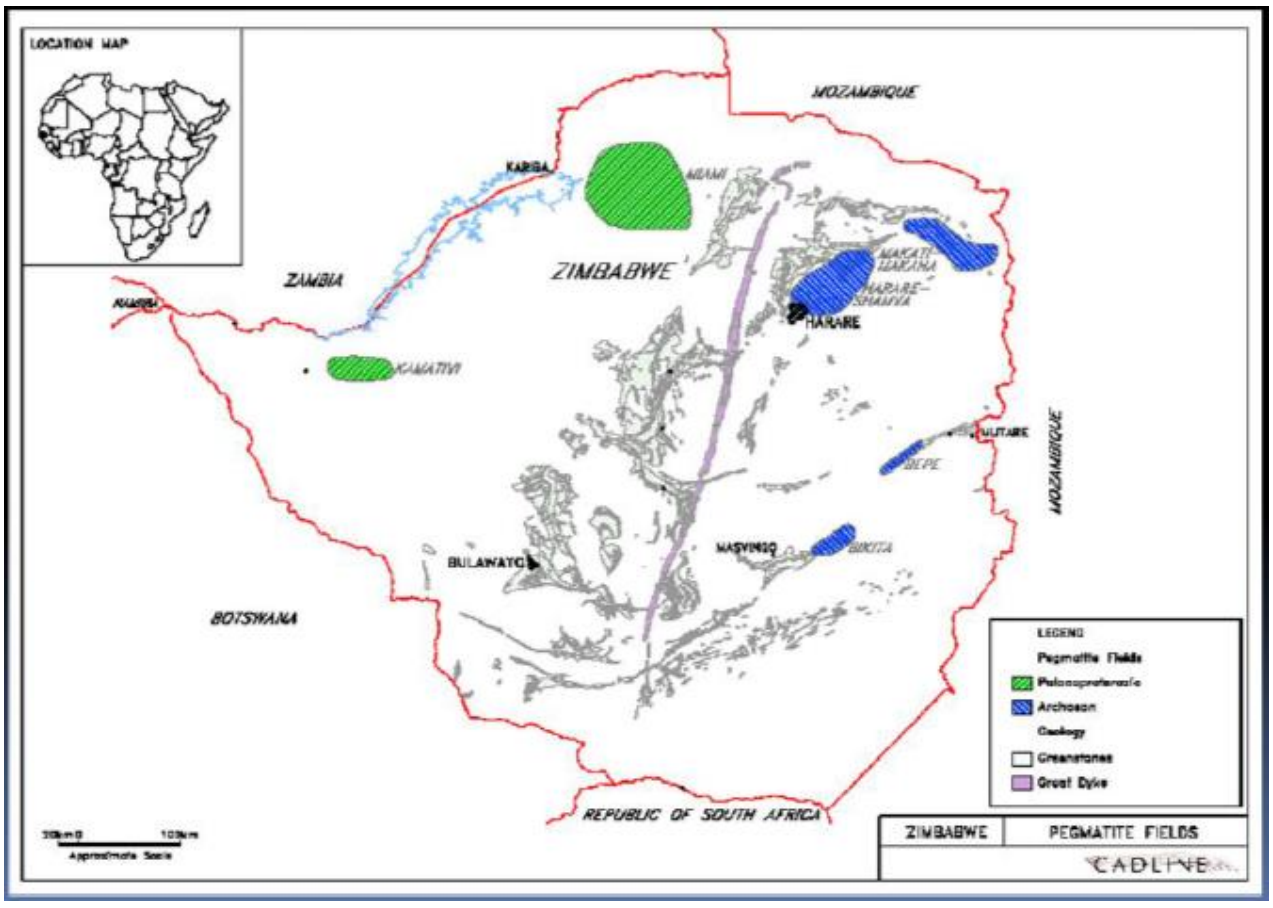

Figure 1. 4: Map of the Zimbabwe pegmatite fields (Barber, 2016).

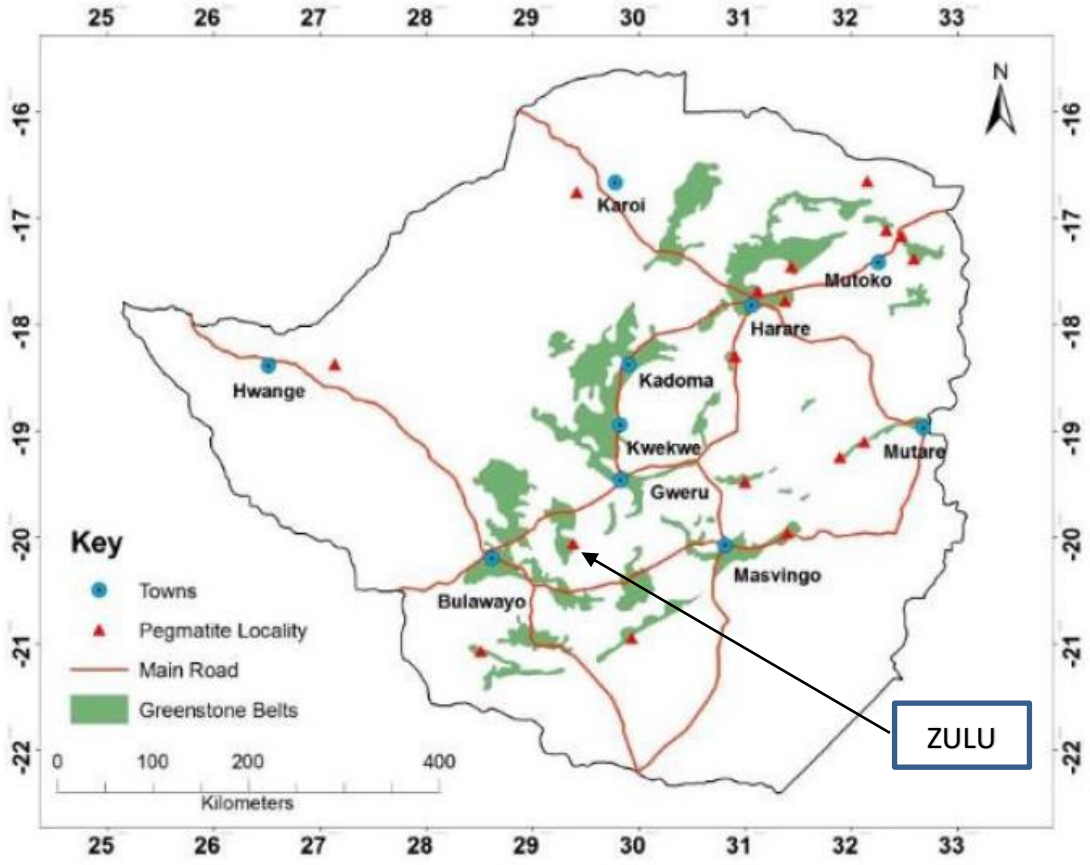

Figure 1. 5: Distribution of pegmatites in Zimbabwe (Modified after Baglow, 1993).

Kamativi Pegmatite Field

The Kamativi tin belt located in the northwestern part of Zimbabwe is one of the pegmatite regions that has in the past decades, proved to be of great economic importance, and from which extensive, flat-dipping cassiterite pegmatites were predominantly emplaced within the Palaeoproterozoic terrane, during the late phase Kibaran orogeny (1000 Ma) (Figure 1.4). The pegmatites were emplaced as dome-like structures in garnetiferous schists, gneisses and granites (Rijks and van der Veen, 1972; Barber, 2016). Although the Kamativi pegmatites are not truly zoned, distinct phases of mineral assemblages have been documented from the Kamativi area namely; microcline-quartz-spodumene, quartz-albite and muscovite-quartz, along with disseminated cassiterite and columbite-tantalite (von Knorring and Condliffe, 1987). Barber (2016) goes on to further classify the pegmatites into four groups namely; the cassiterite-bearing, the mineralised tourmaline-bearing quartz, the non-mineralised tourmaline-bearing and the quartz-bearing. Besides the above mentioned mineralisation, the Kamativi tin belt has also been popular for the production of large bodies of spodumene-rich units as well as accessory minerals such as beryl (von Knorring and Condliffe, 1987).

Miami-Urungwe pegmatite region

The Miami-Urungwe region is located to the east of Lake Kariba in the northern part of Zimbabwe (Figure 1.4). This region comprises numerous pegmatites emplaced in metapelitic gneisses, garnetiferous mica schists and amphibolites of the Magondi mobile belt (Palaeoproterozoic). The

Miami-Urungwe pegmatites have been mined for beryl and industrial sheet mica. The Miami pegmatites are divided into three groups namely the; uneconomic barren, economic mica-bearing and economic beryl-bearing (Barber, 2016). According to Wiles and Tatham (1963), the economic muscovite pegmatites of Zimbabwe occur in already highly micaceous rocks, while the lithium minerals are very rare or limited to a few occurrences of montebrasite in this region. The beryl pegmatites found in Miami-Urungwe are predominantly of the well-zoned, potassium-rich type. A variety of excellent gemstones such as aquamarine, blue topaz, golden beryl and euclase have also been mined from the Miami-Urungwe region (von Knorring and Condliffe, 1987).

Bikita Pegmatites

The world class Bikita pegmatite deposit is found in the southeastern part of the craton within the Masvingo greenstone belt (Figure 1.4), and these pegmatites were emplaced within the Archaean terrane (Barber, 2016). The Bikita pegmatite deposit is one of the most interesting and unique highly fractionated granitic pegmatites in the world, with the highest concentration of lithium within a single pegmatite deposit known and all the major lithium minerals are represented in exceptionally large quantities and include spodumene ($LiAlSi_2O_6$), petalite($LiAlSi_4O_{10}$), eucryptite ($LiAlSiO_4$), lepidolite ($K(Li,Al)_3(Si,Al)_4O_{10}(F,OH)_2$, bikitaite ($Li_2[Al_2Si_4O_{12}].2(H_2O)$and amblygonite-montebrasite (von Knorring and Condliffe, 1987). The Bikita pegmatites exhibit some degree of zonation and are subdivided into sodium-rich and potassium-rich pegmatites (Dasent, 1981). Large quantities of pollucite, cassiterite and a variety of Nb-Ta minerals have also been mined from the Bikita pegmatites (von Knorring and Condliffe, 1987).

Mtoko-Makaha pegmatites (Benson Mine)

Further lithium-mineralised pegmatites occur in the Mtoko-Makaha areas within the central pegmatite region, and these include the Benson pegmatites which are located 30km north of Mtoko district, in the northeastern part of Zimbabwe (Figure 1.4). The Benson pegmatites are emplaced within the Mtoko-Makaha greenstone belt, within the Archaean Terrane, and the claims enclose 40 pegmatites of which 12 are known to contain lithium minerals (von Knorring and Condliffe, 1987). The Benson pegmatites are well zoned, with an extensive lithium-sodium replacement and they contain unusually large concentrations of tantalum minerals. Pronounced metasomatic alteration of the wallrocks of the amphibolites has been documented from the Benson pegmatites, particularly in aureoles where the lithium amphibole holmquistite occurs (von Knorring and Condliffe, 1987). The major lithium minerals that are mined from Benson pegmatites include spodumene, montebrasite and lepidolite. In addition, a variety of accessory minerals found within the highly fractionated Benson pegmatites include, cassiterite, columbite-tantalite, pollucite and caesium beryl (Hornung and von Knorring, 1962).

Bepe Hills pegmatites (Archaean)

The Bepe Hills pegmatites are located about 70km west-southwest of Mutare, and are emplaced within the Archaean aged strata of the Mutare Greenstone Belt (Figure 1.4) (Barber, 2016). The Bepe Hills pegmatites have been mined for beryl, lithium, cassiterite, coltan and microlite (Barber, 2016).

Harare-Shamva Pegmatites (Late Archaean)

The Harare-Shamva Pegmatites located to the northeast of the craton are late Archaean in age and are believed to have intruded the metabasaltic rocks of the Harare-Shamva Greenstone Belt,

gneisses and gabbros in proximity to the Murehwa and the Chinamora batholiths (Figure 1.4) (Barber, 2016). Historically this region has had small mines, producing microlite, however lately there has been an on-going exploration for lithium-bearing minerals within the Harare Greenstone Belt and the surrounding granitic terrane in which the Arcadia mine is located. The lithium-bearing minerals in this area include petalite, spodumene, eucryptite, Spodumene-Quartz-Intergrowth (SQI) and minor lepidolite (Prospect Resources, 2017).

Zulu Pegmatites

The Zulu pegmatite field is located to the southwest of the Zimbabwe craton within the Fort Rixon Greenstone Belt (Figure 1.5). The pegmatite bodies are believed to have intruded along serpentinites and metasedimentary rocks over several kilometres of strike length. It is regarded generally as potentially the largest undeveloped lithium-bearing pegmatite in Zimbabwe (Premier African Minerals Ltd, 2016). Historical exploration results have established the Zulu pegmatites as prospective for lithium and tantalum, and to date the lithium-bearing pegmatites that have been identified from drilling include spodumene and lepidolite.

1.3. Problem Statement

MSA group conducted petrographic studies on selected samples from the Main Pegmatite and Lower Main Pegmatite zones. However, there was still a need for detailed mineralogical and geochemical variation analysis of the above mentioned pegmatite units, in order to understand their genetic affinity, observed paragenetic sequence and to explain the occurrence of the two phases of petalite observed. According to the findings by MSA, it appears that, there are two phases of mineralisation, one primary and the other one secondary, of which the secondary mineralisation involved the alteration of primary petalite and spodumene to spodumene, quartz intergrowth (SQI) and eucryptite. Although isochemical replacements of petalite and spodumene have been documented worldwide from several localities, metasomatic alterations of the two minerals is most common (London and Burt, 1981). According to Ginzburg and Gushchina (1954), late stage hydrothermal alteration of petalite occurs rarely as gem-quality crystals in pegmatitic solution cavities and as sub solidus replacements of spodumene plus quartz. It was therefore essential to establish whether the two phases of mineralisation are present, and also determine the mineral chemistry of a deep pink-coloured mineral (assumed to be petalite), to ascertain if it is indeed another primary version of petalite, or a product of the alteration of the primary petalite.

1.4. Overall Aim

The overall aim of this project was to conduct additional petrographic work and systematic detailed geochemical analysis on the two main stacked pegmatite layers (MP and LMP),and integrate the findings with the results of the MSA report so as to establish the mineralogical and geochemical variations of these pegmatite units, in order to understand their genetic affinity, ascertain and constrain the distribution of the Li-bearing minerals, as well as explain the mineral chemistry of the two phases of petalite observed.

1.5. Specific Objectives

- ✓ To ascertain the lithium mineralogy of the layered pegmatite ore bodies (MP and LMP), and establish their geochemical and mineralogical variations.

- ✓ To establish the phases of mineralisation that characterise the Arcadia pegmatites.

- ✓ To develop a detailed paragenetic sequence of the main lithium-bearing zones.

- ✓ To establish the identity of the deep pink-coloured mineral observed and referred to as petalite, and if it is indeed petalite, then further establish if it is a primary phase or secondary phase, formed during hydrothermal alteration of the primary petalite.

CHAPTER 2: REGIONAL GEOLOGICAL SETTING

2.1. Regional Geology

There are numerous pegmatite occurrences across the granite greenstone terrane of Zimbabwe (Figure 2.1), and of particular interest to this research are the pegmatite zones in the Harare-Shamva region, in which we find the Arcadia pegmatites (Figure 2.1 and Figure 2.2). The geology of the Arcadia area is dominated by greenstone lithologies of the Arcturus Formation of the Harare Greenstone Belt (HGB) (Figure 2.2). The same greenstones are encircled and intruded by a variable suite of granitic rocks, the oldest of which may have been intruded at a similar time with the youngest felsic volcanic rocks of the belt (Figure 2.1 and Figure 2.2). There are small remnants of the older gneissic basement to the greenstone belt and the granitic terrane is dominated by the younger intrusive plutons (Prospect Resources Ltd, 2017). Large dolerite sills and associated dykes are widespread and intrude the greenstone belt and the granitic terrane (Figure 2.2 and Figure 2.3). They are tholeitic, petrographically fresh, and are ascribed to the Mashonaland Igneous Event (1830±230 Ma) (Figure 2.3), which was predominant in the north and northeast of the Zimbabwe craton and involved the emplacement of dolerite sills and dykes in fractures developed in response to the various tectonic events such as the Magondi orogeny to the northwest of the Zimbabwe craton (Figure 2.1). To the extreme southeast of Arcadia, are preserved differentiated ultramafic-mafic sills ascribed to the Manyika Igneous Event (Figure 2.3) (Prospect Resources, 2017).

The HGB takes the form of a complex refolded synform structure (Figure 2.4), which outcrops in two major limbs. An E-W trending Arcturus Limb occupies a broad band across the centre of the area, and to the west of the city of Harare this passes via a fold closure into the N-S trending Passaford Limb which is contiguous northwards with the greenstones of the Bindura area (Figure 2.4) (Baldock et al., 1991). The main HGB lithological units comprise mainly meta-basalts, banded iron formations, meta- andesites, serpentinites, dolerites and the lithium bearing pegmatites that also host beryl, tin and tantalite amongst others (Figure 2.4). Within the meta-volcanics are horizons of banded iron formation, gossanous ironstone, ferruginous quartzite and marble, calc-silicate rocks and some felsic metavolcanics (Prospect Resources Ltd, 2017).

Three pegmatite zones occur in the Harare region and these include the Domboshawa, Chishawasha and the Arcadia-Green Mamba pegmatite zone. The Domoshawa pegmatite zone includes the following mines; Mistress, Mauve and the Hotspur mines, and these mines are located close to the contact of the Harare Greenstone Belt (HGB) and the Sesombi type granodiorite/ tonalite (Prospect Resources, 2017). The Chishawasha pegmatite zone is located immediately to the east of the city of Harare and includes the following claims; Pope, Moonstone-Barakat and Patronage, situated at the margin of the Chishawasha granodiorite. The third zone which is the Arcadia-Green Mamba pegmatite zone occurs to the east of Arcturus town within the basaltic volcanics (greenstones) of the Arcturus Formation (Figure 2.5).

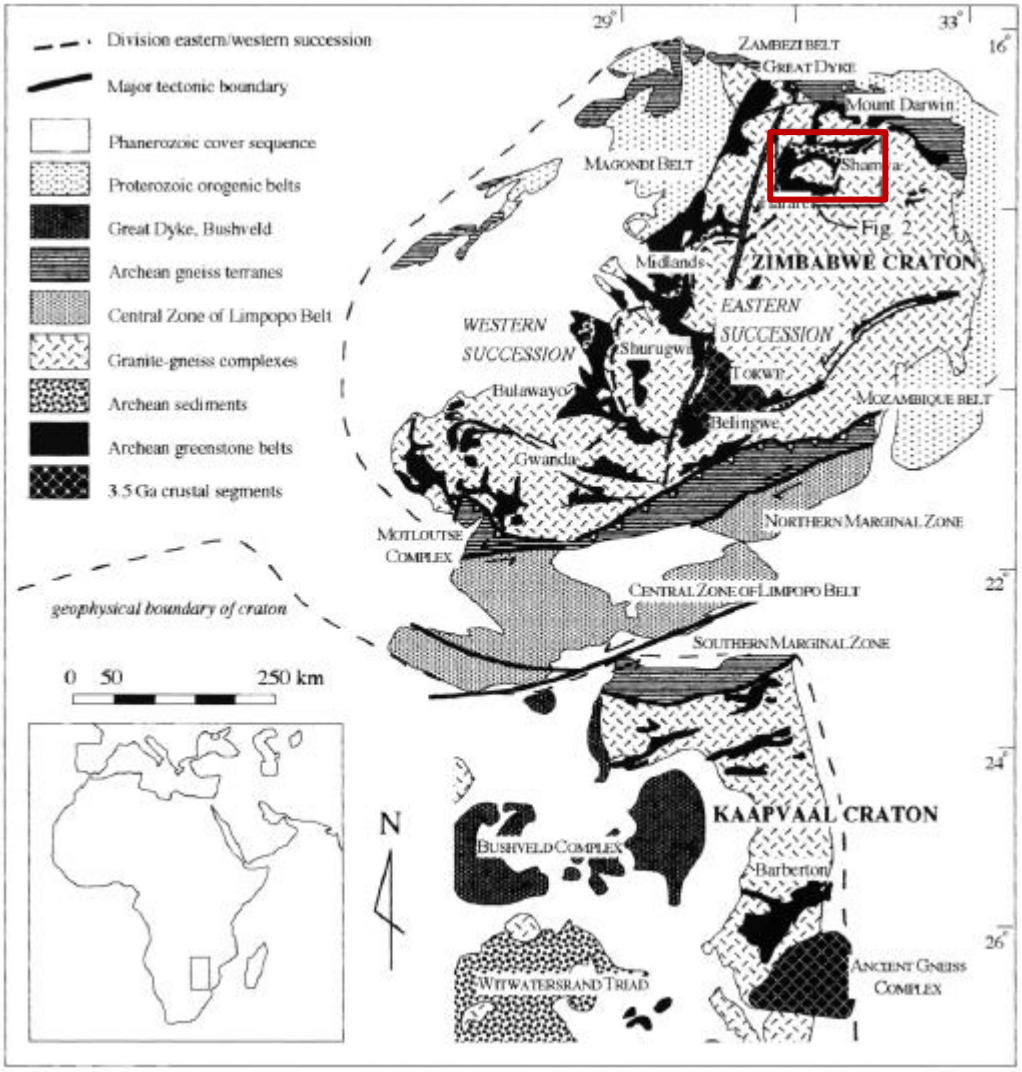

Figure 2. 1: General geology of the Southern Africa craton, surrounding Archean high-grade gneiss and Proterozoic terranes. Note the division between the late Archean eastern and western greenstone successions in the Zimbabwe craton. Insert shows the location of the Harare-Shamva greenstone belt (Jelsma and Dirks, 2000).

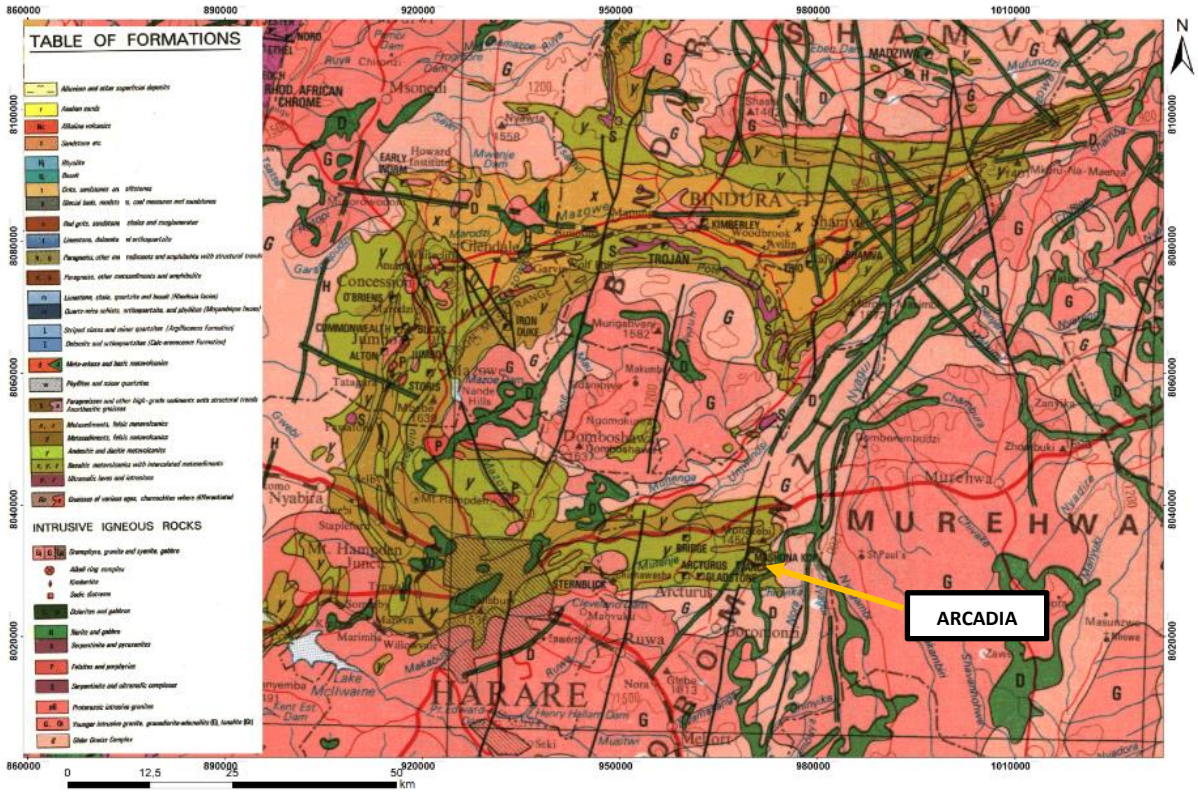

Figure 2. 2: Map showing the Harare greenstone belt, the location of the study area, the dolerite dykes and sills, and the intrusive granite rocks. (Geological Society of Zimbabwe, 1990).

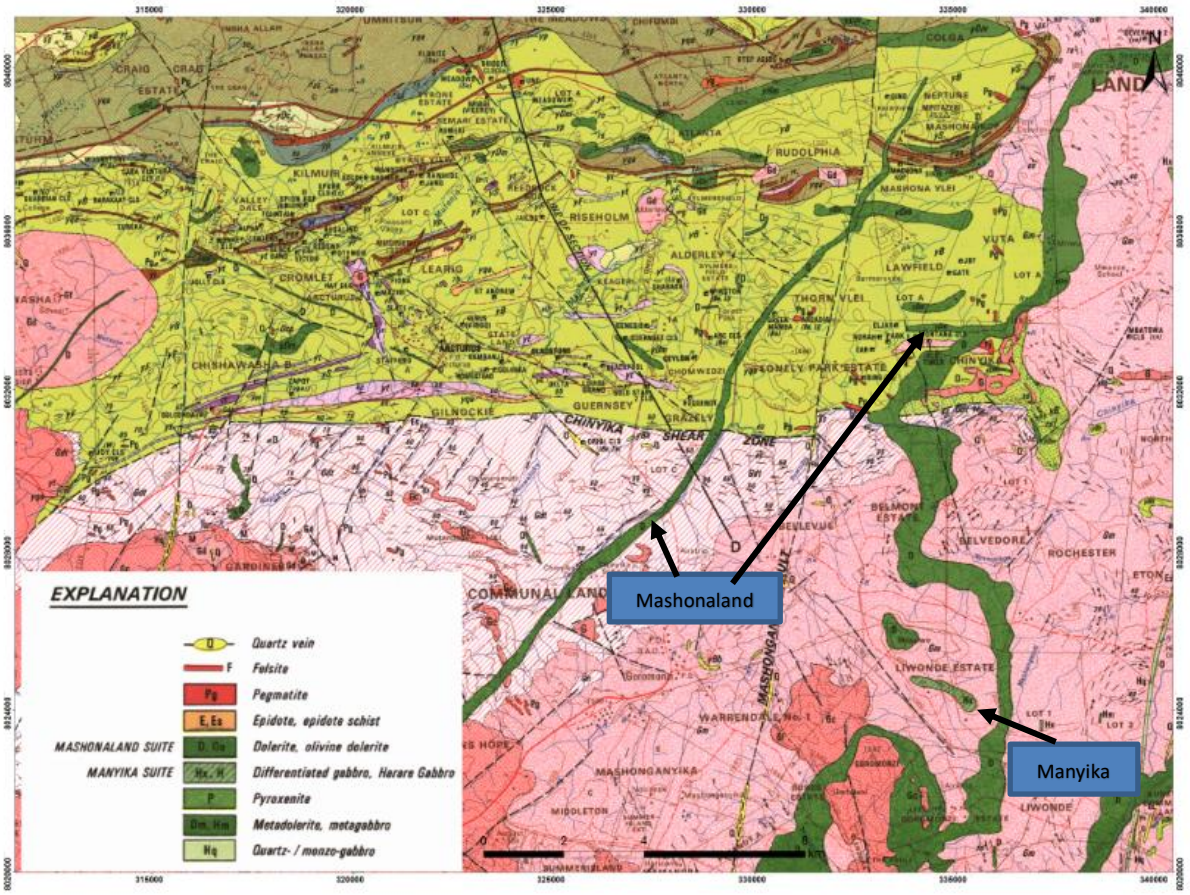

Figure 2. 3: Map showing preserved differentiated ultramafic-mafic sills ascribed to the Manyika Igneous Event, southeast of Arcadia and the dolerite dykes and sills of the Mashonaland Igneous Event (Baldock et al, 1991).

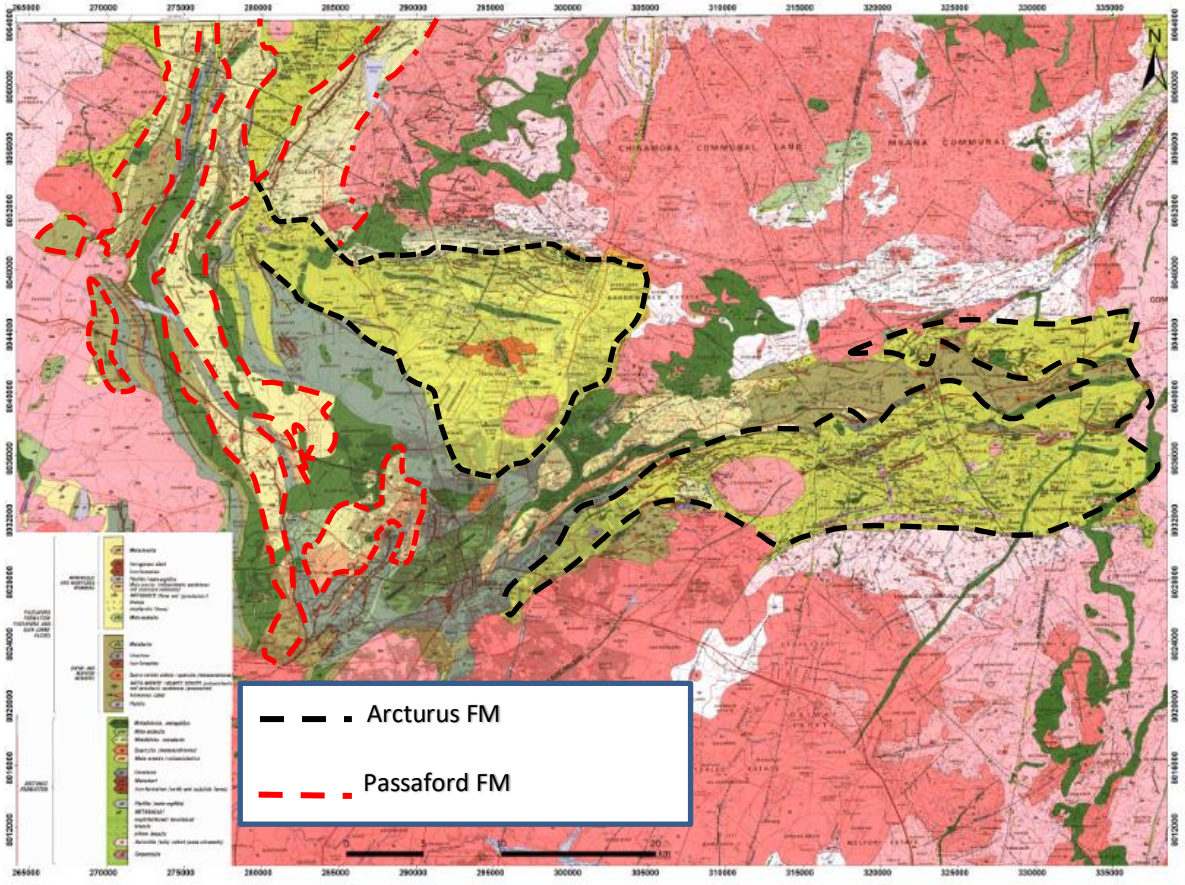

Figure 2. 4: Map showing the complex refolded synform structure of the Harare Greenstone Belt (HGB), the E-W trending Arcturus Limb and the N-S trending Passaford limb (Baldock et al, 1991).

2.2. Local geology

The Arcadia pegmatite deposits include the Winston, Takashi, Green Mamba, Bing, Tourit and the Oribi Li-Be claims (Figure 2.5), and of interest to this research is the Arcadia-Green Mamba claims. The Arcadia-Green Mamba area is surrounded by numerous granodioritic and tonalitic plugs of the Chishawasha suite (Figure 2.5), and according to the regional sampling conducted by Prospect Resources, the Arcadia pegmatites are believed to be genetically related to these intrusions, although this is yet to be proved (Prospect Resources, 2017). The Chishawasha suite includes the Chikwakwa Injection Complex, to the east of Arcadia, the Chinamora Igneous Complex to the north and northeast of Arcadia and the Chinamora Porphyritic Granite.

Four different rock types are found on the Arcadia-Green Mamba claims, namely the metabasalt, pegmatite, dolerite and quartz veins, listed from relatively oldest to youngest. The exploration drilling programme conducted by Prospect Resources Ltd, unveiled a package of up to 14 significant stacked, sub-parallel pegmatites sheets, with a unique mineralisation style. From uppermost to lowermost these are namely the; Upper Pegmatites (UP), U3, U2, U1, Main Pegmatite Zone (MP), Lower Pegmatites; L1, L2, L3, L4, L5, L6, L7 and L8. The L4 and L5 have coalesced in large parts of the claim to form the Lower Main Pegmatite (LMP) and likewise the L7 and L8 form the Basal Pegmatite (BP) (Prospect Resources Ltd, 2017). The Upper and the Intermediate pegmatite units together comprise the Main Pegmatite Zone (Figure 2.6). The Main Pegmatite and the underlying Lower Main

Pegmatite, are the most significant bodies both in terms of lithium grade, thickness, and lateral consistency, with thicknesses of 7-10m and 25-50m respectively (Figure 2.6) (Prospect Resources Ltd, 2017). These two major zones, the MP and the LMP are the main focus in this project. Figure 2.7, shows the Arcadia Pit with the outcropping Main Pegmatite exposed overlain by the metabasalt.

The Arcadia-Green Mamba pegmatite bodies are concentrically zoned, with the outermost zones namely the wall and aplitic zones (albite zone), being fine-grained and comprising mostly feldspar, quartz and muscovite with some rare lepidolite. The intermediate zone is the widest of all the zones and has a coarse to very coarse-grained texture, and furthermore, hosts lithium-bearing ore minerals (petalite and spodumene), along with feldspar and quartz. The core zone, is dominated by coarse-grained quartz and muscovite, but is not always developed. It is important to note that the thickness of each zone varies, depending on the thickness of the entire pegmatite body (MSA, 2017).

The only known recorded production is from the Arcadia-Green Mamba claims which took place between 1962 and 1978, and then premature closure of the operation occurred in 1978 due to war along with economic sanctions. None of these claims have been in formal production since the early 1970's. In the 1980's, Rand Mines private limited undertook a drilling program of unknown size, but reportedly defined circa 18 Mt of ore, with high peak grades of Li_2O (3-5 %). However due to the absence of any QAQC on assay data and the associated uncertainty in the positioning of some drill holes, the Rand Mine results were not JORC compliant and as a result could not be incorporated into the current work by Prospect Resources Ltd. Zimbabwe. Between the years 2016-2018, Prospect Resources Ltd embarked on an exploration and drilling feasibility programme on the Arcadia-Green Mamba claims, and six drilling phases have been conducted to date by the company, in which a total of 23,724m of ground was covered by 81 diamond drill (DD) holes and 194 reverse circulation (RC) holes in a bid to evaluate the economic viability of the deposit (Prospect Resources, Ltd, 2017).

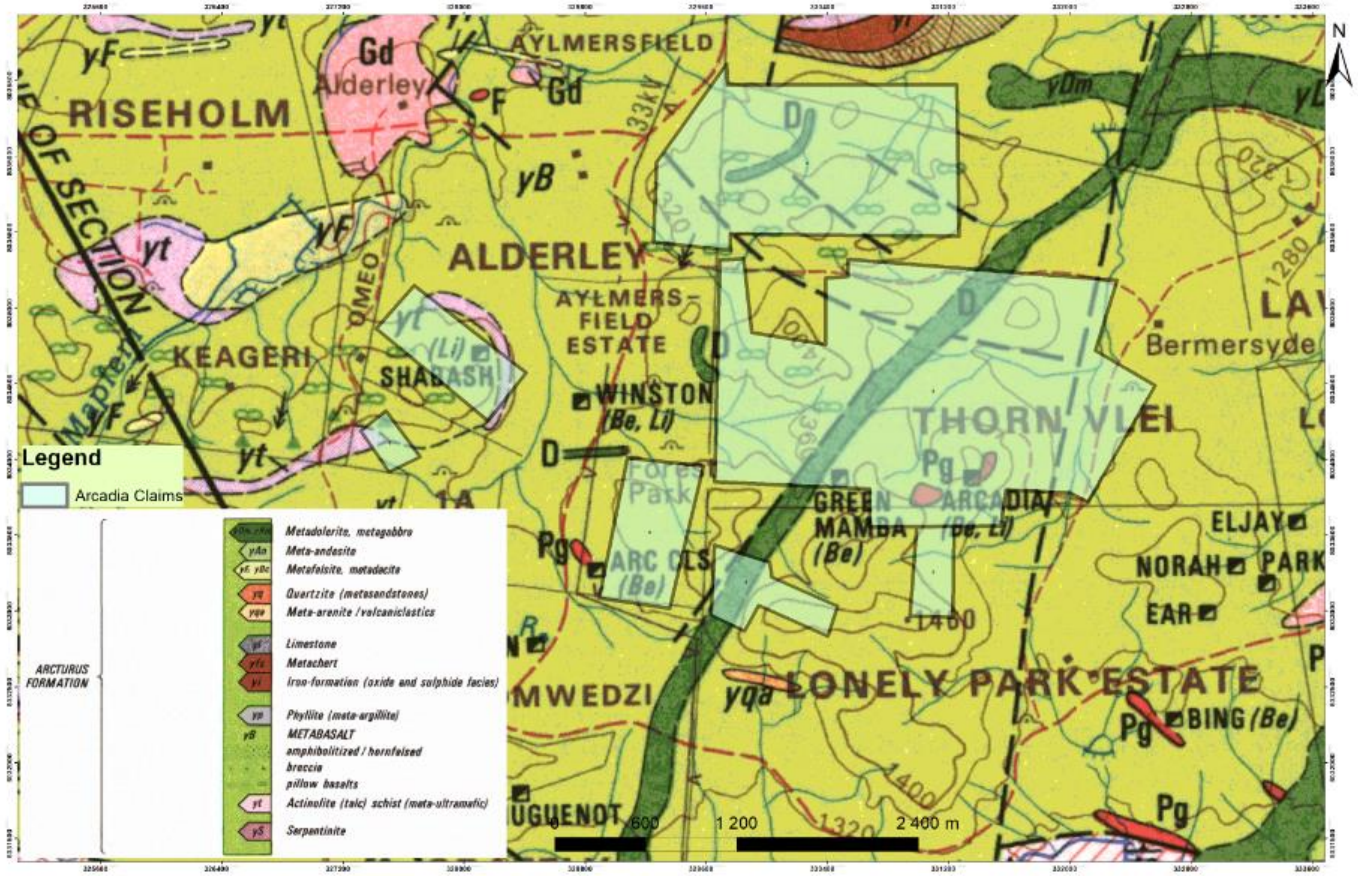

Figure 2. 5: Map showing the Arcadia Mining Claims. (Prospect Resources Ltd. 2017).

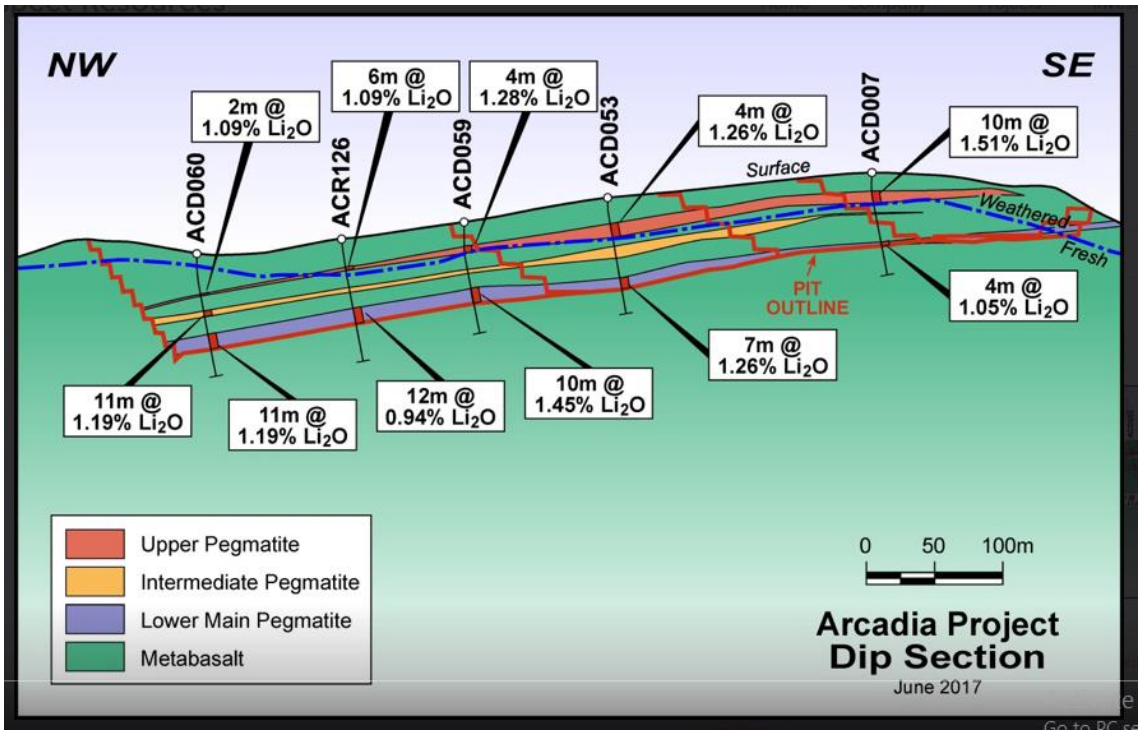

Figure 2. 6: Arcadia Dip Section, showing the stacked sub parallel pegmatite units. Intermediate and the Upper Pegmatite make up the Main Pegmatite (Source: Prospect Resource Ltd, 2017).

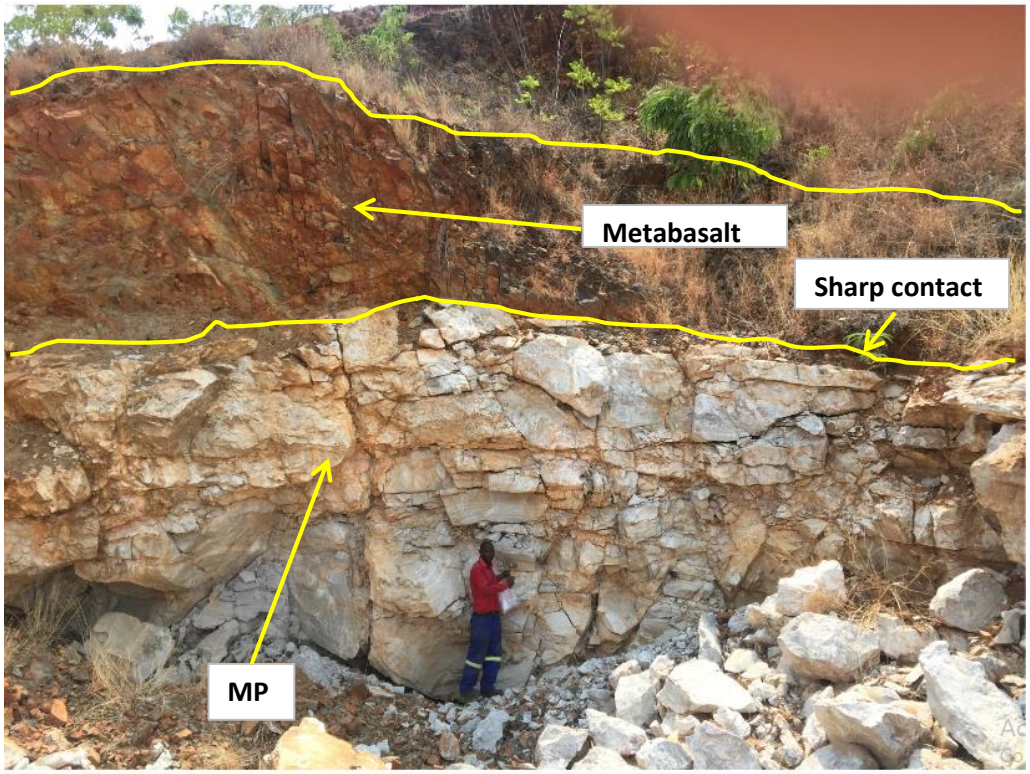

Figure 2. 7: Arcadia Pit showing outcrop of Main Pegmatite and hanging wall metabasalt.

CHAPTER 3: FIELDWORK

3.1: Introduction

This chapter will cover the fieldwork done at Arcadia which included core logging, hand specimen description and a description of some key geological observations within Arcadia Pit.

3.2. Core logging

Core logging was done for the 13 boreholes from which samples were collected and documented in a log sheet (Table 3.1). The location of the samples is shown in Figure 3.1. The major rock units that were observed from the core included the pegmatite and the metabasalt which hosts the pegmatite units. Generally, the Arcadia pegmatites are coarse-grained, although aplitic textures can be observed in some sections of the core in both the MP and the LMP units (Table 3.1; ACD 069; 75.00-75.20m). The aplitic texture also appeared to have some vitreous fine-grained muscovite and spodumene (Figure 3.2). Sharp contacts were also observed between the aplitic and the coarse-grained textures and where the aplitic dykes cut across the metabasalt (Figure 3.2 and Figure 3.3). The lithium minerals petalite and spodumene appeared more abundant in the MP unit than in the LMP unit. The grey coloured petalite appeared brecciated, fractured and with a general abundance of 1-2% within the MP unit (Figure 3.4), while in the LMP unit its abundance was predominantly ≤ 1%, although it would occasionally have ≤ 2% petalite abundance (ACD 068; Table 3.1). Spodumene was the second most abundant Li-bearing mineral in both units and was identified by its vitreous lustre and radial texture from needle-like crystals. A deep pink-coloured mineral was also observed on core in both the MP and the LMP units. It was coarse-grained and with an abundance that varied between 1-2% (Table 3.1). This deep pink-coloured mineral would more often appear adjacent to the grey petalite within the MP unit as was observed in borehole ACD074 (24.62-25.22m), while in some rare instances it appeared without the grey petalite within the LMP unit as observed in borehole ACD068 (85-91.7m; Table 3.1). The other dominant rock-forming minerals that were observed on core included coarse-grained quartz, coarse-grained pink-coloured K-feldspar, albite and the vitreous muscovite (Figure 3.4). Quartz was present as milky quartz, clear transparent quartz and in some instances as smokey quartz. It was also present as quartz veins of varying thicknesses of 1-2.5mm cutting across the metabasalt (Figure 3.3). The coarse-grained K-feldspar had inclusions of quartz, albite and muscovite (Figure 3.5). Accessory opaque minerals that were medium to coarse-grained were observed in borehole ACD071 (90-105.2m) within the LMP zone. Lepidolite, a lithium-bearing mineral that is very rare at Arcadia was also identified in accessory amounts (<0.5%) in borehole ACD041. Weathering of feldspars was also observed at the top part of borehole ACD013, which also appeared poorly mineralised (Figure 3.6). The other borehole that was poorly mineralised was ACD066 and the same borehole had the widest aplite intercept (Table 3.1).

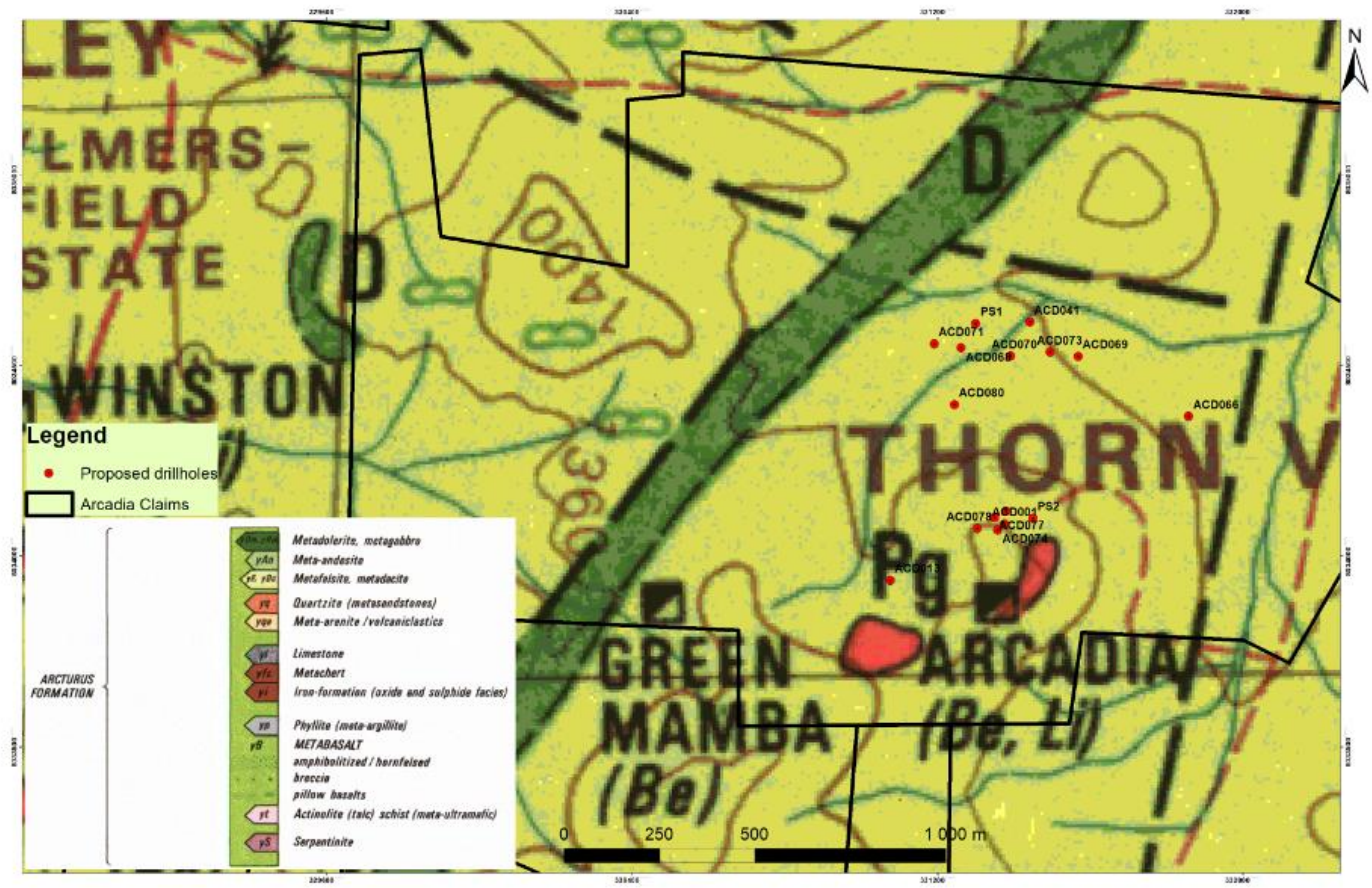

Figure 3. 1: Map showing the location of the samples.

Table 3. 1: Core Logging and Sampling exercise conducted at Arcadia Lithium Mine on 11/10/ 2019

Hole ID	From (m)	To (m)	Length (cm)	Sample ID	Eastings	Northings	Elevation (m)	Lithology	Comments	Region/Zone
ACD041	105	105.2	20	S001	331442	8034614	1321	PEG	qtz,feldspars,muscovite- rich ,Lower main, generally coarse grained	LMP
	108	108.2	20	S002				PEG	grey Pet 1-2% , qtz,fd,ms- rich ,Lower main, generally coarse grained (aplitic zone present&sharp contact)	LMP
	123	123.2	20	S003				PEG	Lepidolite, <0.5%,Lower main	LMP
ACD066	29	29.2	20	S004	331858	8034367	1316	PEG	qtz,feldspars,muscovite, poor in Li- mineralisation, wide aplitic zone	LMP
	44.13	44.54	41	S005 *				PEG	Minor deep-pink coloured mineral ,Mba vein@56.15-56.35m,, generally poor Li-mineralisation (aplitic zone)	LMP
	61.33	61.63	30	S006 *				PEG	qz,fd,ms-rich,, generally poor Li-mineralisation, L5,(aplitic texture)	LMP
ACD068	85	85.2	20	S007	331262	8034547	1333	PEG	Brecciated,Pink mineral <2%,Lower main, plg, qtz, minor K-Feldspar	LMP
	90	90.2	20	S008				PEG	Brecciated,Pink mineral <2%,Lower main, plg, qtz, minor K-Feldspar	LMP
	91.5	91.7	20	S009				PEG	Brecciated,Pink mineral <2%,Lower main, plg, qtz, minor K-Feldspar	LMP
ACD071	90	90.2	20	S013	331191	8034557	1332	PEG	Grey Pet<1%,Lower main, feldspars, qtz, opaque minerals, medium- coarse grained-albitization	LMP
	100	100.2	20	S014				PEG	Grey Pet<1%,Lower main, feldspars, qtz, opaque minerals, medium- coarse grained-albitization	LMP
	105	105.2	20	S015				PEG	Grey Pet<1%,Lower main, feldspars, qtz, opaque minerals, medium- coarse grained- albitization	LMP
ACD074	24.62	24.82	20	S016	331358	8034069	1410	PEG	Intermidiate Pegmatite ,Grey Pet 1-2% ,Deep- Pink mineral 1-2% Main Zone, Spodumene, K-feldspar, qtz, fd	MAIN ZONE
	24.82	25.02	20	S017				PEG	Intermidiate Pegmatite ,Grey Pet 1-2% ,Deep-Pink mineral 1-2% Main Zone, Spodumene, K-feldspar, qtz, fd	MAIN ZONE
	25.02	25.22	20	S018				PEG	Intermidiate Pegmatite ,Grey Pet 1-2% ,Deep Pink mineral 1-2% Main Zone, Spodumene, K-feldspar, qtz, fd	MAIN ZONE
ACD073	100	100.2	20	S019	331495	8034535	1325	PEG	minor Grey Pet,L5, plg, quartz, k-feldspar	LMP
	100.2	100.4	20	S020				PEG	minor Grey Pet,L5, plg, quartz, k-feldspar	LMP
	100.4	100.6	20	S020B				PEG	minor Grey Pet,L5, plg, quartz, k-feldspar	LMP
ACD081	36.61	36.81	20	S021	331379	8034119	1402	PEG	Grey Pet 1-2%, qtz, k-feldspars,ms rich, , L1	MAIN ZONE
	37.03	37.23	20	S022				PEG	Grey Pet 1-2%, qtz, k-feldspars,ms rich, , L1	MAIN ZONE
	37.23	37.43	20	S023				PEG	Grey Pet 1-2%, qtz, k-feldspars,ms rich, , L1	MAIN ZONE
ACD080	32.85	33.05	20	S024	331244	8034398	1349	PEG	Grey Pet 1-2%,U1, feldspars, qtz veins variable thicknesses (1-2mm)	MAIN ZONE
	33.05	33.25	20	S025				PEG	Grey Pet 1-2%,U1, feldspars, qtz veins variable thicknesses (1-2.5mm)	MAIN ZONE
	33.25	33.45	20	S026				PEG	Grey Pet 1-2%,U1, feldspars, qtz veins variable thicknesses (1-2.5mm)	MAIN ZONE

Hole ID	From (m)	To (m)	Length (cm)	Sample ID	Eastings	Northings	Elevation (m)	Lithology	Comments
ACD078	28.56	28.76	20	S030	331304	8034073	1409	PEG	Minor Grey Pet,L1, K-feldspar, qtz
	34	34.2	20	S031				PEG	Grey Pet<1%,L2, K-feldspar, qtz
	34.33	34.53	20	S032				PEG	Grey Pet<1%,L2, K-feldspar, qtz
ACD077	27	27.2	20	S033	331349	8034102	1403	PEG	Grey Pet 1-2% ,Pink mineral<1%, qtz, fd
	30	30.2	20	S034				PEG	Grey Pet<1%,qtz, fd
	35	35.2	20	S035				PEG	Grey Pet 1-2% ,Pink mineral <1%,fd, qtz
ACD069	65	65.2	20	S040	331568	8034524	1429	PEG	Grey Pet 1-2% ,Lepidolite < 1% ,Spodumene (radial needles), feldspars, qtz
	75	75.2	20	S041				PEG	Aplitic Pegmatite,sugary texture, fd, qtz, ms
	90	90.2	20	S042				Metabasalt	Metabasalt with small Pegmatite vein @ 89.40-89.50m, fd, qtz,ms
ACD001	10.65	10.85	20	S043	331375	8034085	1407	PEG	Grey Petalite, Spodumene (radial needles), K-feldspars, qtz, ms,(Upper Pegmatite band 1)
	25.4	25.6	20	S044				PEG	Spodumene (radial needles), petalite, k- feldspars, albite, qtz, ms,- weathered zone
	58.33	58.53	20	S045				PEG	Spodumene (radial needles), fault weathered zone present
ACD013	13.58	13.78	20	S046	331076	8033937	1391	PEG	Top part of borehole heavily weathered - Generally Poorly mineralised- L1 (Lower Pegmatite band 1).

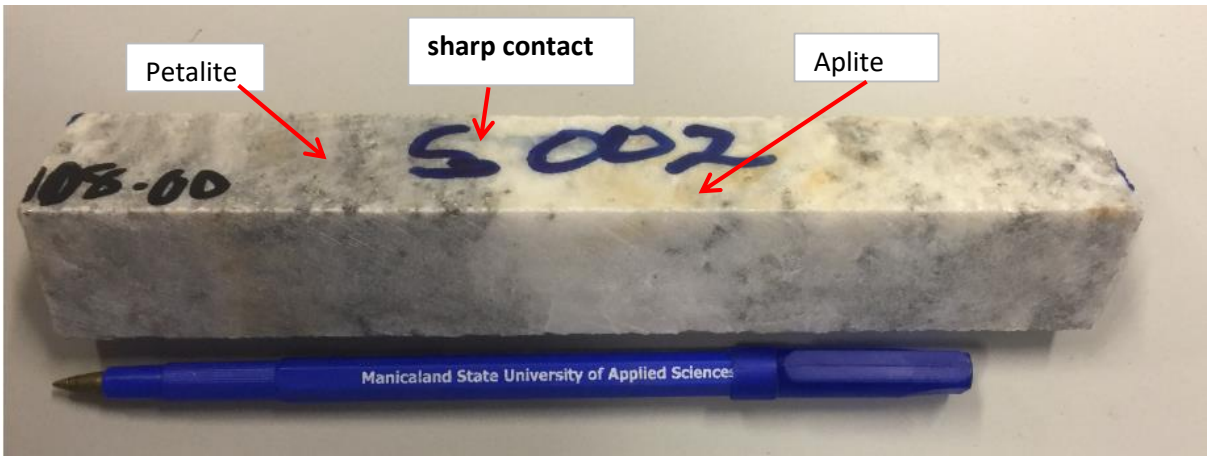

Figure 3. 2: Sharp contact between the coarse-grained petalite and the aplitic zone ACD 041.

Figure 3. 3: Aplite dyke showing a sharp contact with metabasalt. Quartz veins of variable thickness also present within the metabasalt ACD069.

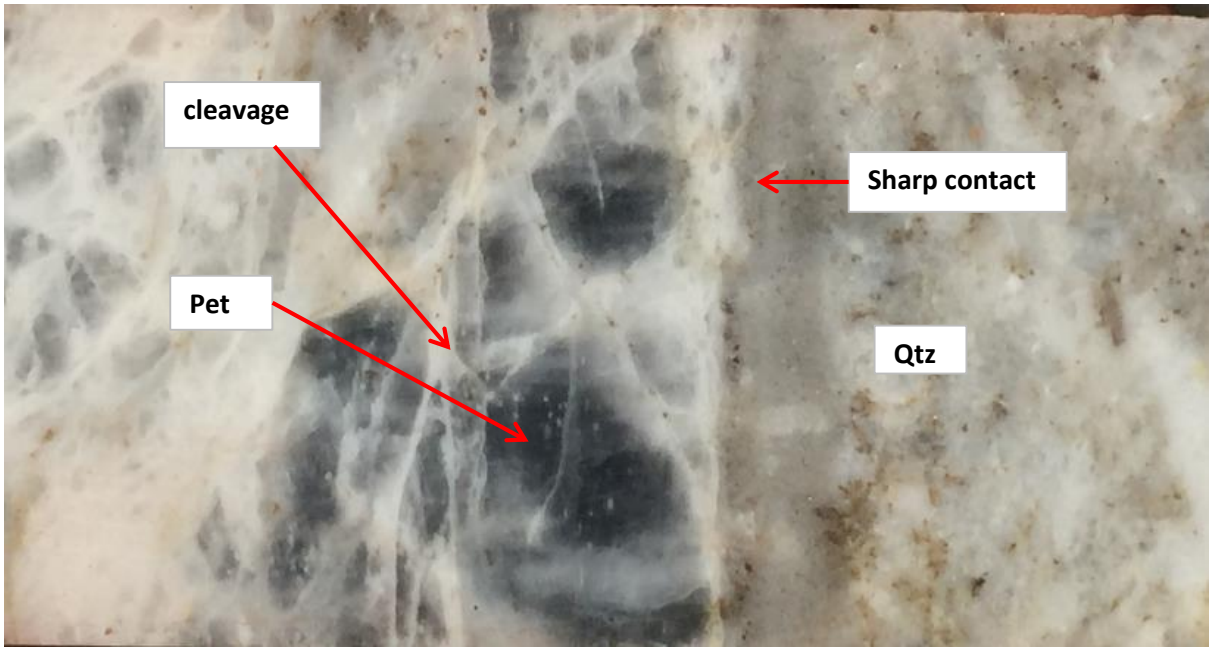

Figure 3. 4: Coarse-grained and brecciated petalite (pet) with prominent cleavage planes and fractures. A sharp contact defined by a change in texture and a change in mineral phase is also present.

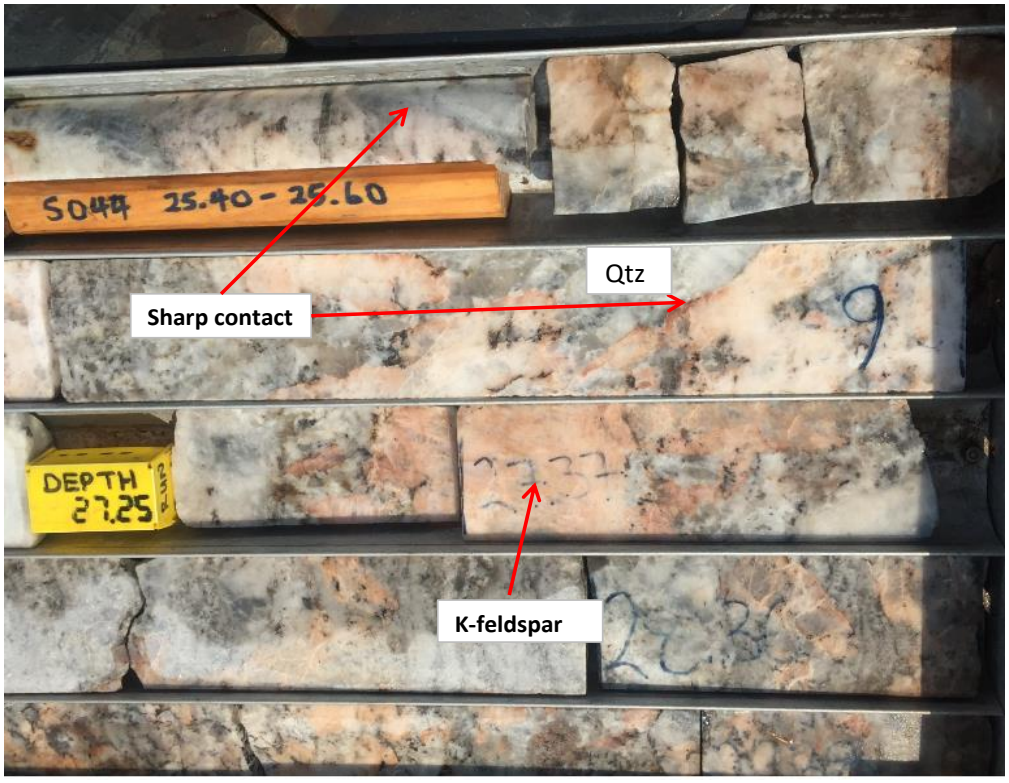

Figure 3. 5: Monomineralic coarse-grained K-feldspar and a sharp contact with milky quartz. Inclusions of quartz, albite, muscovite and opaque minerals in K-feldspar present (ACD 001).

Figure 3. 6: Weathering of feldspars in the upper part of borehole ACD013.

3.3. Hand specimen description

A pit visit was conducted to collect a few hand specimens for petrographic and geochemical analysis. The most interesting aspects observed from the hand specimens included the different mineralogical make up, textures, contacts and alteration processes. The Li-bearing minerals that were identified from hand specimen included the dominant petalite and spodumene and other minerals such as K-feldspar, albite, quartz, muscovite and accessory opaque minerals. The deep pink-coloured mineral observed on core was also visible on the pit samples. The textures that were identified varied between coarse-grained, medium to fine-grained, graphic, aplitic / sugary, radial and replacement textures. The contacts observed were predominantly sharp and the alteration was mainly hydrothermal alteration of feldspars and petalite. The replacement texture was prevalent on the cleavage planes of the coarse brecciated petalite. Weathering of feldspars to clays was also visible on the exposed MP unit within the pit.

3.3.1. Li- Bearing minerals

Petalite

Petalite exhibited a grey colour and was coarse-grained, with subhedral crystals exhibiting a prominent cleavage, in some instances creating a brecciated texture (Figure 3.7). Pervasive alteration was also prevalent along the cleavage planes and microfractures in petalite, and in some instances the cleavage planes and fractures appeared filled by the alteration product which in the majority of the samples appeared to be feldspars (albite) (Figure 3.7), while in other instances the microfractures and cleavage planes showed an infilling of vitreous spodumene intergrown with

quartz (Figure 3.8). The cleavage within petalite appeared to be at a high angle to the observed microfractures (Figure 3.7 and Figure 3.8).

A deep pink-coloured mineral was also identified adjacent to the grey petalite and also exhibited cleavage planes (Figure 3.9). The mineral was still yet to be verified if it was petalite and whether it is primary or secondary.

Figure 3. 7: Pit sample PS1, showing coarse-grained subhedral, brecciated grey petalite, with prominent microfractures and alteration along the cleavage planes (8034610N/331300E).

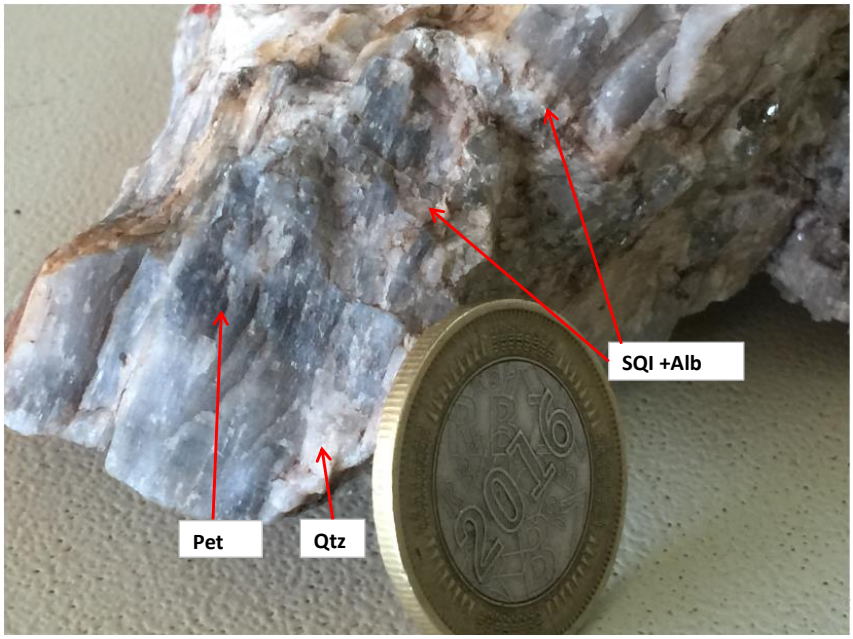

Figure 3. 8: Selected photograph of pit sample PS2 from the Main Pegmatite Zone showing petalite cleavage planes and microfractures, filled in with Spodumene+Quartz Intergrowths (SQI), albite and vitreous needle-like fine-grained spodumene(8034100N/331450E).

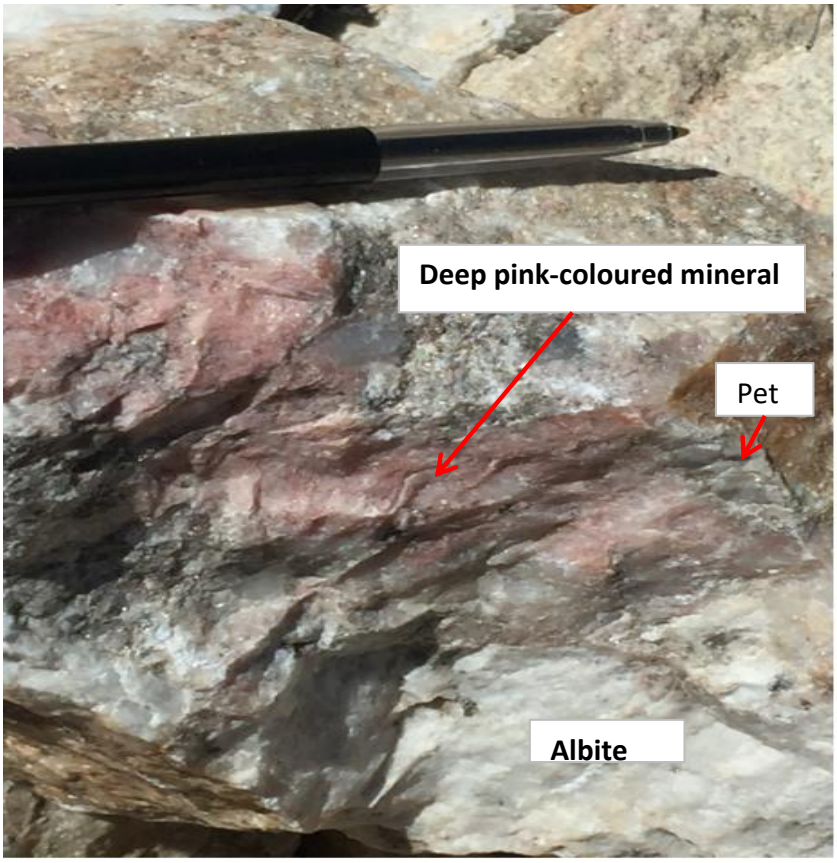

Figure 3. 9: PS1 showing the deep-pink coloured mineral occuring adjacent to the grey petalite and the albite showing a perfect cleavage (8034610N/331300E).

Spodumene

Spodumene in hand specimen appeared as fine-grained needle-like vitreous crystals (Figure 3.10), occuring along cleavage planes of other minerals such as petalite and as an intergrowth with quartz. It was a challenge to identify it in hand specimen but with a hand lens the vitreous, fine needle-like grains that were radially and sparsely distributed were apparent (Figure 3.10).

Figure 3.10: Pit Sample, showing the vitreous needle-like fine-grained crystals of spodumene (8034250N/331220E).

3.3.2. Rock Forming Minerals

The major rock forming minerals that were identified in hand specimen included coarse-grained albite, quartz and medium to fine-grained muscovite, and these minerals appeared to define a mineral zonation (Figure 3.11). Quartz crystals appeared clear, transparent and in some instances milky white and are coarse-grained and subhedral in shape, with a vitreous lustre and no alteration. Both clear and milky quartz appeared intergrown with albite creating a graphic texture (Figure 3.11). Medium to fine-grained muscovite appeared silver-greyish in colour with some ruby brown tint and green in some instances, exhibiting a perfect cleavage. The muscovite seemed to form a sheet-like structure occupying a zone between the albite rich zone and the quartz zone, with some of the medium to fine-grained muscovite also occurring as inclusions within the coarse-grained albite. The

vitreous medium to fine-grained muscovite was also identified in most of the aplitic zones (Figure 3.12). The coarse-grained albite exhibited a perfect cleavage (Figure 3.11).

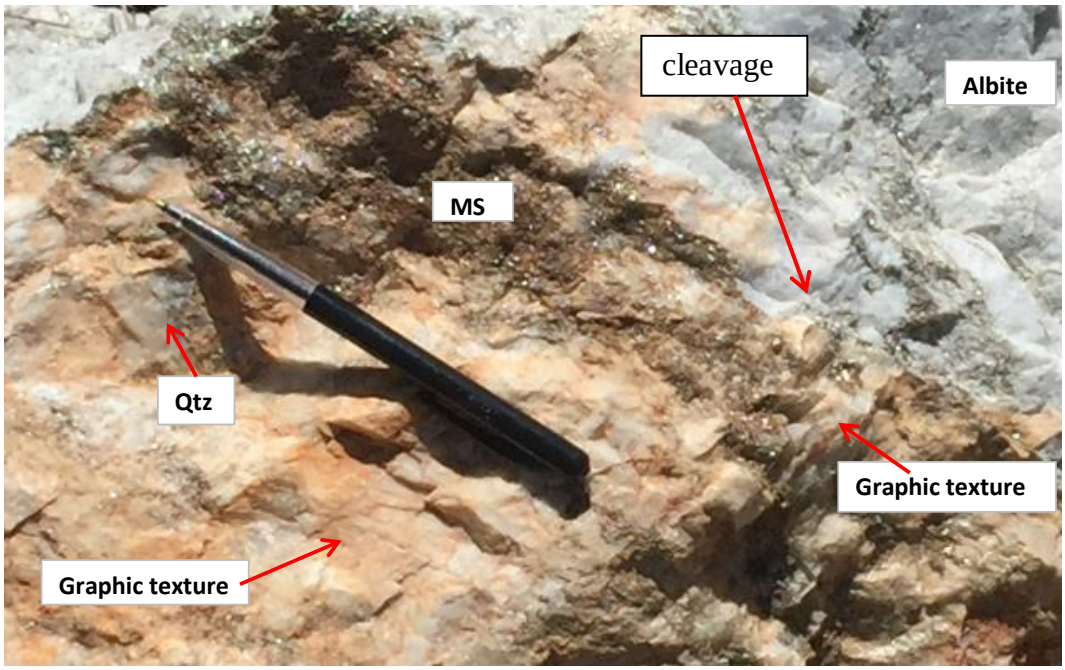

Figure 3. 11: Pit Sample showing mineral zonation patch of quartz (Qtz), muscovite (ms) and albite. Quartz and albite appear intergrown exhibiting a graphic texture. Albite is exhibiting a perfect cleavage (8034240N/331530E).

Figure 3. 12: Aplite showing the aplitic (sugary) texture, with medium to fine-grained vitreous muscovite and fine-grained vitreous spodumene (8034110N/331290E).

3.4. Other geological features

The Arcadia pit is approximately 200m long southwest to northeast strike and has been excavated in a southwest-northeast direction. Pegmatites intruded into the deformed metamorphosed greenstones and the granitic terrane with the dominant visibly extensive metabasalt covering all the Arcadia-Green Mamba claims (Figure 3.13). Small discontinuous lenses of thin, stacked sub-parallel pegmatite units, dipping towards the north and truncated by a series of sub-parallel northeast southwest trending normal faults were observed within the exposed Main Pegmatite unit (Figure 3.13). The hanging wall metabasalt is separated from the underlying Main Pegmatite zone by a sharp contact.

The mapping of pit features revealed irregular mineralised concentric patchy zones within the MP unit. The zonation was defined by a mineralogical and textural change. From the upper margin inward, the visible zones were the intermediate zone and the aplitic zone. The intermediate zone is characterised by a coarse-grained texture and comprises the mineral assemblage, petalite+ spodumene+ K-feldspar+ quartz +garnet. The aplitic zone is characterised by a medium to fine-grained texture and the following mineral assemblage, quartz+albite+ muscovite+ garnet. The aplitic zone appeared patchier than the intermediate zone. The two zones are generally demarcated by sharp contacts. The other zone present within the Arcadia pegmatites is the core zone enriched in coarse-grained quartz but poorly mineralised. This zone was only visible within some sections of core and not at the pit. The rock units within the pit appeared to have undergone some regional deformation and metamorphism (Figure 3.14), with the deformation resulting in some mineral lineations of albite observed on some outcrop units. The lineations were of centimetre scale plunging northeast (Figure 3.14).

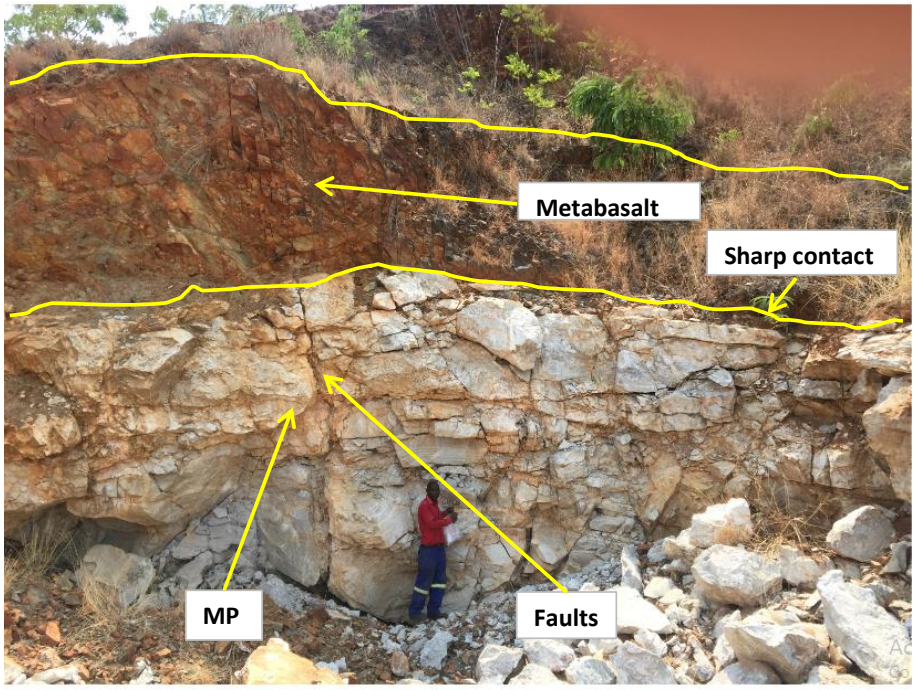

Figure 3. 13: Outline of the pit showing the hangingwall metabasalt overlying the Main Pegmatite zone separated by a sharp contact. A series of parallel faults across both units.

Figure 3.14: Mineral lineations of albite in a metamorphosed pegmatite unit, within the pit plunging northeast (8034070N/331310E).

3.5. Discussion

Fieldwork revealed the various lithologies, textures, contacts and the mineralisation that characterize the Arcadia pegmatites. The main lithological units comprise the pegmatite and the metabasalt. The coarse-grained texture appears to be the dominant texture followed by the aplitic texture and these two textures are separated by sharp contacts. The dominant lithium-bearing minerals are the grey coarse-grained brecciated petalite and the fine-grained spodumene, with petalite being the most abundant one in both the MP and the LMP units. The dominant rock forming minerals at Arcadia are albite, quartz, K-feldspar and muscovite. Albite is white to greyish in colour, massive, coarse-grained, and exhibits some striations and two perpendicular perfect cleavage planes, while the coarse-grained quartz appeared as either clear, smokey and milky, intergrown with albite and spodumene. Fine-grained silver-green muscovite appeared concentrated between the albite and quartz zones and is also common in the aplitic zones. The coarse-grained K- feldspar had a pink colour and exhibited perpendicular cleavage planes and had no striations. Discernible alteration of feldspars and spodumene intergrown with quartz appeared prevalent along the fractures and cleavage planes of the grey primary petalite. Weathering and albitisation of feldspars to clays was visible at the pit and within core. Irregular concentric zoning of the intermediate and aplitic zones was also observed within the pit and it was characterized by a change in texture and the presence of certain mineral assemblages mentioned in section 3.4, with the coarse-grained intermediate zone hosting the mineralisation. The deep pink-coloured mineral appeared to be coarse-grained and present in both the LMP and the MP units, occurring adjacent to the primary grey petalite in the MP zone, while in the LMP zone it was present without the primary grey petalite.

3.6. Conclusion

From the above findings, it can be concluded that petalite is the dominant lithium mineral that occurs at Arcadia, with spodumene occurring in minor quantities as either a primary phase or as an alteration product of petalite intergrown with quartz. It can also be concluded that the pegmatites do not show clear zonation from the margins of the pit inwards as observed by the presence of irregular patchy concentric zones, with the mineralized intermediate zone better visible than the aplite zone within the exposed MP unit. The transition between the aplitic and the coarse-grained textures is abrupt and sharp, which is an indication of the fast cooling of magma. According to Nabelek et al., (2009), the observed transition from the aplitic zones to the pegmatite zones represents a transition from zones of high nucleation density and rapid growth to zones of low nucleation density, with even more rapid crystal growth. The pink-coloured coarse-grained mineral, the identity of which is still to be verified, also occurs adjacent to the grey petalite within the intermediate zone. The presence of the observed mineral lineation of albite, confirms the presence of the extensional force component during the regional deformation that took place which is evident from Figure 3.13 and Figure 3.14 (Fossen, 2016).

It can therefore be concluded that there is no significant mineralogical variation observed between the MP and LMP zone other than the abundance of petalite and spodumene which seemed to be higher in the MP zone as compared to the LMP zone. The textural variance is that the LMP appears to have more of the aplitic textures than the MP unit as observed from core logging, while the coarse-grained and graphic textures appeared dominant in the MP unit (Table 3.1).

CHAPTER 4: PETROGRAPHY AND MINERALOGY

4.1. Introduction

This chapter will cover the petrography and XRD analyses conducted on the selected representative samples from the MP and the LMP units. The X-Ray Diffraction analysis was conducted at a lab in Pretoria (South Africa) by XRD Analytical & Consulting, while the petrographic analysis was conducted at Wits University using the Olympus BX 53M/DP74 microscope. The two methods corroborate each other, with the XRD technique playing a critical role in the direct identification and quantification of the mineral phases that are a challenge to identify using the microscope.

Petrographic analysis was conducted on 19 representative samples from 13 boreholes intersecting the Main Pegmatite zone (MP) and the Lower Main Zone (LMP). The petrographic analysis was essential to determine the overall mineralogy and the various textural relationships between minerals within the two units. The petrographic analysis was conducted under both plane polarised light (PPL) and cross polarised light (XPL). The detailed petrographic properties of all the analysed samples have been tabulated in Appendix A and below is a summary on the petrographic analysis describing the outstanding features for the selected representative samples.

4.2. Petrographic analysis

The petrographic analysis of the Arcadia pegmatite samples in thin section, identified petalite and spodumene as the major Li-bearing minerals respectively, with the abundance of petalite varying from 0.2-62%, while that of spodumene varied from 0-50%. The other minerals identified within the thin sections included albite, quartz, microcline and garnet. Albite and quartz seem to be the predominant rock-forming minerals with the abundance of albite varying from 5-92%, while that of quartz varied from 3-46%. Microcline varied in abundance from 0-59%.

4.2.1. Li-Bearing Minerals

Petalite

Petalite seemed to be the dominant Li- bearing mineral in samples S040, PS1 and S016 (Appendix A), displaying a low relief with the subhedral to anhedral crystals varying in size between 0.25-11mm. The coarse-grained megacrystals of petalite exhibited prominent cleavage (Figure 4.1 and Figure 4.2). In instances where petalite was in accessory amounts it was medium to fine-grained and occurred within a fine-grained matrix of altering albite and quartz (Appendix A). Where petalite was undergoing alteration, its edges or rims seemed to be resorbed in the fine-grained matrix of spodumene and quartz, resulting in a reaction or replacement texture (Figure 4.1 and Figure 4.2). The resorption of petalite around its edges, and its alteration to spodumene can be clearly seen in Figure 4.2. Inclusions of spodumene+ quartz (SQI) and albite in petalite were also identified in this suite of pegmatites (Figure 4.1, Figure 4.2 and Figure 4.3). There appeared to be two versions of petalite in some thin sections, one was primary and the other one secondary (Figure 4.1 and Figure 4.3).

Spodumene

Spodumene exhibited a diagnostic high relief and cleavage, which enabled its identification particularly in samples PS2 and PS1 (Figure 4.1, Figure 4.2 and Figure 4.3), where its abundance in PS2 accounted for about 50% including the bulk of the matrix. Spodumene appeared both as a primary phase and as a product of alteration of petalite intergrown with quartz and albite, within the cleavage planes of petalite or within the fine-grained matrix (Figure 4.1, Figure 4.2 and Figure 4.3). The secondary fine-grained spodumene was also interstitial to petalite (Figure 4.2). Generally, the crystal size of spodumene varied from 0.25- 3mm (Appendix A).

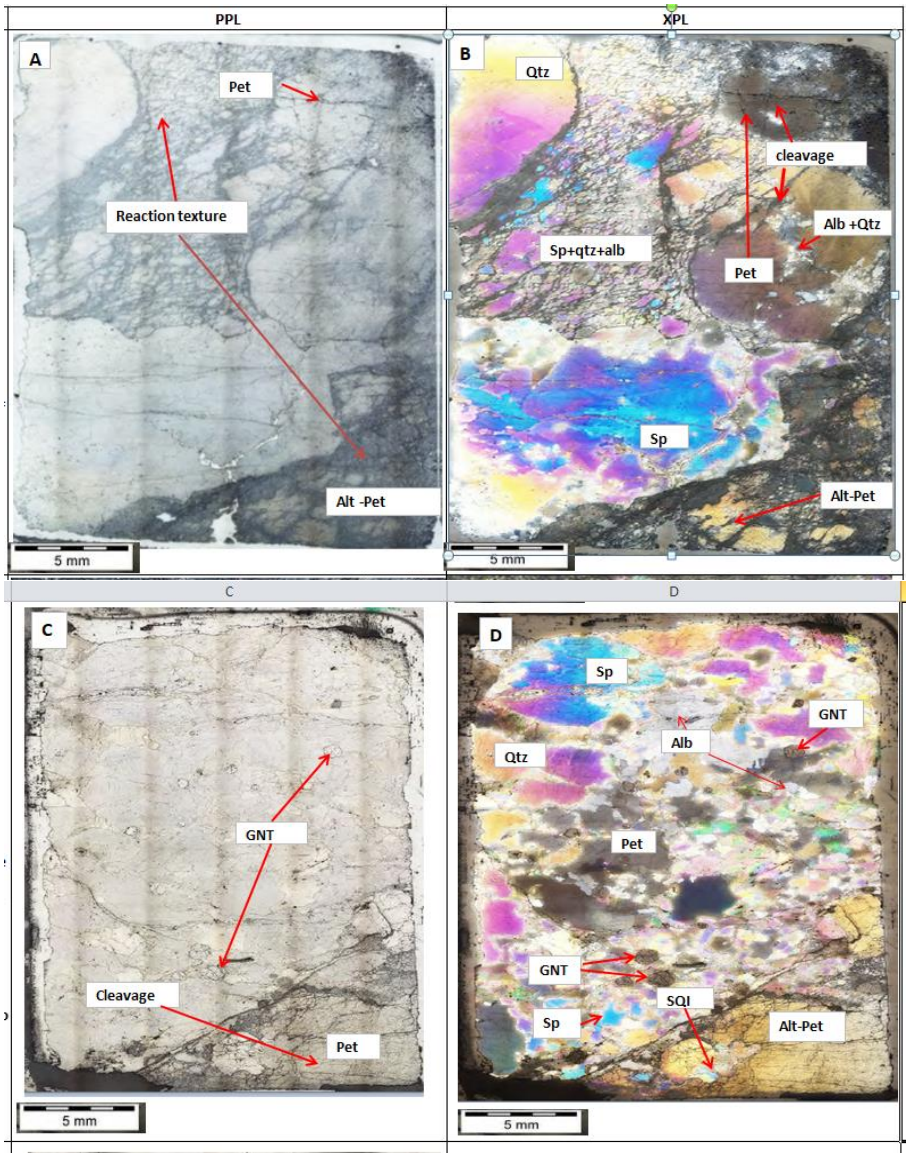

Figure 4.1: Selected thin sections showing petalite and spodumene occurrences. (A). Low relief coarse-grained primary petalite (pet) with its prominent cleavage and the altering petalite with fractures and showing a reaction texture in PPL (Sample PS1-MP). (B). Spodumene (Sp) with its high diagnostic relief and cleavage plane appears intergrown with quartz (qtz) +albite (alb) in a fine-grained matrix. Inclusions of sp+qtz +alb in petalite (Sample PS1-MP) in XPL. (C). Disseminated accessory euhedral garnets present. Low relief petalite with distinctive cleavage planes in PPL (S040-LMP). (D). Primary petalite with inclusions of albite. Petalite altering to spodumene, intergrown with quartz+albite in XPL (S040-LMP).

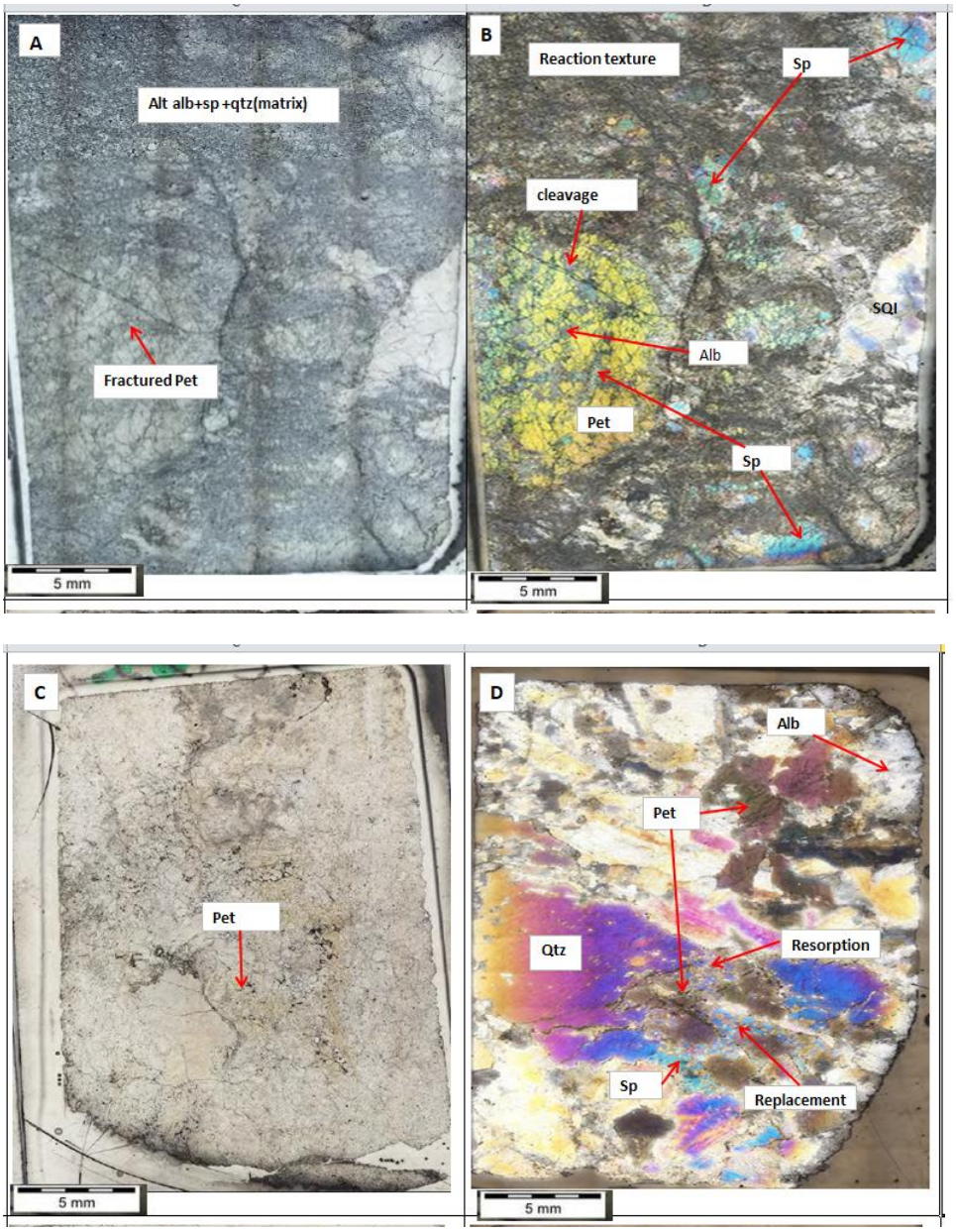

Figure 4. 2: Selected samples showing the alteration of petalite (pet) and albite (alb) as well as the alteration textures. (A). Fractured petalite showing a low relief under PPL (Sample PS2-MP). (B) Reaction texture produced by the alteration of albite (alb) and this makes up the fine-grained matrix with the altering spodumene (sp) +quartz. Prominent fractures and distinctive cleavage planes present in the altered petalite megacrystal. Spodumene is dominant in this section within the fine-grained matrix and is also interstitial to the megacrystic petalite and appears intergrown with quartz (SQI). Albite and quartz are also interstitial to the megacrystic petalite (XPL). (C). low relief petalite in PPL (Sample S022-MP). (D). Alteration of primary petalite to spodumene creating a replacement texture and petalite also getting resorbed around its edges where it is rimmed by quartz in XPL (Sample S022-MP).

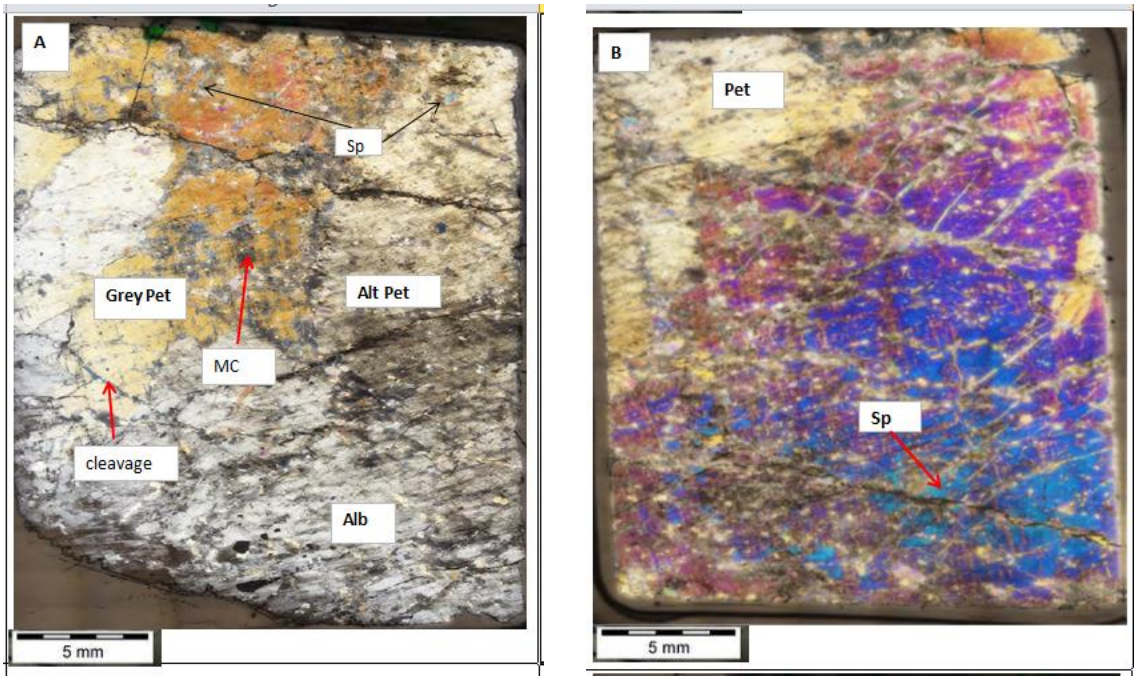

Figure 4.3: Selected thin sections exhibiting the grey petalite and the deep-pink coloured petalite. (A). The grey primary petalite is present, with visible cleavage and inclusions of fine-grained spodumene (sp) +fine-grained qtz+ microcline (mc). There is also altered petalite with cleavage planes and inclusions of quartz+sp+alb. (S016). (B). Anhedral coarse-grained petalite with cleavage planes filled with spodumene+qtz. Spodumene (sp) can be seen with its diagnostic high relief and cleavage, present within the section S016.2.

4.2.2. Rock-Forming Minerals

Albite

Albite is the most abundant rock forming mineral varying from coarse to medium and to fine-grained in texture. The crystals are anhedral and vary in size between 0.05-6mm (Appendix A). The medium to fine-grained albite occurs as inclusions within microcline, petalite or intergrown with quartz creating a graphic texture (Figure 4.1; Figure 4.2 and Figure 4.4). The graphic texture is very visible in Figure 4.4. Albite twinning was also observed in samples, S034A and S034B (Figure 4.4). Alteration of albite was also observed in some of the thin sections with the intense alteration occurring in sample S015-LMP (Figure 4.5).

Quartz

Quartz appeared generally coarse-grained and subhedral to anhedral in most of the sections, with some sections exhibiting medium to fine-grained quartz, ranging between 0.05-10mm in size (Appendix A). The medium to fine-grained quartz occurs as inclusions in microcline, petalite and intergrown with spodumene and albite (Figure 4.4).

Microcline

Microcline was generally coarse-grained in most of the thin sections. Where it was present it showed tartan plaid or cross-hatch twinning, and a perthitic texture as well as inclusions of quartz and albite

(Figure 4.4). The microcline megacrystals were anhedral in shape and ranged in size between 0.5->6mm (Appendix A). However, microcline was not present in all the thin sections analysed.

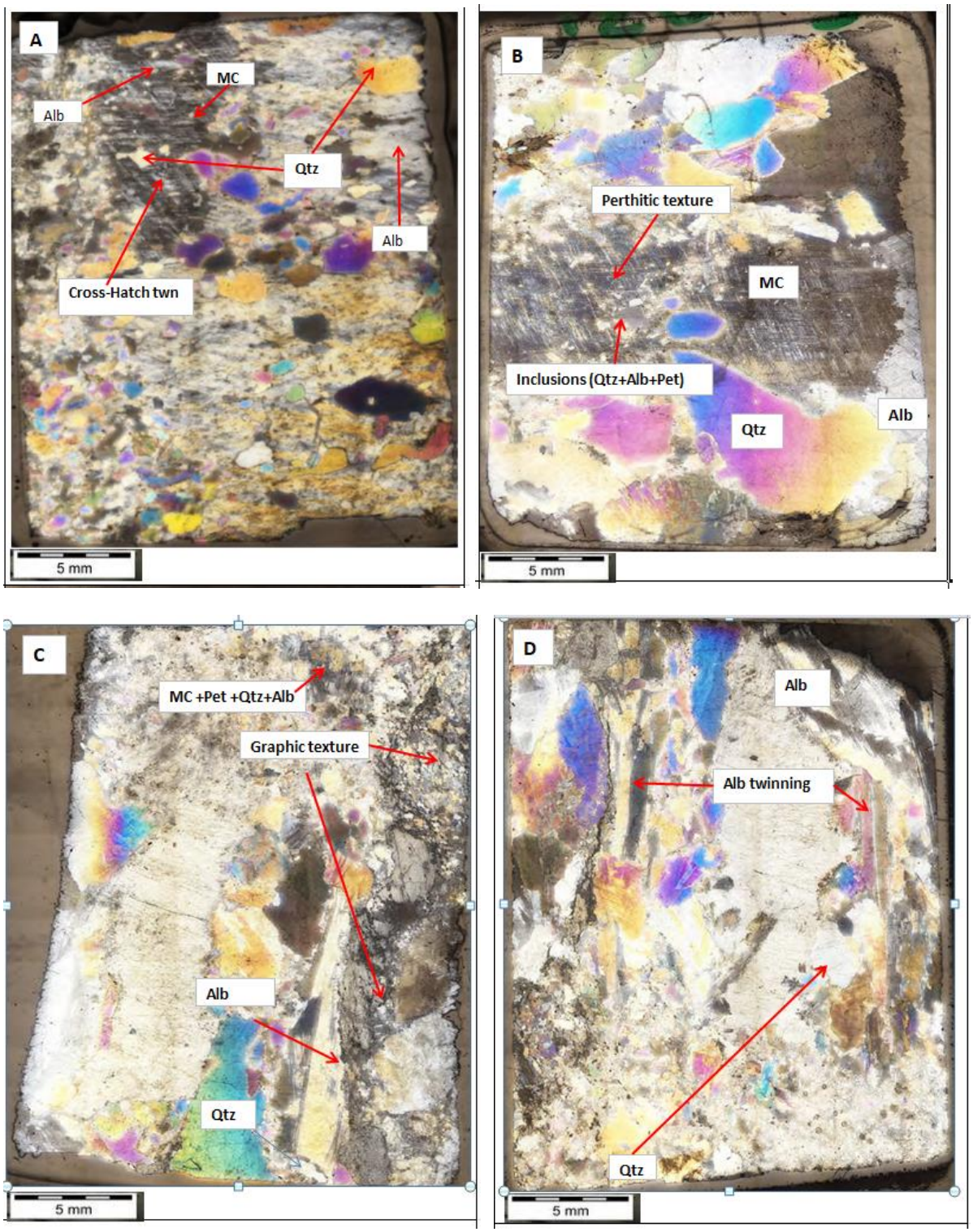

Figure 4. 4: Selected images of thin sections showing the occurrences of the rock-forming minerals under XPL. (A). Coarse- grained microcline (MC), showing cross- hatch twinning and has inclusions of quartz and albite (S020B-LMP). (B). Microcline showing a perthitic texture and also has inclusions of fine-grained qtz+alb+pet. Coarse-grained quartz and albite also present (S031-MP). (C). Graphic texture exhibited by the intergrowth of albite and quartz (S034B-MP). (D). Albite twinning exhibited (S034A-MP).

Other Accessory minerals

Accessory, disseminated, euhedral garnets were identified in only one of the thin sections S040 (Figure 4.1) from the LMP zone, with the grain size varying from 0.5-1.0mm. There were also other accessory opaque minerals and secondary minerals, particularly in the highly altered sample S015 (Figure 4.5), that were a challenge to identify through the microscope, and could only be identified and quantified by the XRD technique, the results of which will be discussed later in this chapter.

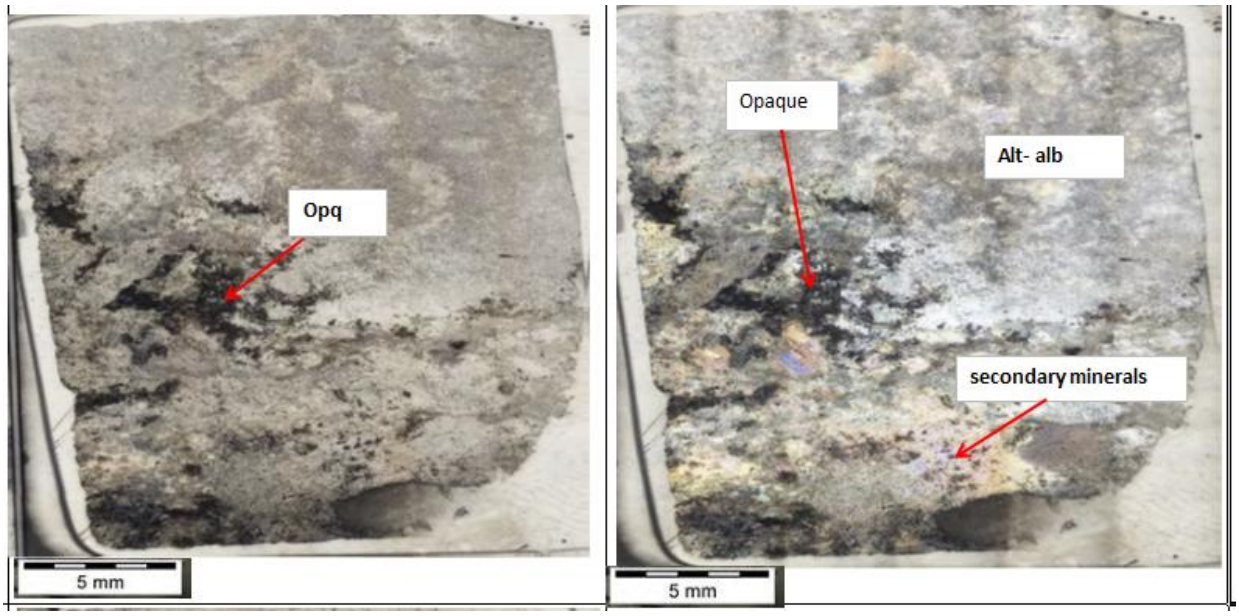

Figure 4. 5: Thin section sample S015 under PPL and XPL showing high degree of alteration. (A) medium to fine-grained opaque (opq) minerals in a fine-grained matrix in PPL. (B). Alteration of albite producing secondary minerals, some of which have shades of pink in sample S015.

4.3. X-Ray Diffraction Technique

The XRD Rietveld analytical method was used to determine the mineral composition of the 15 selected representative samples from both the MP and LMP units (Table 4.1). The XRD analysis proved to be very useful in the direct identification and quantification of Li-bearing minerals as well as the accessory minerals that were a challenge to identify under the microscope. According to Bruker (2006), the XRD method is regarded as the most direct and accurate method in the semi-quantitative determination and analysis of mineral species in a sample, although it does not provide accurate quantitative data on the elemental composition of the samples.

The Rietveld XRD method is an accurate quantitative analysis technique that has been widely accepted due to its whole- pattern fitting approach instead of a single peak analysis (Rietveld, 1969). The main advantage of the Rietveld XRD method is its ability to effectively minimise or eliminate the inaccuracies associated with overlapping peaks, preferred orientation which gives incorrect intensities, micro-absorption, polarisation effects, particle statistics, as well as inaccuracies associated with the detection of amorphous and trace phases (Djerdj, 2019). The Rietveld method is regarded as a full pattern refinement method, consisting of a whole range of a measured spectrum and eliminating any problems associated with crystalline materials.

4.3.1. XRD Results Analysis

The XRD analysis technique was able to directly identify and quantify the following minerals within this suite of pegmatites: plagioclase (albite), quartz, siderophyllite, bikitaite, calcite, smectite, pollucite, eucryptite, petalite, microcline, spodumene, amblygonite-montebrasite and stilbite (Table 4.1).

4.3.2. Rock-forming minerals

Plagioclase

Albite is the predominant mineral in this suite of pegmatites (Table 4.1), with the samples S025, S034, S032 and S009 registering significant amounts greater than 70wt%. Sample S025 recorded the highest concentration value of 91.8wt% for albite, while sample PS1 recorded the least amount of albite, which was 5.3wt%. In samples where albite was a minor phase, the same samples registered significant amounts of petalite and spodumene (Table 4.1).

Quartz

Quartz was also identified as one of the major mineral components of the Arcadia suite of pegmatites, with significant concentrations ranging between 3.1%-45.6wt%. S042, S001 and S005, had significant concentrations of quartz; 45.6wt%, 44.7wt% and 44.5% respectively, but registered trace amounts of petalite and spodumene (Table 4.1).

Microcline

Microcline was detected and quantified in 60% of the analysed samples, while in the other 40% (6 samples) it could not be detected (Table 4.1). This confirms the petrographic observations where the mineral was also visualised in about 7 samples (Appendix A). Where present the mineral ranges from trace amounts of 0.1wt% for sample S005, to significant concentrations of 58.7wt% for sample S031. However, it should be highlighted that microcline could not be detected in three of the four samples with significant concentrations of petalite and spodumene namely S040, PS1 and PS2 (Table 4.1).

4.3.3. Li-bearing minerals

Petalite

Petalite was detected in significant concentrations ranging from 17.7-61.6wt% in samples S040, S016, PS1 and PS2, with sample S040 from the LMP, registering the highest value of 61.6wt%. The rest of the significant concentrations were from samples within the Main Pegmatite Zone. Sample S032 registered minor amounts of petalite (11.4wt%), while the rest of the remaining pegmatite samples only showed trace or accessory amounts of the mineral ranging from 0.2-1.8wt% (Table 4.1).

Spodumene

Spodumene comprised 49.6wt% of sample PS2 from the Main Pegmatite Zone, while minor concentrations were detected in samples PS1-13wt%, S040-9.3wt% and S016-7.2wt%. Trace amounts were recorded for 6 samples and no spodumene was detected for the remaining 5 samples namely, S020B, S025, S031, S032 and S034 (Table 4.1).

Other Accessory Minerals

The XRD analysis was also very useful in detecting and quantifying the accessory minerals that were a challenge to visualise and identify in thin sections. These minerals included some Li-bearing minerals namely bikitaite, eucryptite and amblygonite-montebrasite. The other accessory minerals identified and quantified included siderophyllite, smectite, stilbite, calcite and pollucite (Table 4.1). The minerals eucryptite and bikitaite registered significant values of 8.4wt% and 15.6wt% respectively for the sample S015, but the two minerals could not be detected in 60% (9 samples) of the bulk samples. Sample S015 was the only sample in which the mineral pollucite was detected with a concentration value of 0.3wt%. Amblygonite-montebrasite appeared to occur in trace amounts in 6 samples, with the highest value detected being 2.1wt% for sample S001, while siderophyllite (mica), a rock forming mineral was detected in trace amounts in 60 % of the samples (9 samples), with the highest value of 4.2wt % detected in sample S042. The clays smectite and stilbite were also detected in trace amounts, with the XRD detecting smectite in three samples and stilbite detected in eight samples. The highest smectite abundance was 6.6wt% in sample S015, while stilbite registered its highest concentration of 1.4wt% in sample PS2. Calcite is another accessory mineral that was identified and quantified by the XRD in one sample S015 with a trace concentration of 0.2wt% detected (Table 4.1).

Table 4. 1. Record of minerals identified by the XRD Rietveld Method

ZONE	Sample	Plg	Qtz	Siderophyllite	Bikitaite	Calcite	Smectite	Pollucite	Eucryptite	Petalite	Microcline	Spodumene	Amblygonite-montebrasite	Estilbite
MP	PS1	5.3	37.1	0	0	0	0	0	0	44.5	0	13	0	0
MP	PS2	10.5	19.8	0.3	0	0	0.5	0	0.3	17.7	0	49.6	0	1.4
LMP	S001	47.8	44.7	2.3	0	0	0	0	0	1.4	0	1.6	2.1	0.1
LMP	S005	55	44.5	0	0	0	0	0	0	0.2	0.1	0.1	0	0
LMP	S009	71.9	20.8	0	0.3	0	0.1	0	0	0.9	5.4	0.4	0.2	0.1
LMP	S015	56	7.8	0	15.6	0.2	6.6	0.3	8.4	1.1	0	4	0	0.1
MP	S016	19	10.7	0.1	0	0	0	0	0	51.7	11.2	7.2	0	0
LMP	S020B	58.9	24.9	1.2	0	0	0	0	0	1.8	13.1	0	0	0.1
MP	S021	33.9	30.8	0.2	0	0	0	0	0	0.4	34.6	0.1	0.1	0
MP	S025	91.8	6.9	0.1	0	0	0	0	0	0.9	0.3	0	0	0
MP	S031	28.1	11	0	0	0	0	0	0	0.2	58.7	0	1.9	0.1
MP	S032	75.6	3.1	0	0	0	0	0	0	11.4	9.9	0	0	0
MP	S034	79.4	12.3	0.4	0	0	0	0	0	1.5	6.4	0	0	0
LMP	S040	10.1	15.5	0.4	1.7	0	0	0	0.1	61.6	0	9.3	1.2	0.1
LMP	S042	46.8	45.6	4.2	0	0	0	0	0	1.7	0	0.3	1.3	0.1

4.4. Discussion

The petrographic analysis indicated that samples, S040, PS1, S016 and PS2, were enriched in the Li-bearing minerals petalite and spodumene. This was also corroborated by the XRD analysis which detected and quantified significant amounts of lithium in these samples. Petrography also showed the abundance of the rock forming minerals albite and quartz and this analysis was also confirmed by the XRD results where significant concentrations of these two minerals where recorded. The samples with significant concentrations of albite and quartz registered trace amounts of petalite. An association of albite, quartz and spodumene was common in the samples where primary petalite was altered and the same association was present as inclusions within microcline. Petalite and spodumene appear to occur in association, as can be observed from the XRD results in which both minerals registered their significant concentrations in similar samples (S040, S016, PS1 and PS2). This association is also confirmed by petrographic analysis, which showed the same samples exhibiting petalite as the dominant phase in association with the minor phase spodumene, either as a primary or a secondary phase from the alteration of petalite.

Petrographic analysis revealed intense alteration of albite and the presence of accessory opaque minerals in sample S015 (Figure 4.5), of which the identification and quantification of the fine-grained alteration products and the accessory opaque minerals was detected by the XRD technique, thus confirming the corroborative nature of the two analytical methods. The XRD technique identified the minerals in the highly altered sample S015 as bikitaite, eucryptite, smectite, stilbite and calcite (Table 4.1). The same minerals had their significant concentrations detected in sample S015 (Table 4.1). The minerals appear to be hydrothermal alteration products of the primary mineral phases. Bikitaite and eucryptite appear to be products of the hydrothermal alteration of primary petalite and spodumene, while smectite, stilbite and calcite appear to be hydrothermal alteration products of plagioclase feldspars. The hydrothermal alteration replacement reaction of primary petalite and spodumene is supported by Hurlbut (1957) and Charoy et al (2001), who documented the replacement of primary spodumene by K-feldspar + eucryptite, while bikitaite occurs as a late-formed mineral in fractures of Li-rich pegmatites replacing spodumene and in some cases possibly replacing eucryptite.

Garnet was identified in one thin section S040 (Figure 4.1) from the LMP zone and it appears to be present in accessory amounts but in the LMP. This observation is consistent with the MSA findings regarding garnet's presence in this unit (MSA, 2017). The garnets could be part of the country rock (metabasalt) material that contaminated the pegmatites during their intrusion, implying that the garnets are xenoliths in these pegmatites and therefore they crystallised earlier before the Li-phases. The pink coloured mineral observed during core logging in sample S016 and in pit sample PS1, both from the MP unit (Figure 3.8), was identified in thin sections as altered or secondary petalite (Figure 4.1 and Figure 4.3). Petrographic analysis confirmed the core logging observation of the abundance of this secondary pink coloured petalite in the MP unit.

Generally, the XRD and petrographic analyses revealed the LMP as having a higher or significant concentration of secondary minerals as compared to the MP unit (Table 4.1). On the other hand, the MP appears to have a significant concentration of primary lithium minerals, petalite and spodumene as well as the primary rock forming minerals as confirmed by the XRD and petrographic analyses as

well as the fieldwork conducted. The textural variation observed from petrography was the dominance of fine-grained textures as well as replacement textures in the LMP unit.

4.5. Conclusion

The petrographic and XRD analyses revealed that there is no significant variation in the mineralogical makeup of the LMP and the MP other than the abundances of the lithium minerals and the secondary minerals. The lithium minerals are more abundant in the MP unit than in the LMP unit while the secondary minerals are more abundant in the LMP unit than in the MP unit. The other variation is the presence of accessory garnets in the LMP unit and none observed within the MP unit. The presence of garnets could be an indicator of a highly evolved or increased fractionation of the pegmatite melt.

The textural variation observed is the dominance of the coarse-grained and the graphic textures in the MP zone as compared to the LMP zone as observed from petrographic analyses. The LMP unit appears to be dominated by fine-grained and replacement textures as a result of intense alteration of feldspars within this unit as exhibited by most of the thin sections (Appendix A), particularly sample S015 (Figure 4.5).

CHAPTER 5: GEOCHEMISTRY

5.1. Introduction

The XRF analyses were undertaken using a Panalytical PW2404, X-Ray Fluorescence spectrometer housed at the Earth Laboratory at the Witwatersrand University. The analysis was conducted so as to further understand the genesis of Arcadia pegmatites, their emplacement environment, and the compositional variation of this suite of pegmatites. The Norrish Fusion [35] technique was used and the XRF samples for major oxide data were prepared and run using the standard guidelines and procedures outlined in the methodology by Wilson (2012). A carbon steel jaw crusher was used to crush the samples and they were then milled using a carbon-steel swing mill. The Johnson Matthey Spectroflux 105 was used to fuse the major elements at a temperature of 1100^0 C and in-house software was used for the correction of the raw data. The following primary International Reference Material, NIM series (South Africa) and the USGS series (USA) were used as standards for the calibration and to provide a control for the analytical instruments. The XRF analyses undertaken, provided data on the following major oxides, SiO_2, Al_2O_3, K_2O, Na_2O, CaO, Fe_2O_3, MnO, MgO, P_2O_5, TiO_2 and Cr_2O_3 and the results are presented in Table 5.1.

5.2. XRF Analysis

It can be observed that SiO_2 recorded the highest concentrations in all the analysed samples, with mean values ranging from 66.22 to 88.64wt%, followed by Al_2O_3 (6.56 to 20.69wt%), K_2O (0.05 to 9.04wt%), Na_2O (-0.03 to 9.21wt%), CaO (0.08 to 3.11wt%), Fe_2O_3 (0.30 to 1.36wt%). MnO, MgO, P_2O_5, TiO_2 and Cr_2O_3 recorded concentrations of less than 1wt%, while the loss on ignition (LOI) varies from 0.14 to 3.94wt% (Table 5.1).

The samples appear to be SiO_2-Al_2O_3 rich with sample S005 recording significant concentration for SiO_2 (88.64wt%), while the highest concentration value for Al_2O_3 (20.69wt%), was detected in sample S015. The same sample S015 also detected a significant concentration of MgO (0.48wt%) and a highest value of loss on ignition (LOI) of 3.94wt%. Sample S025 recorded the highest major oxide concentration for Na_2O (9.21wt %), and the same sample registered the lowest concentration for the major oxide K_2O (0.55wt%). Significant concentrations of the major oxide K_2O (9.04wt%) were detected in sample S031. The XRF results also showed sample S042 as having the highest concentration of the major oxide Fe_2O_3 (1.36wt%) and a low concentration of MgO (0.02wt %). Sample S001, recorded significant concentrations for the following major oxides; MnO (0.33wt%), P_2O_5 (0.19wt%), and TiO_2 (0.05wt%). The XRF results also indicated significant concentrations of SiO_2 and Al_2O_3 and low values for the major oxides MgO, Na_2O and K_2O for the following Li- bearing samples; S040, S016, PS1 and PS2 (Table 5.1). Sample S040 from the LMP unit which had accessory garnets recorded more Fe_2O_3 (0.48wt%) than MnO (0.12wt%) (Table 5.1).

Binary variation plots were constructed for the various major oxides against SiO_2 to determine their relationship with silica (Figure 5.1) and relevant ratios were also calculated in order to classify and geochemically characterise the Arcadia pegmatites. Some of the binary plots of the calculated oxide ratios were used to try and understand magma evolution and any magmatic processes such as fractional crystallisation, contamination and magma mixing that might have taken place resulting in any observed mineralogical or geochemical variation between the MP and LMP units (Table 5.2).

Table 5. 1: XRF Major Oxide Data

ZONE	wt%	SiO2	Al2O3	Fe2O3	MnO	MgO	CaO	Na2O	K2O	TiO2	P2O5	Cr2O3	NiO	LOI	Total
LMP	S020B	75.05	13.91	0.67	0.08	0.02	0.23	3.99	4.64	0.01	0.07	0.01	0.00	0.40	99.08
MP	S025	71.68	16.98	0.41	0.20	0.02	0.57	9.21	0.55	0.01	0.06	0.01	0.00	0.20	99.89
MP	S016	76.65	15.71	0.39	0.02	0.03	0.08	1.57	2.47	0.01	0.04	0.00	0.00	0.14	97.10
LMP	S009	74.50	13.40	0.49	0.04	0.19	3.11	4.82	1.86	0.01	0.03	0.00	0.00	1.29	99.74
LMP	S005	88.64	6.56	0.49	0.02	0.02	0.16	3.32	0.56	0.01	0.03	0.00	0.00	0.16	99.97
LMP	S001	81.43	10.26	0.91	0.33	0.03	1.09	2.79	1.20	0.05	0.19	0.00	0.00	0.82	99.10
MP	S021	79.76	11.33	0.49	0.13	0.01	0.11	2.76	4.69	0.02	0.07	0.01	0.00	0.29	99.65
MP	PS1	87.53	9.26	0.45	0.02	0.02	0.10	-0.03	0.05	0.01	0.01	0.00	0.00	0.26	97.67
MP	S032	69.98	18.24	0.49	0.11	0.02	0.53	6.66	2.80	0.00	0.07	0.00	0.00	0.23	99.13
MP	S034	73.74	15.44	0.47	0.17	0.01	0.37	6.70	2.66	0.01	0.08	0.00	0.00	0.15	99.79
LMP	S040	77.39	15.66	0.48	0.12	0.05	0.33	0.49	0.94	0.01	0.02	0.01	0.00	0.98	96.47
LMP	S015	66.22	20.69	0.30	0.13	0.48	0.71	5.20	0.21	0.01	0.04	0.00	0.00	3.94	97.94
LMP	S042	82.94	10.45	1.36	0.09	0.02	0.22	2.99	1.53	0.02	0.04	0.00	0.00	0.62	100.29
MP	PS2	73.81	17.50	0.44	0.30	0.11	0.78	0.44	0.25	0.01	0.02	0.00	0.00	2.73	96.38
MP	S031	70.41	16.07	0.33	0.02	0.02	0.12	2.92	9.04	0.01	0.12	0.01	0.00	0.23	99.30

5.3: Discussion

Binary plots

The binary plots of the major oxides Al_2O_3, Na_2O, K_2O, MgO, CaO, MnO and P_2O_5 exhibited a negative correlation with SiO_2, while Fe_2O_3 and TiO_2, showed a positive correlation, suggesting the compatibility of these two oxides with silica (Figure 5.1). MgO, CaO and TiO_2 did not show a linear trend with silica, but rather exhibited clustering of samples horizontally revealing the abundance of silica. The binary plot of Al_2O_3 vs SiO_2, revealed a better linear trend than all the oxides, even though the two oxides showed a negative correlation, with Al_2O_3 recording the highest correlation coefficient value out of all the oxides (Al_2O_3, R^2-0.892). The binary plots for Na_2O, K_2O, MnO and P_2O_5 exhibited a similar trend that was characterised by scattered sample points spreading upwards and showing a negative correlation with silica (SiO_2) (Figure 5.1). The negative correlation is an indication of a non -association with silica, while a positive correlation reveals an association with silica (SiO_2), this therefore implies, as stated earlier, that only Fe_2O_3 and TiO_2 have some association with silica, but a weak one as revealed by their low correlation coefficient values with silica (Fe_2O_3, R^2-0.1847) (TiO_2, R^2-0.1242) (Figure 5.1).

The binary plot of Na_2O/ Al_2O_3 against K_2O/ Al_2O_3 (Figure 5.2), revealed the samples plotting in both the igneous and the sedimentary/metasedimentary regions, with the majority of the samples plotting within the igneous region and the four samples with significant concentrations of lithium minerals plotting within the sedimentary/metasedimentary region. The plotting of the samples within these two different regions suggests a mixed source for the materials making up the protolith from which the pegmatites were partially melted. This analysis is supported by Obasi and Madukwe (2016), who confirm the existence of a mixed plutonic source for some pegmatitic melts. The binary plot of Na_2O+K_2O-CaO vs SiO_2 (Figure 5.3) revealed scattered plots, and such spread of data is consistent with the pegmatite being derived from an S-type granite, or from partial melting a metapelite.

Major Oxide Calculated Ratios

The ratio values for Na_2O/K_2O range from -0.60-24.76, with sample PS1 having the lowest ratio value of -0.61 and sample S015 registering a high ratio value of 24.76 (Table 5.2). According to Pettijohn, et al., (1987), the ratio values of Na_2O/K_2O can be used to establish if the magma was extremely fractionated or not and the results from Table 5.2 generally exhibit low ratio values for Na_2O/K_2O with the exception of S025 and S015, indicating that the magma for this suite of pegmatites was highly evolved or extremely fractionated. The ratio values for $Na_2O+ K_2O+ CaO/ Al_2O_3$ appear to be less than unity ranging between 0.01-0.75 (Table 5.2) and according to Pearce et al., (1984), if this ratio value is less than 1, it implies that the rocks are peraluminous. The alumina (Al_2O_3) value for individual samples appears to be higher than the sum of the total alkali $Na_2O+ K_2O+ CaO$, which according to Obasi and Madukwe (2016), suggests that the pegmatites were derived from a parent S-type granite, or from another source, such as partial melting of a metapelite. The ratio values of Na_2O/ Al_2O_3 and K_2O/ Al_2O_3 appear to be low ranging between 0-0.54 and 0.01-0.56 respectively. These low ratio values also point to the abundance of alumina which further confirms the peraluminous character of the Arcadia rocks.

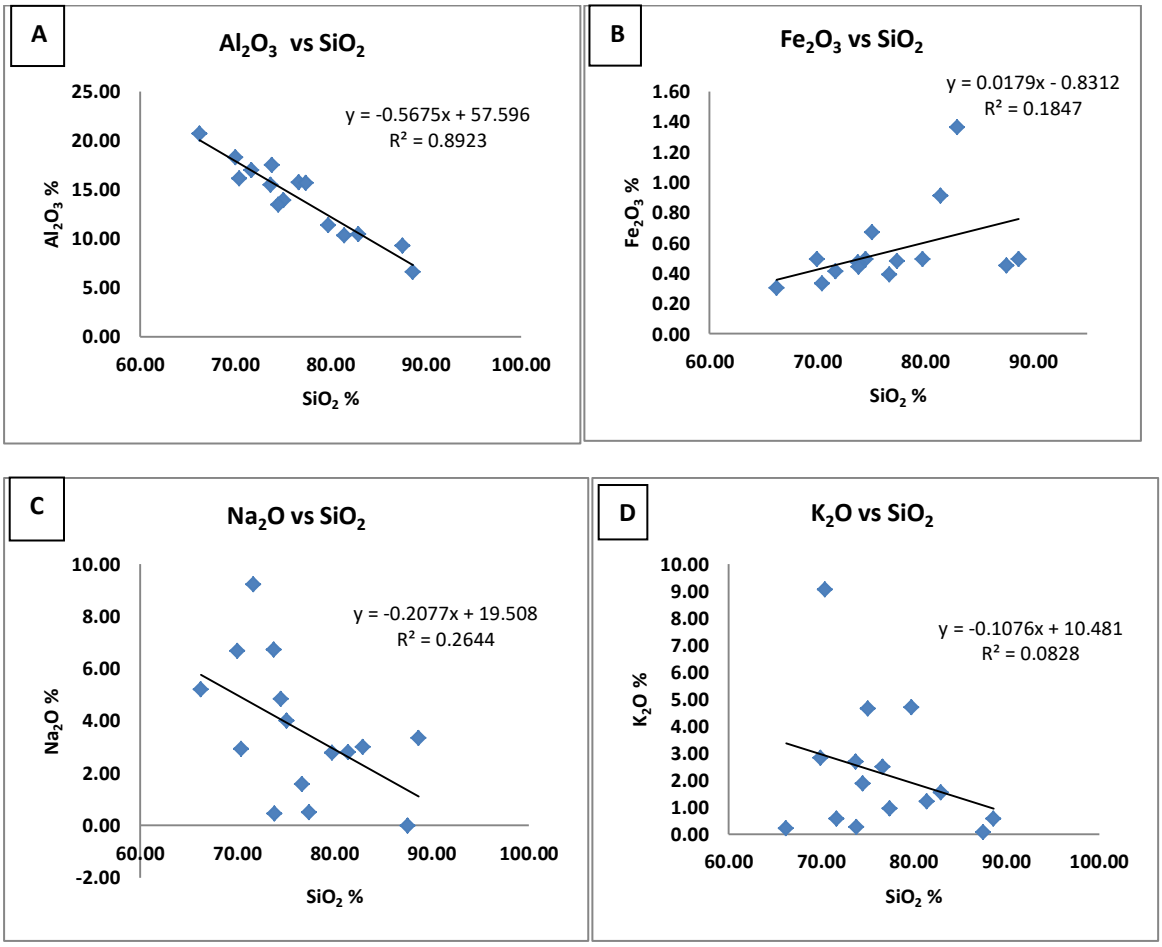

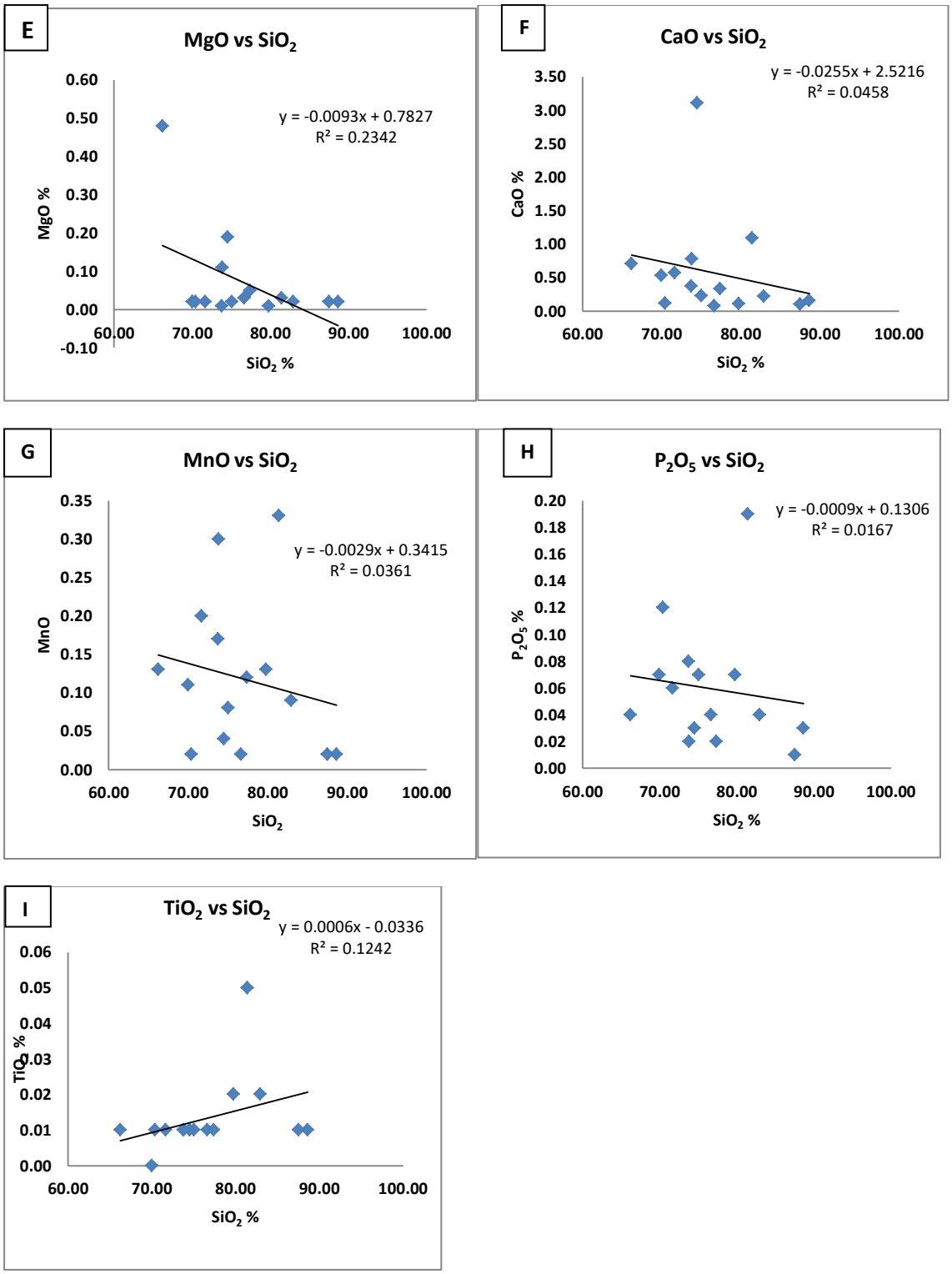

Figure 5. 1: Binary variation plots for the major oxides vs Silica (SiO_2). (A). Al_2O_3 vs SiO_2, showing a linear trend however with a negative correlation with SiO_2 (B). Fe_2O_3 vs SiO_2 showing a weak positive correlation with SiO_2. (C). Na_2O vs SiO_2, showing a negative correlation with SiO_2. (D) K_2O vs SiO_2, showing a negative correlation with SiO_2. (E). MgO vs SiO_2, showing a negative correlation with SiO_2 and the points are clustered and not scattered (F). CaO vs SiO_2, showing a negative correlation with SiO_2 with clustered points (G). MnO vs SiO_2, showing a negative correlation with SiO_2. (H). P_2O_5 vs SiO_2 showing a negative correlation with SiO_2. (I) TiO_2 vs SiO_2 showing a positive correlation with SiO_2.

Table 5. 2: Calculated Major Oxide Ratios

Zone	wt%	SiO2	Al2O3	Na2O	K2O	CaO	Na2O+K2O+CaO	Na2O+K2O+CaO/Al2O3	Na2O+K2O-CaO	Na2O/K2O	Na2O/Al2O3	K2O/Al2O3
LMP	S020B	75.05	13.91	3.99	4.64	0.23	8.86	0.64	8.40	0.86	0.29	0.33
MP	S025	71.68	16.98	9.21	0.55	0.57	10.33	0.61	9.19	16.75	0.54	0.03
MP	S016	76.65	15.71	1.57	2.47	0.08	4.12	0.26	3.96	0.64	0.10	0.16
LMP	S009	74.50	13.40	4.82	1.86	3.11	9.79	0.73	3.57	2.59	0.36	0.14
LMP	S005	88.64	6.56	3.32	0.56	0.16	4.04	0.62	3.72	5.93	0.51	0.09
LMP	S001	81.43	10.26	2.79	1.20	1.09	5.08	0.50	2.90	2.33	0.27	0.12
MP	S021	79.76	11.33	2.76	4.69	0.11	7.56	0.67	7.34	0.59	0.24	0.41
MP	PS1	87.53	9.26	-0.03	0.05	0.10	0.12	0.01	-0.08	-0.60	0.00	0.01
MP	S032	69.98	18.24	6.66	2.80	0.53	9.99	0.55	8.93	2.38	0.37	0.15
MP	S034	73.74	15.44	6.70	2.66	0.37	9.73	0.63	8.99	2.52	0.43	0.17
LMP	S040	77.39	15.66	0.49	0.94	0.33	1.76	0.11	1.10	0.52	0.03	0.06
LMP	S015	66.22	20.69	5.20	0.21	0.71	6.12	0.30	4.70	24.76	0.25	0.01
LMP	S042	82.94	10.45	2.99	1.53	0.22	4.74	0.45	4.30	1.95	0.29	0.15
MP	PS2	73.81	17.50	0.44	0.25	0.78	1.47	0.08	-0.09	1.76	0.03	0.01
MP	S031	70.41	16.07	2.92	9.04	0.12	12.08	0.75	11.84	0.32	0.18	0.56

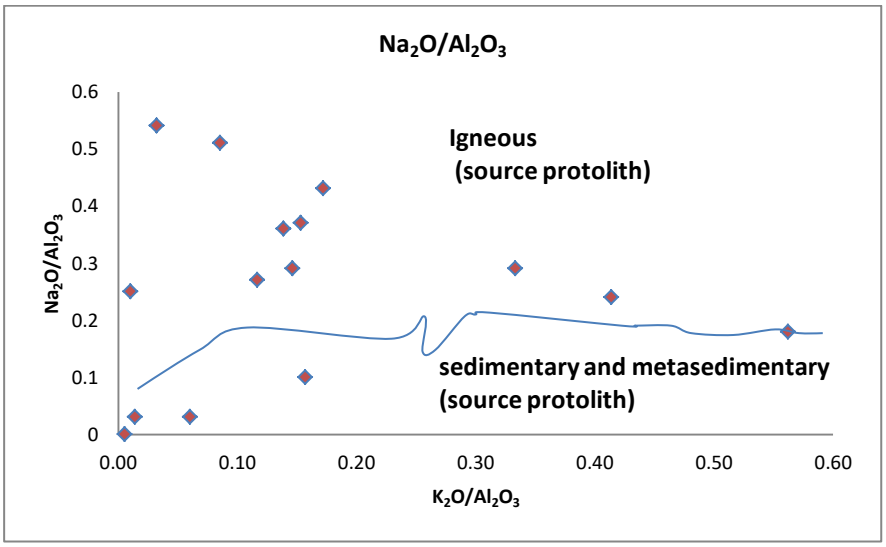

Figure 5. 2: Geochemical classification graph; Na_2O/ Al_2O_3 vs K_2O/Al_2O_3 (After Garrels and Mckenzie, 1971)

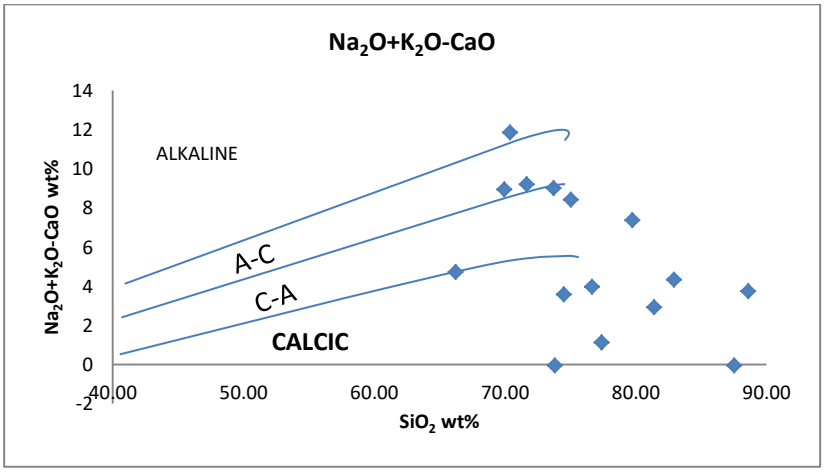

Figure 5. 3: Na_2O+K_2O-CaO vs. SiO_2: Classification of Arcadia pegmatite suite, A-C (Alkali-Calcic); C-A (Calcic-Alkali). Source: After Frost et al (2001).

5.4. Conclusion

From the above discussion, it can be concluded that the majority of the major oxides show a non-association with silica except for Fe_2O_3 and TiO_2, which showed a weak association with silica. It can also be concluded that the Arcadia pegmatites are highly evolved and peraluminous in nature as confirmed by the calculated low ratio values of Na_2O/K_2O, the abundance of alumina (Al_2O_3) and the abundance of silica which for the 13 samples out of 15 appeared to be greater than 70wt%. According to Frost et al (2001), a rock with silica > 70wt% is peraluminous in nature. It can also be concluded that the material that makes up the magma from which these pegmatites were formed is from mixed sources. The MP and the LMP units do not show any significant geochemical variation other than the slight variations in the significant concentrations of CaO (3.11wt%), MgO (0.48wt%), P_2O_5 (0.19wt%) and TiO_2 (0.05wt%) in the LMP unit as compared to the MP unit (Table 5.1). The geochemical classification of the samples revealed the majority of the analysed samples from both units as calcic-rich (Figure 5.3). The LOI values that varied between 0.14 to 3.94wt% are an indication of the presence of fluxing and volatile components which are critical in the development of the observed pegmatitic textures (London, 2005). According to Thomas et al., (2012), Martin and De Vito (2009), Nabelek et al., (2009) and London (2005), volatiles and fluxing components play a vital role in lowering the liquidus temperature of the pegmatite forming melts. Water is key in pegmatite petrogenesis as it promotes rapid growth of large crystals and controls rapid supraliquidas emplacement. Water drastically diminishes the rate of nucleation by undercooling the melt so that the few nuclei eventually grow into large crystals.

CHAPTER 6: DISCUSSIONS AND CONCLUSIONS

6.1. Overview

Fieldwork

The fieldwork revealed the Arcadia suite of pegmatites as enriched in the lithium-bearing minerals petalite and spodumene, with petalite in higher abundance than spodumene. The rock-forming minerals present included albite, quartz, K-feldspar and muscovite. The above mentioned minerals exhibited different textures such as coarse-grained, brecciated, aplitic, medium to fine-grained, graphic, replacement and radial textures. Irregular patchy concentric internal zonation of the pegmatites was observed on the exposed MP unit in the pit. The zonation is characterised by a textural and a mineralogical phase change and the zones are demarcated by sharp contacts. The coarse-grained intermediate zone appeared to be the most visible zone within the MP unit in the pit, although it appeared patchy and irregular hosting the lithium mineralisation. The aplitic zone could also be identified, occurring sporadically and also in patches, being characterised by the fine-grained aplitic texture, yet devoid of lithium mineralisation. The core zone, enriched in the coarse-grained quartz and poorly mineralised, was only visible on some sections of the core and not in the pit. According to Simmons and Webber (2008), the observed textural characteristics of many pegmatites is as a result of strong undercooling.

Deformation and metamorphism were also observed and were characterised by a series of parallel normal faults and mineral lineation of feldspars plunging northeast. The faults might have acted as conduits to the mineralising fluids or the hydrothermal fluids that resulted in the observed alteration of feldspars, petalite and spodumene.

Petrography

Petrographic analysis was useful in establishing the textural and mineralogical variations that exist between the MP and the LMP pegmatite units. The analysis indicated the presence of two mineralisation phases, one characterised by the presence of primary magmatic minerals, and the second characterised by alteration products of the primary mineral phases. The dominant alterations comprised the hydrothermal alteration of petalite and that of the feldspars, of which the secondary minerals were identified by XRD. Petalite alteration involved, (1) the alteration of primary magmatic petalite and spodumene to secondary petalite and to spodumene intergrown with quartz (SQI) and albite and; (2) the alteration of the primary magmatic petalite and spodumene to eucryptite and bikitaite, and these secondary minerals seemed to be in high abundance in the highly altered sample S015 of the LMP unit (Figure 4.5 and Table 4.1). Calcite, smectite and stilbite are all products of the hydrothermal alteration of plagioclase feldspars and these minerals also are associated with the second mineralisation phase. Another observed mineralogical variation between the two units was the presence of the accessory disseminated euhedral garnets which were only observed in the LMP unit sample S040 (Figure 4.1). The presence of garnet is very crucial in understanding the evolutionary path of the pegmatitic melt. It appears the garnets might have crystallised earlier within the country rocks and were incorporated into the pegmatites as xenoliths.

The garnets are also a good indicator of the degree of fractionation of the magma of which in this case their presence is an indication of highly evolved or extremely fractionated peraluminous pegmatites. This analysis is further confirmed by Clemence and Wall (1981), who stated that the observed accessory garnets could be a product of the early magma crystallisation of peraluminous, evolved magmas of the host rock at medium pressure. The secondary petalite observed as the deep-pink coloured mineral in hand specimen and from core appears to occur in both units, but is present in significant concentration within the MP unit as observed from the logging of core and petrographic analysis.

The textural variation observed from the petrographic analysis between the two units was the dominant presence of the coarse-grained texture in the MP unit as a result of the primary mineral phases, while the fine-grained and replacement textures were common in the LMP unit as a result of intense hydrothermal alteration.

XRD Rietveld Analysis

The ability of the XRD Rietveld method to directly identify and quantify both primary and secondary mineral phases assisted in confirming the two modes of mineralisation that characterise the Arcadia pegmatites. The first phase is characterised by the primary magmatic crystallisation of petalite and spodumene, and the second phase is characterised by the alteration products of the primary mineral phases that include eucryptite, bikitaite and SQI. The XRD analysis was also very useful in giving the actual abundances of both primary and secondary lithium mineral phases that characterise both the MP and the LMP units, thus confirming the overall abundance of petalite and spodumene in the MP unit, and the abundance of the secondary lithium mineral phases, eucryptite and bikitaite in the LMP unit (Table 4.1).

Whole Rock geochemistry

The XRF major oxide data was useful in the classification of the pegmatites and in understanding the magmatic processes that characterise this deposit. It was also useful in corroborating the XRD results. An example on the corroborative aspect of the XRF technique is observed on the results of sample S042, which registered significant concentrations of the major oxide Fe_2O_3 (1.36wt%) and a low concentration of MgO (0.02wt %) (Table 5.1), which is characteristic of siderophyllite that was detected in significant amounts of 4.2 % for sample S042 by the XRD (Table 4.1). The XRF analysis also confirmed the presence of the rare lithium-phosphate mineral, amblygonite-montebrasite in significant concentrations in sample S001 by registering a high concentration value of (0.19wt%) for the major oxide P_2O_5, which is characteristic of this mineral series. This result corroborates the XRD results in which the mineral amblygonite-montebrasite was detected in significant concentrations of 2.1wt% in sample S001. The highly altered sample S015, had the highest concentration of Al_2O_3, thus confirming the presence of the alteration products smectite, stilbite, bikitaite and eucryptite which have significant alumina in their chemical composition. The high loss on ignition of 3.94wt% exhibited by the same sample S015 is an indication of the presence of hydrothermal alteration, which was also visible in the petrographic analysis of this section. Sample S040 from the LMP unit with the observed accessory garnets registered a higher iron content (0.48wt%) than MnO (0.12wt%), suggesting that the garnets are almandine-spessartine in nature. Cerny (1998) and Selway et al (2005) indicated that within an individual pegmatite, garnets with more Fe content than Mn often occur in contact and wall zones, while garnets with Fe almost equal to Mn occur in

intermediate mineral assemblages and the Mn-rich garnets often occur within the inner and replacement zones. In the case of Arcadia, the Fe-rich garnets appear to occur within the contact zones which are aplitic in nature.

The major oxide data revealed a wide compositional range for the Arcadia pegmatites, which appeared to be silica (SiO_2) and alumina (Al_2O_3) rich, which is characteristic of peraluminous rocks. The binary plots for most of the oxides exhibited a non-compatible relationship with silica. The graph of Na_2O/Al_2O vs K_2O/Al_2O indicated a mixed source (igneous/sedimentary) for the protolith material for this suite of pegmatites. The geochemical classification of this suite of rocks revealed the majority of the samples from both the MP and the LMP units as calcic-rich (Figure 5.3).

There is no significant geochemical variation between the MP and the LMP other than the significant abundances of the following major oxides within the LMP unit as compared to the MP unit: CaO, MgO, P_2O_5 and TiO_2. The samples from both units seem to show similar geochemical trends that plotted within the same regions and showing similar trends as portrayed in the binary plots.

Paragenetic Sequence

From the petrographic analysis and XRD, two phases of mineralisation characterise the Arcadia pegmatites.

1. The first phase is characterised by the primary magmatic crystallisation of petalite and spodumene.
2. The second phase is characterised by the hydrothermal alteration of the primary mineral phases, petalite and spodumene producing eucryptite, bikitaite and SQI.

Finally, hydrothermal alteration of plagioclase feldspar, which is still part of the second mineralisation phase occurred and it produced the secondary mineral phases; calcite, smectite and stilbite. The accessory garnets observed are interpreted to be products of early magma crystallisation of the evolved peraluminous magma (possibly an S-type granite), and could have been incorporated as xenoliths in the pegmatites. Pollucite ($CsAlSi_2O_6$) was detected in one sample (S015), which is highly altered, and this mineral according to London (2019), crystallises as one of the latest primary mineral phases in the extreme fractionation of LCT pegmatites, or as a product of later hydrothermal alteration (albitisation) of the primary mineral phases. Minerals of the amblygonite-montebrasite series (Li- phosphate), usually occur in the inner zone associated with spodumene or associated with quartz in the quartz-rich core in zoned complex LCT pegmatites (London and Burt 1981). It therefore qualifies as a primary magmatic mineral phase although it is very sensitive to its physico-chemical environment and quickly gets metasomatised to secondary amblygonite-montebrasite by residual metamorphic fluids, and sometimes occurs as inclusions within albite, lepidolite, pollucite and elbaite (London and Burt, 1981). Below is a paragenetic sequence of the Arcadia pegmatite Table 6.1.

Table 6. 1: Paragenetic sequence for the Arcadia pegmatites.

Mineral	Early Magmatic crystallisation	Late crystallisation stage (Vein & alteration)	Late Alteration (Hydrothermal)
Quartz			
Microcline			
Albite			
Siderophyllite			
Petalite			
Spodumene			
Eucryptite			
Bikitaite			
SQI			
Amblygonite- montebrasite			
Garnet			
Pollucite			
Smectite			
Stilbite			
Calcite			
		Key-	primary phase
			secondary phase

6.2: Various Theories on the genesis of pegmatites.

Two models have been used to describe pegmatite formation that is either as products of extended fractional crystallisation of granitic magmas or as products of partial melting of rocks (anatexis) (London, 2005; Martin and De Vito, 2005). According to Simmons and Webber (2008), there is no universally accepted model for pegmatite genesis that satisfactorily explains all various aspects of granitic pegmatites.

6.2.1. Pegmatites formed by fractional crystallisation

Most researchers favour the formation of pegmatites from the fractional crystallisation of residual melts of granitic plutons. The fractional crystallisation model which supports rare-earth element enrichment of pegmatites by differentiation of fertile granites suggests concentration of volatiles and rare elements in pools of residual melts during consolidation of granitic plutons (Cerny, 1991). According to Cerny (1991), the fractional crystallisation model is supported by; the physical links observed between the mineralised pegmatites and their plutonic parents; the continuous

mineralogical, textural and geochemical evolution from the parent granites to the associated pegmatites; the similarity between the late crystallising pegmatite pods trapped in parent granites and the exterior pegmatites in metamorphic roofs of the same granites and the bulk compositions of the rare element pegmatites corresponding to the experimental minima in granite systems modified by accumulation of fluxes such as water, lithium, boron, fluorine and phosphorus. According to Martin and De Vito (2005), the evolved felsic magmas from plutonic rocks undergoing fractionation are found in two distinct settings. The first is associated with orogenic magmas where there is crustal shortening, collision and subduction, while the second one is associated with anorogenic magmas characterised by rifting and crustal attenuation.

6.2.2. Pegmatites formed by anatexis

According to Simmons and Webber (2008), pegmatites can form from the low-degree partial melts produced around plutons in orogenic settings. Metasedimentary rocks containing evaporites provide a source of fluxing components of incompatible elements such as lithium and boron. In collisional tectonic settings, a sedimentary volcanic sequence contains incompatible elements and fluxing components that can ultimately end up in a granitic melt, which can undergo fractional crystallisation to form a pegmatite, and the same incompatible elements and fluxing components can be preferentially partitioned into a low-degree partial melt that can directly form a pegmatite. The evidence in support of the anatexis model is presented by London (2005), who outlined it as follows; (1) The challenge of relating highly evolved magmas to the comparatively primitive chemistry of the possible plutonic sources; (2) The tendency for some pegmatite groups to mirror compositions of their host rocks with respect to major elements and, (3) The common isolation of thin pegmatite dykes from any known plutonic source. Nabelek et al., (2009), Simmons and Webber (2008), Martin and De Vito (2005), amongst others have presented classic cases of anatectic pegmatites derived from both crustal and mantle rocks. The authors further state that many batches of anatectic melts can coalesce to form a pluton-size mass of magma.

The anatexis model appears to have been the process that ultimately produced the source of magma for the Arcadia pegmatites. The possible source rocks which were partially melted to form the pematitic melt, could have been the Chinyika tonalities and the Chishawasha granodiorite (Prospect Resources, 2017).

6.3. Geological and Tectonic settings of pegmatites

Structural controls and large geological settings have changed during crustal evolution (Cerny, 1991). In the late Archean, pegmatite fields appear confined to mobile sedimentary troughs, within and around the margins of the greenstone terranes as well as along the lithologic boundaries, especially the batholithic contacts (Cerny, 1991). On the other hand, the Phanerozoic pegmatite population tends to be confined to the fertile granites within linear orogens of the Alpine or Appalachian type (Cerny, 1991). The lithologic environment for pegmatite fields in Archean greenstone terranes is characterised by a volcanic or sedimentary sequence (Superior Province), while the Phanerozoic pegmatite fields have a lithologic environment characterised by metasedimentary rocks or remobilised segments of older crystalline terranes that have been penetrated by numerous granitoid plutons under both retrograde and prograde conditions.

The rare-element pegmatite fields of Arcadia lie within the Archean greenstone belts (HGB), which has been intruded by various granitoids and whose lithologic environment is characterised by a

volcanic sedimentary to metasedimentary sequence (Figure 2.2 and Figure 2.5). According to Martin and De Vito (2005), the tectonic setting ultimately affects the pattern of enrichment in most pegmatites. In the case of Arcadia, the regional deformation and metamorphism that occurred was a key factor in creating the conduits which enhanced the mineral enrichment of the pegmatites.

6.4: Economic Mineralisation Processes of the Arcadia Pegmatites

According to Thomas and Davidson (2012), this observation of significant concentrations of silica and alumina is expected in economic pegmatites, whereby high concentrations of alkalis in pegmatitic fluids tend to increase the solubility of Si and Al, thus increasing the capacity of the pegmatites to sequester significant concentrations of rare elements and in some instances to economic concentration of which, the Li mineralisation in Arcadia pegmatites is interpreted to have been the result of these processes. The volatiles were also key in the mobilisation of the incompatible elements which constituted the ore and in the hydrothermal alteration processes which gave rise to the observed second phase of mineralisation at Arcadia.

6.5. Exploration for LCT pegmatites

The exploration techniques that can be adopted for rare-element LCT pegmatites at Arcadia, entail reconnaissance exploration, involving the regional mapping of pegmatite dykes that cut across the various granitic plutons and evaluating their mineralisation potential. The exploration should also include examining the regional zoning of fertile granitic plutons that intrude the Harare Greenstone Belt. According to Selway et al, (2005), the degree of fractionation and rare-element content of pegmatite dykes increases with increasing distance from their fertile parent granite hence the need to target these dykes regionally and then locally. The authors further indicate that fertile granites have rare-element contents at least three times that of an average upper continental crust, that can be determined from the whole rock compositions and the compositions of K-feldspar and muscovite (Selway et al., 2005). Cerny (1991) also adds that fertile granites, exposed, or hidden, represent the origin of more or less zoned concentric to unidirectional pegmatite groups. The other exploration target would be pegmatites associated with rare-element enriched metasomatised host rocks (Selway et al., 2005). Primary dispersion haloes or metasomatic aureoles in country rocks can also be examined using the whole rock analysis tool for rare-element content, since the rare-element enriched pegmatite fluid intrudes the country rock and alters its composition. The hidden or blind pegmatites can also be detected from whole rock analysis of metasomatised host rocks. Secondary dispersion haloes within the overburden and stream sediment sampling of both heavy and light minerals (e.g. spodumene, tantalite-columbite, beryl, tourmaline) may also be used in identifying target areas, both regionally and locally (Sinclair, 1996). Generally, an understanding of the internal zoning of pegmatites is a useful key tool in the exploration of granitic pegmatites and their mineralisation potential.

Geophysical methods such as regional and local radiometric and gravity surveys are critical in identifying parent granites associated with pegmatites. Radiometric survey will be used to identify parent granites associated with pegmatites enriched with the radioactive elements, thorium and uranium, while the gravity survey may be used to delineate pegmatites from their host rocks using the density contrast aspect (Sinclair, 1996).

6.6: Conclusions

From the above discussions it can be concluded that two phases of mineralisation characterise the Arcadia pegmatites, and the first phase being the early primary magmatic crystallisation of petalite and spodumene, and the second phase which comprises alteration products of petalite and spodumene, namely eucryptite, bikitaite and SQI. The hydrothermal alteration process that constitutes the second phase of mineralisation resulted in the enrichment of the pegmatites with incompatible elements of economic interest. The peraluminous nature of the Arcadia pegmatites was confirmed by the geochemical data and the calculated ratio data which revealed the abundance of alumina and silica, which is characteristic of peraluminous rocks. The Arcadia pegmatites crystallised from a highly evolved magma which was extremely fractionated and this was confirmed by the presence of the accessory garnets whose presence indicates extreme fractionation of peraluminous magmas. This is further confirmed by the presence of the observed graphic textures, which according to Cerny et al (1991) are common in highly evolved granites and pegmatites. It can also be concluded from the geochemical classification of rocks that the Arcadia pegmatites are calcic-rich.

There is no significant mineralogical and geochemical variation between the Main Pegmatite zone (MP) and the Lower Main Zone (LMP), other than slight variations, such as the high abundance of lithium minerals petalite and spodumene in the MP unit as compared to the LMP unit, and the presence of accessory garnets and abundance of secondary minerals in the LMP zone. There were textural differences observed between the two units, with the MP unit exhibiting coarse-grained and graphic textures, while the LMP unit was dominated by aplitic, fine-grained and replacement textures. The slight variations observed between the MP and the LMP units, is an indication that the magma that gave rise to this suite of pegmatites was the same, although the protolith might have been from a mixed igneous/sedimentary source. Moreover, from the above discussions it is also apparent that the pegmatites were formed from one magmatic intrusive event, but underwent complex internal crystallisation that resulted in the observed variable grain sizes and mineral assemblages making up the pegmatite zones within the Arcadia pegmatites.

It can also be concluded that the deep-pink coloured mineral is secondary petalite from the alteration of primary petalite, as confirmed by the petrographic analysis. The secondary petalite is present in both the MP and the LMP units, although it appears more abundant in the MP unit where it occurs adjacent to the primary grey petalite.

6.7. Recommendations

The author recommends sampling of possible source rocks in addition to pegmatites and conducting a detailed geochemical analysis using the electron microprobe, in order to understand the mineral chemistry of feldspars and muscovite, which are key in understanding the pegmatite body evolution. The immobile trace element ratios obtained from the geochemical analysis results will also further assist in understanding the genetic affiliation of the Main Pegmatite zone (MP) and the Lower Main Pegmatite Zone (LMP). It is also recommended that more geochemical tests be conducted to provide a detailed mineral chemistry of the pink-coloured petalite. Research exploration geochemistry on pollucite is also recommended to further understand its mineral chemistry and occurrence, as well as find out if the mineral has the potential of becoming a mineable economic ore deposit in the future.

References

Baglow, N., 1993. Bindura 1:100 000 Geological Map. Geological Survey of Zimbabwe.

Baldock, J.W., Styles, M.T., Kalbskopf, S., Muchemwa, E. (1991). The bulletin of the Harare Greenstone Belt and the surrounding granitic terrane. Zimbabwe Geol. Surv.Bull., 94, pp. 222.

Barber, B., (2016). Overview of Tantalum-Niobium Mineralisation in Zimbabwe. Available at; www.geologicalsociety.org.zw. Accessed on the 2nd of February 2020.

Bohlsen, M., (2019).Lithium Miners news for the Month of December 2019.Available at; https://seekingalpha.com/article/4314058-lithium-miners-news-for-month-of-december-2019. Accessed on the 4th of April 2020.

Bruker Designs, (2006). Quantitative analysis of geological samples. Combined XRD and XRF analysis Bruker AXH GMBH, Karlsruhe, Germany.

Cerny, P., (1991). Rare-element granitic pegmatites. Part 1: Anatomy and internal evolution of pegmatitic deposits. Geoscience Canada.

Cerny, P., (1998). The classification of granitic pegmatites revisited. Geoscience Canada.

Charoy, B., Noronha, F., and Lima, A., (2001). Spodumene- petalite-eucryptite. Mutual Relationships and patterns of alteration in Li-rich aplite pegmatite dykes from northern Portugal: Canadian Mineralogist, v. 39, p. 729-746.

Cooper, D.G. 1964. The Geology of the Bikita pegmatite. In The Geology of Some Ore Deposits in Southern Africa (S.H. Haughton, ed) Geol.Soc.S.Af. Monogr.**2,** pp 441-462.

Dittrich, T., Seifert, T., Schulz, B., Pfander, J.A., Gerdes, A, (2017). Formation of LCT Pegmatites in Archaean Cratons: Constraints from $_{40}Ar/_{39}Ar$ mica, U-Th-Pb monazite and U-Pb tantalite/ columbite dating.

Djerdj, I. (2019). Rietveld Refinement in the characterization of Crystalline Materials- MDPI.

Forster, J. (2011). A Lithium Shortage: Aare Electric Vehicles under Threat. Energy Economics and Policy Lecture.

Fossen, H. (2016). Structural geology (2nd Edition). Cambridge University Press, Cambridge. Hardback, 524pp.

Frost, B.R., Barnes, C.G. & Collins, W.J. (2001). A geochemical classification for granitic rocks. Journal of Petrology, 42 (11) 2033-2048.

Garrels, R. M. & McKenzie, F.F. (1971): Evolution of Sedimentary Rocks. WM Norton and Co., New York, p 394.

Geological Society of Zimbabwe (1990). Bulletin **94**. Harare- Shamva-Bindura greenstone belt.

Ginzburg, A. I and Gushchina, N.S. (1954). Petalite from pegmatite of eastern Transbaikalia.Trudy Miner. Museum Acad. Sci. USSR 6.71-85; Russia. (Chemical Abstracts, 51, #4223, 1957).

Hornung, G, and von Knorring, O. (1962). The pegmatites of the North Mtoko region. Southern Rhodesia. Translations of the Geological Society of South Africa, 65, 153-180.

Hurlbut, C.S., Jr. (1957) Bikitaite, LiAlSi2O6.H2O. a new mineral from Southern Rhodesia. Am. Mineral.**42**, 792-797.

London, D. (2019). Reading Pegmatites: Part 5- What Pollucite Says. Rocks and Minerals. Volume **94:5,** p420-427.

London, D. 2008. Pegmatite Deposits. The Canadian Mineralogist, Special Publication 10.

London, D. 2005. Granitic pegmatites. An assessment of current concepts and directions for the future. *Lithos,* vol. 81, p281-303.

London, D., and Burt, D.M., (1981a). Lithium aluminosilicate occurrences in pegmatites and the lithium aluminosilicate phase diagram. (Manuscript submitted to American Mineralogist).

Longstaffe, F.J. (1982). Stable isotope in the granite pegmatite and related rocks. Mineral Association of Canada. Short course Handbook. Vol.6. 373-404.

Mamuse, A.1999. Geological, geochemical and petrogenetic features of tantalum pegmatites: A study of the Benson Mine area (NE Zimbabwe) and implications for tantalum exploration. Unpubl. Hons thesis, pp 1-43.

Martin, F.R and De Vito, C. 2005. The patterns of enrichment in felsic pegmatites ultimately depend on tectonic setting. The Canadian Mineralogist, vol. 43, no. 6, p. 2027-2048.

Middlemost. E.A.K. (1985). Magmas and Magmatic Rocks. An Introduction to Igneous Petrology. 226pp. London, New York: Longman.

MSA Group Services (Pty) Ltd, (2017). Prospect Resources- Petrography of Arcadia's lithium bearing pegmatite addendum. Zimbabwe.

Mugumbate, F., Oesterlen, P.M., Masiyambiri, S., Dube, W. 2001. Industrial Minerals and Rock Deposits of Zimbabwe. Zim. Geol.Surv. Mineral Resources Series No.**27**, pp.100-109.

Nabelek, P.I., Whittington, A.G. and Siberscu, M.C. 2009. The role of H2O in rapid emplacement and crystallisation of granite pegmatites. Resolving the paradox of large crystals in highly undercooled melts. *Contribution to Mineralogy and Petrology*. Springer –Verlag. 12p.

Obasi, R.A and Madukwe, H. (2016). Geochemistry Classification Characteristics of Pegmatites from Ijero-Ekiti, Ekiti-State, Southwest Nigeria. International Research Journal of Natural Sciences. Vol. 4, No. 4, pp. 1-18.

Peacock, M. A. (1931). Classification of Igneous series. Journal of Geology, **39**, 54-67.

Pearce, T.H., Harris, N.B.W. & Tindle, A.G. (1984). Trace element discrimination diagrams for the tectonic interpretation of granitic rocks. Journal of Petrology, **25**,956-983.

Pettijohn, F. J, Potter, P.E. and Siever, R. (1987). Sand and Sandstone. Springer- Verlag Publication, New York Vol. **6**. 926p.

Premier African Minerals Ltd Report (2016).Available at, http://www.premierafricanminerals.com.Accessed on the 4th of February 2020.

Prospect Resources Ltd Report (2017). Available at, https://www.prospectresources.com.au/projects/arcadia-lithium-project.Accessed on the 31st of March 2019.

Rijks, H.R.P., and van der Veen, A.H. (1972). The geology of the tin-bearing pegmatites in the eastern part of the Kamativi district. Rhodesia Mineral Deposita, **7**, 383-395.

Rietveld, H.M. (1969). A profile refinement method for nuclear and magnetic structures. Journal of Applied Crystallography 2 (2), 65-71. Iucr.org.

Selway, J.B., Breaks, F.W. and Tindle, A.G. 2005. A review of rare element (Li-Cs-Ta) pegmatite exploration techniques for the Superior Province, Canada and Large Worldwide Tantalum Deposits. *Exploration and Mining Geology*, vol. 14, no. 1-4, p. 1-30.

Simmons, W.B. and Webber, K.L. 2008. Pegmatite genesis. State of the art. *European Journal of Mineralogy,* vol.20, no. 4, p. 421-438.

Sinclair, W.O. 1996. Granitic Pegmatites. In: Canadian Mineral Deposit types (ed). O.E. Eckstrand, W.O. Sinclair, and R.I. Thorpe. Geological Survey of Canada. Geology of Canada. no 8, p. 503-512.

Thomas, R, Davidson, P and Baulern, H. (2012). Competing models for the origin and internal evolution of granitic pegmatites in the light of melt and fluid inclusion research. *Minerology and Petrology*. Springer Verlag, vol **106**, p 55-73.

USGS (2010) Lithium. Available at; http://minerals.usgs.gov/minerals/pubs/commodity/lithium/mcs-2010-lithi.pdf. Retrieved on the 3rd of March 2020.

Von Knorring, O.V., Condliffe, E. (1987). Mineralised Pegmatites in Africa.Geological Journal, Department of Earth Sciences, University of Leeds, UK. Vol.**22**, Thematic Issue, 253-270.

Wiles, J.W. and Tatham, N.A. (1963). The muscovite pegmatites of southern Rhodesia and their exploitation. Pegmatites in Southern Rhodesia, a Symposium.Instn. Min.Metall.S. Rhodesia, 10-18.

Wilson, A.H. (2012). A chill sequence to the Bushveld complex: Insight into the first stage of emplacement and implications for the parental magmas. J. Petrol.**53**, 1123-1168

APPENDIX A

Detailed Petrography of the thin sections

Sample Information	Description	PPL	XPL
Sample ID: PS1-MP (Zone) **MINERALOGY:** Petalite (Major)- >3mm Quartz (Major)- > 2mm Spodumene (Minor)- <1.5mm Albite (Minor)-0.5-1mm	The dominant mineral is petalite and its coarse- grained and euhedral- subhedral. Both coarse- grained primary petalite and medium-fine grained highly fractured altered/secondary petalite is also present in the sample, with distinctive cleavage planes characterised by pervasive alteration. Inclusions of albite and quartz can also be seen within both the primary and secondary petalite. Spodumene can also be identified with its diagnostic high relief. The spodumene seems to be intergrown with quartz and albite making up the matrix creating a replacement or reaction texture whch could be a product of the alteration of petalite.	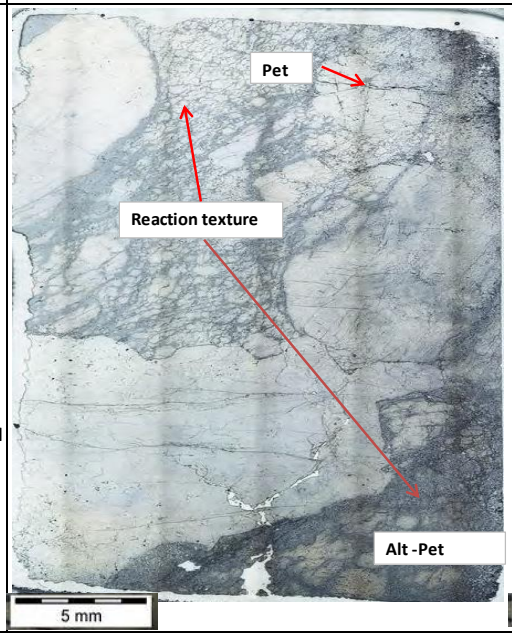	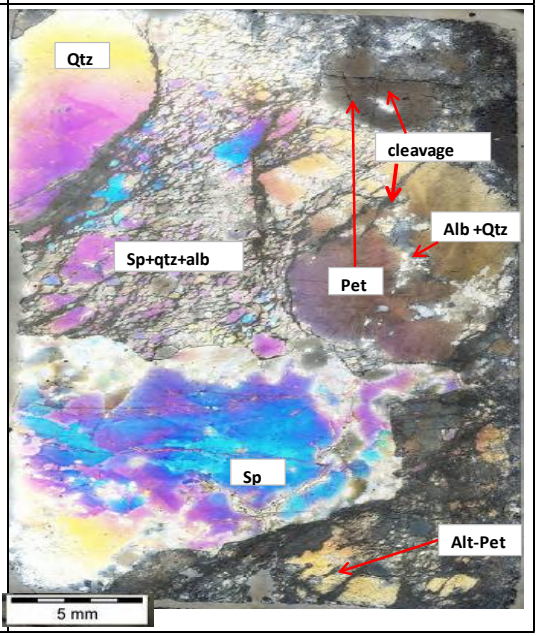

Sample PS1- MP ZONE- PPL and XPL

Sample ID: **PS2- MP (Zone)** **MINERALOGY:** **Spodumene (Major)-0.5-3mm** **Quartz (Minor)- 1-3mm** **Petalite (Minor)- 6-8mm** **Plagioclase (Minor) 0.05-0.2mm**	**Spodumene with its distinctive high relief is dominant within the fine- grained meshy matrix, and the matrix contains quartz and alterered plagioclase.** **Megacrystic petalite with fractures and prominant cleavage planes also characterised by alteration can be identified within the thin section.** **Interstitial spodumene can be identified within the fractured petalite magacrystal.** **Quartz intergrown with albite and Spodumene can also be identified on the far right side of the XPL image (SQI + Albite)**	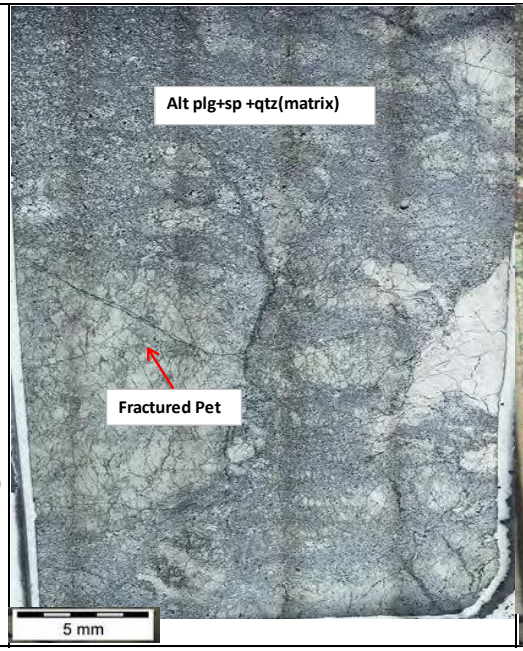	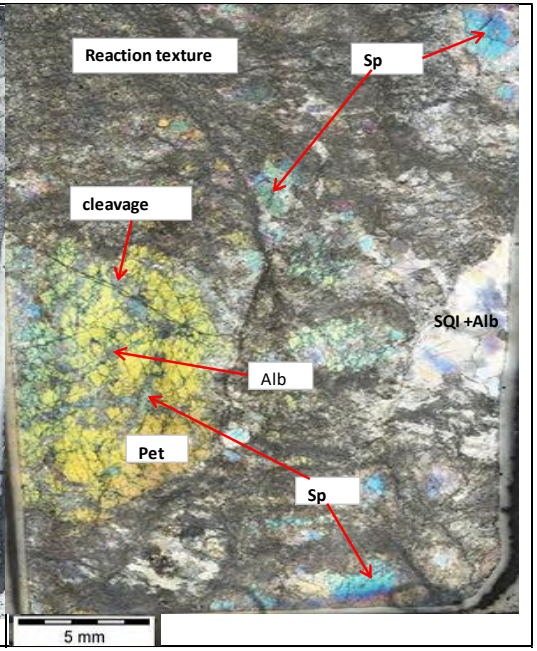

Sample PS2- MP ZONE- PPL and XPL

Sample ID: **S001- LMP (Zone)** **MINERALOGY:** **Albite(Major)- 0.1-1.5mm** **Quartz (Major)-0.1-1.5mm** **Spodumene(Accessory)-0.2-1mm** **Petalite (Accessory)-0.1-0.5mm**	**The major minerals in this setion are albite and quartz. The sample appears to be altered (albitization) and the matrix is fine-grained and meshy .Quartz e can be identified within the fine-grained matrix.** **Spodumene and Petalite are in accessory amounts and can be seen within the fine grained matrix and also intergrown with albite and quartz.**	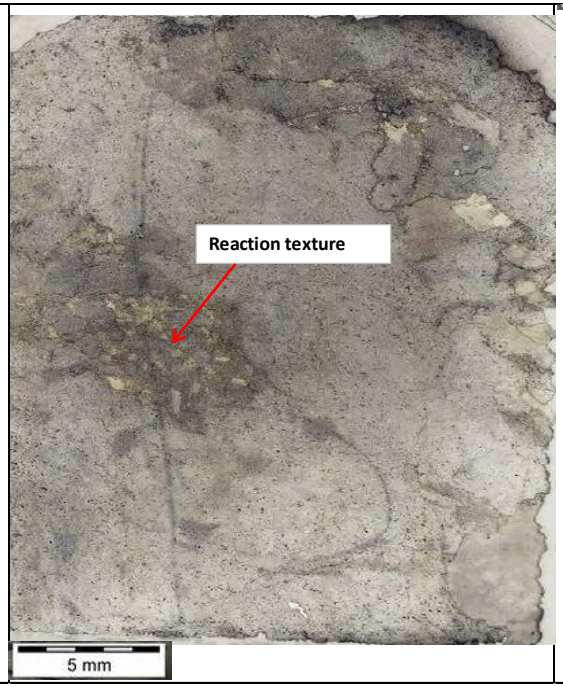	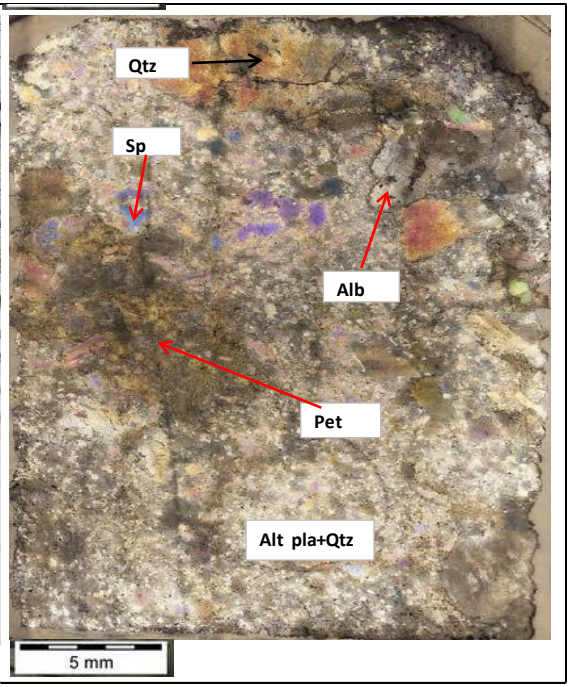

Sample S001- LMP ZONE- PPL and XPL

Sample ID: **S005- LMP(Zone)** **MINERALOGY:** **Albite (Major)-0.5-2mm** **Quartz (Major)-1-10mm** **Petalite (Accessory)->0.1mm** **Spodumene (Accessory)>0.5mm** **Microcline (Accessory)>0.1mm**	**The sample contains coarse- grained quartz and albite as the major minerals.The quartz megacrystal has veins running across it. Acessory amounts of petalite, spodumene and microcline are also present.**	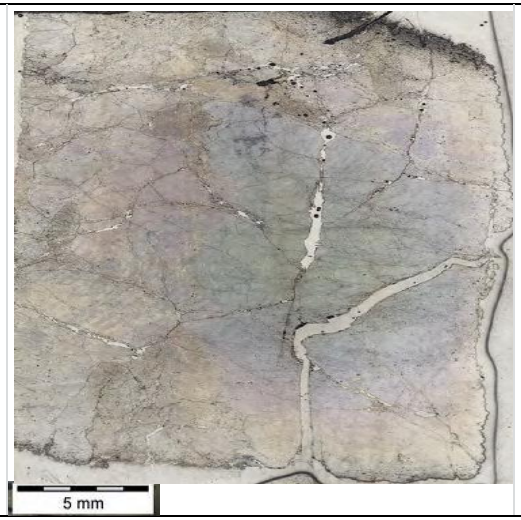	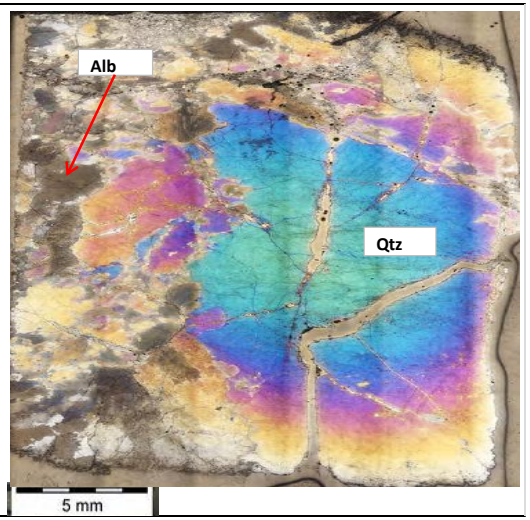

Sample S005- LMP ZONE- PPL and XPL

Sample ID: **S009- LMP (Zone)** **MINERALOGY:** **Albite (Major)-0.25-1.5mm** **Quartz (Minor)- 0.05-2.5mm** **Microcline (Accessory)>0.5mm** **Petalite (Accessory)>0.5mm** **Spodumene (Accessory)- 1-2mm** **Other opaque minerals(Accessory)->0.5mm**	**Albite is the dominant mineral in the section and there is high degree of alteration, with a lot of sericite. Quartz is also present and can be identified within the fine grained matrix.** **The other mineral present in accessory amounts is microcline within the fine grained matrix as well as some petalite, spodumene and some opaque minerals.**	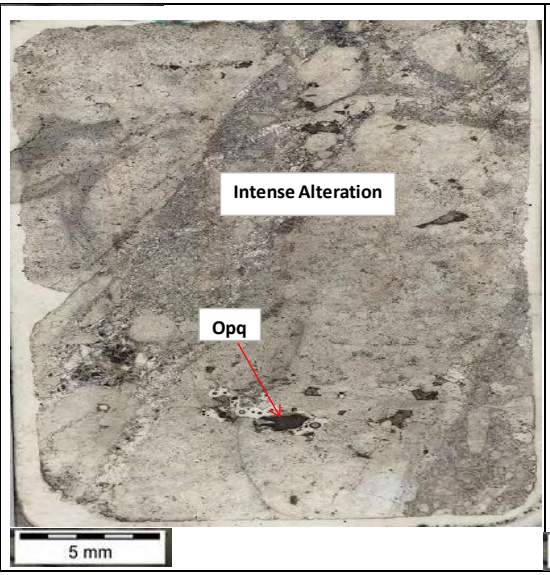	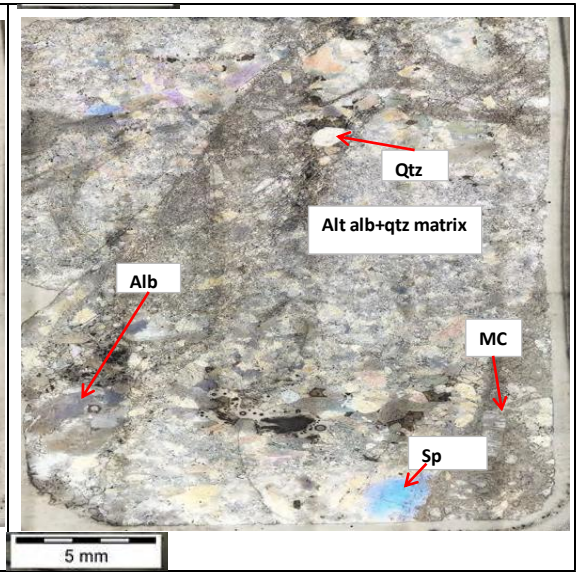

Sample S009- LMP ZONE- PPL and XPL

Sample ID: **S015- LMP (Zone)** **MINERALOGY:** **Altered Albite (Major)- 0.05- 1mm** **Quartz (Minor)-0.05-2mm** **Spodumene (Accessory)-0.25mm** **Petalite (Accessory)->0.1mm** **Other opaque->2mm minerals(Minor to Accessory proportions)**	**There is high degree of alteration particurlarly of albite. The other minerals present within the fine-grained matrix are quartz, spodumene and petalite,as well as some opaque minerals in minor to accessory proportions.** **There also seems to be some pink and green minerals that appear like products of alteration, within the fine-grained matrix.**	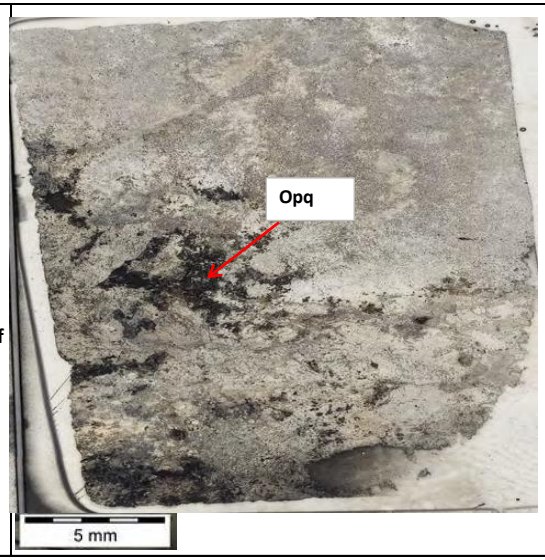	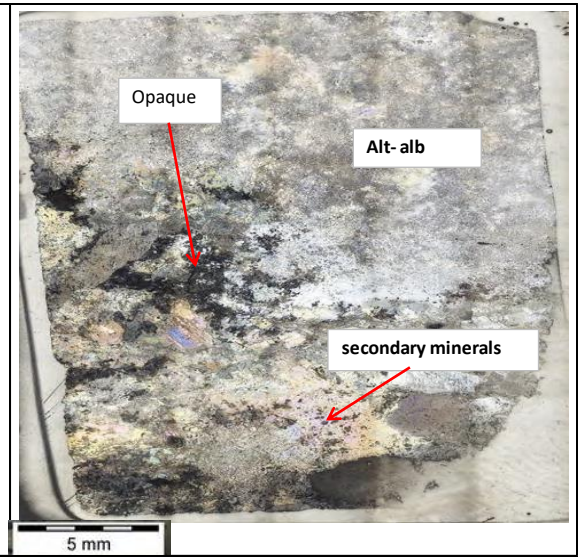

Sample S015- LMP ZONE- PPL and XPL

Sample ID: **S016.2 - MP (Zone)** **MINERALOGY:** **Petalite (Major)->8mm** **Microcline (Minor)->3mm** **Albite(Minor)-0.05-1mm** **Spodumene (Minor)- 0.5-2mm** **Quartz (Accessory)->0.5mm**	**This thin section is dominated by altering coarse-grained anhedral petalite exhibiting prominent fractures and cleavage planes with spodumene occurring interstitial to petalite and within the fractures and cleavage planes of petalite.** **Inclusions of spodumene, albite, quartz and microcline can be seen within petalite.** **Spodumene can be identified with its diagnostic high relief .**	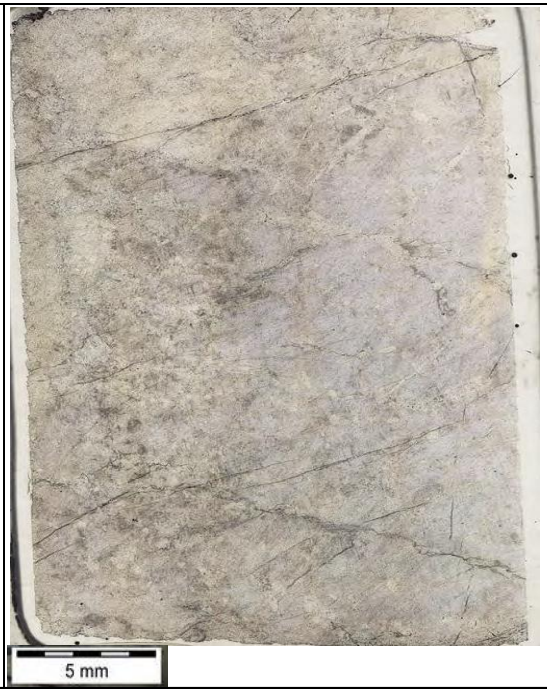	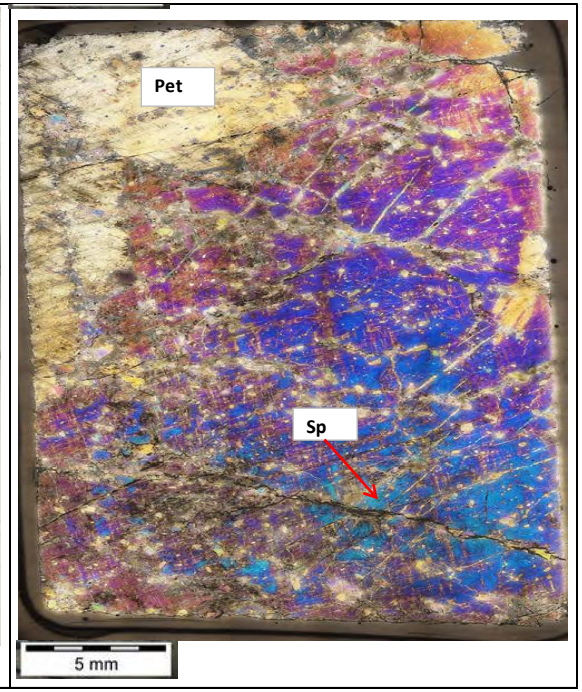

Sample S016.2- MP ZONE- PPL and XPL

Sample ID: **S016 - MP (Zone)** **MINERALOGY:** **Petalite (Major)- >7mm** **Albite(Minor)0.05-3mm** **Microcline (Minor) >0.5mm** **Quartz (Minor)-0.5-2mm** **Spodumene (Accessory)->0.25mm**	**This thin section is dominated by petalite showing its distinctive cleavage planes. It appears there might be two versions of petalite one primary and the other one probably secondary highly altered, both with distictive cleavage planes.** **Microcline is present as inclusions within petalite, its cross-hatch twinning seems oscured by petalite.** **Inclusions of fine-grained albite, quartz and spodumene can be identified within petalite along the cleavage planes and around the edges of the coarse- grained altering petalite and the primary petalite. Quartz and albite appear coarse-grained in some areas within the section. Albite appears to also have inclusions of quartz and some opaque accessory minerals**		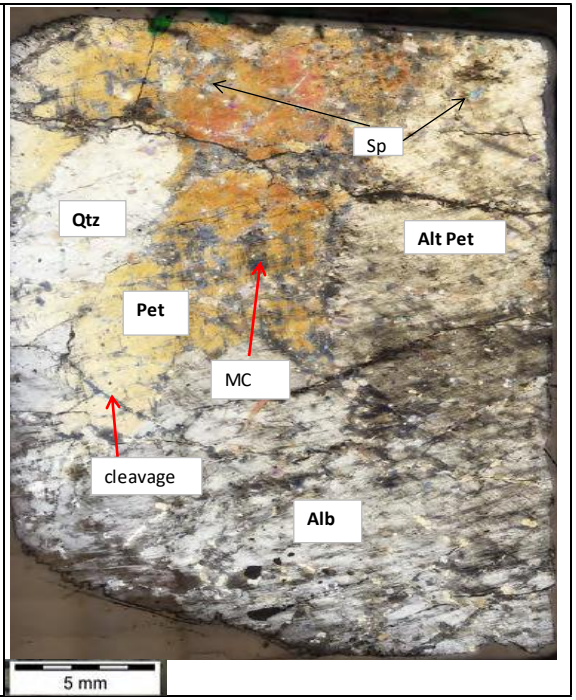

Sample S016- MP ZONE- PPL and XPL

Sample ID: **S020B - LMP (Zone)** **MINERALOGY:** **Albite (Major)- 0.25-2mm** **Quartz (Minor)-0.25-3mm** **Microcline (Minor)->6mm** **Petalite (Accessory)-0.25-1m** **Accessory minerals**	**This thin section is dominated by albite followed by quartz.** **A megacrystal of microcline with cross-hatch twinning is also present, with inclusions of quartz and albite . Accessory minerals can also be identified within the section. Petalite is also present but in accessory amounts within the fine-grained matrix.**	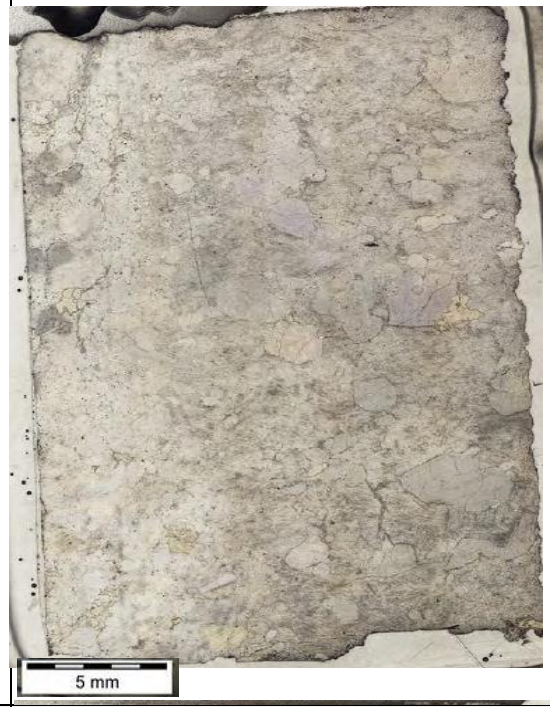	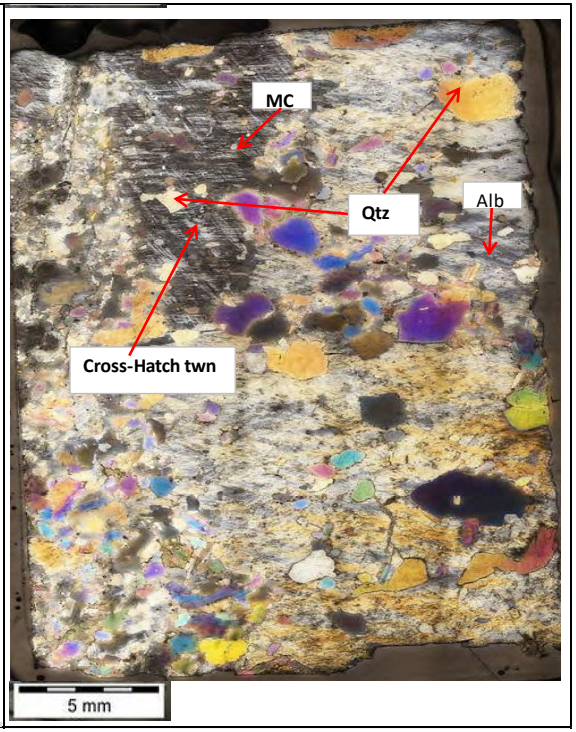

Sample S020B- LMP ZONE- PPL and XPL

Sample ID: **S020B duplicate-LMP (Zone)** **MINERALOGY: Same as previous but cut in a different orientation** **Albite(Major)- 0.25- >3mm** **Quartz (Minor)0.25->2.5mm** **Microcline (Minor)->6mm** **Petalite (Accessory)->1mm**	**This thin section is dominated by albite, followed by microcline which appears to have inclusions of quartz and albite. Cross-hatch twinning of microcline can also be identified within the section. Accessory mineral sare also present within the matrix. Accessory amounts of petalite are also present.**		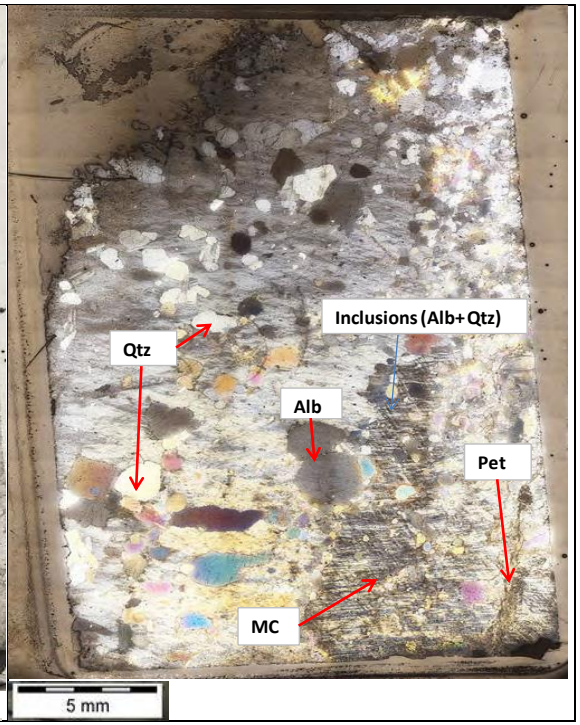

Sample S020B DUPLICATE- LMP ZONE- PPL and XPL

Sample ID: **S021- MP (Zone)** **MINERALOGY:** **Microcline (Major)- >1mm** **Plagioclase (Major)->1mm** **Quartz (Minor)- >6mm** **Petalite (Accessory)->0.5mm** **Spodumene (Accessory)->0.5mm**	**The thin section is dominated by altered microcline and plagioclase . Mega crystals of coarse grained quartz can be identified within the section and within the fine-grained matrix of the altered plagioclase.**		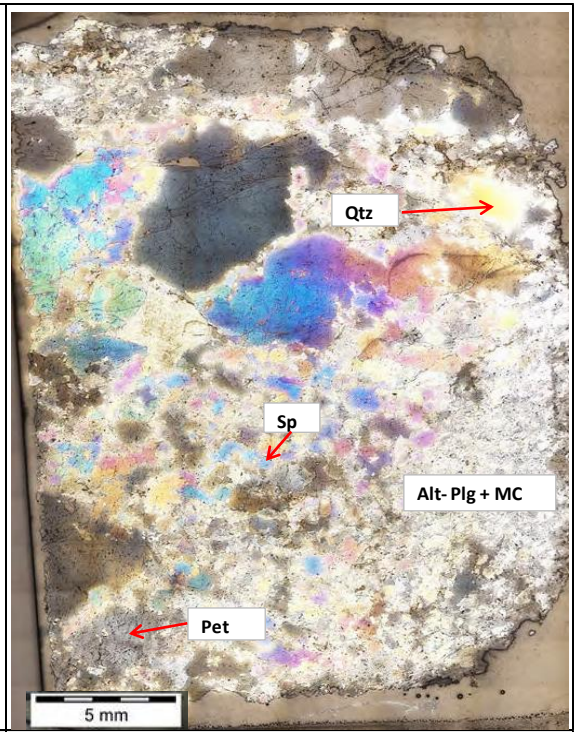

Sample S021- MP ZONE- PPL and XPL

Sample ID: **S022- MP (Zone)** **MINERALOGY:** **Quartz (Major)- >8mm** **Albite (Major)->3mm** **Petalite (Accessory)-1-3mm** **Spodumene(Accessory)-0.05-0.8mm**	**Quartz and albite are the dominant minerals in this section. Quartz seems to occur in two forms as megacrystals which are coarse- grained and as medium- fine-grained interstitial to petalite . The petaite appears resorbed around its edges where its rimmed by quartz.** **A replacement or reaction texture which could be a product of the alteration of petalite can also be observed within the section particurlarly where spodumene appears interstitial to petalite.** **The distinctive cleavage planes of petalite can also be observed.**		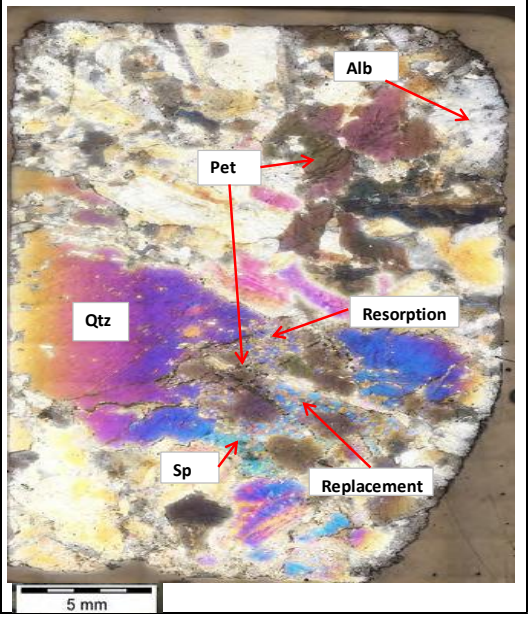

Sample S022- MP ZONE- PPL and XPL

Sample ID: **S025- MP (Zone)** **MINERALOGY:** **Albite (Major)- 0.5-2mm** **Quartz (Minor)->2mm** **Petalite (Accessory)->0.1mm** **Microcline (Accessory)->0.1mm**	**Albite seems to be the dominant or major mineral component in this section with minor amounts of quartz and accessory amounts of petalite and microcline in the fine- grained matrix. Plagioclase alteration is also present.**		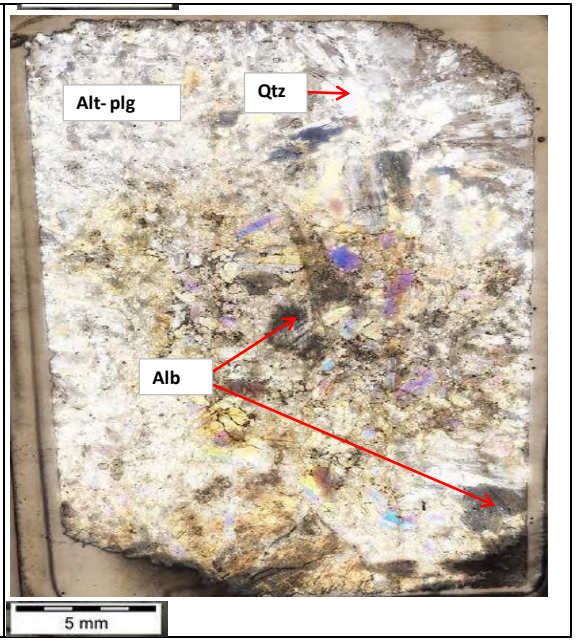

Sample S025- MP ZONE- PPL and XPL

Sample ID: **S031- MP (Zone)** **MINERALOGY:** **Microcline (Major)- >5mm** **Albite (Major)->2.5mm** **Quartz (Minor)->6mm** **Petalite (Accessory)- >0.25mm**	**Microcline apears to be the dominant mineral with a perthitic texture, second in abundance is albite followed by the coarse-grained quartz and these two minerals (albite +qtz) also occur as inclusions within microcline.** **Accessory petlite appears to be present also as an inclusion within the microcline.**		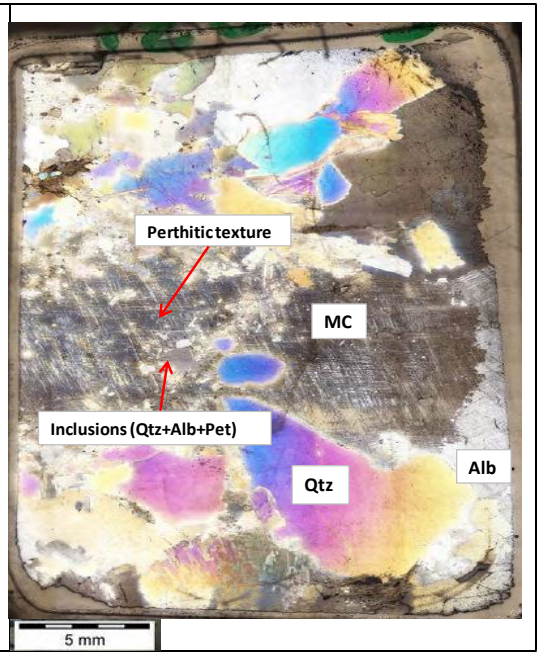

Sample S031- MP ZONE- PPL and XPL

Sample ID: **S032- MP (Zone)** **MINERALOGY:** **Albite (Major)- >6mm** **Petalite (Minor)->2mm** **Microcline (Minor)->2mm** **Quartz (Minor)-0.5-1mm**	**Coarse-grained albite is dominant in this section. Primary petalite appears to be present as well as microcline and qaurtz Quartz appears to occur as inclusions in albite.**		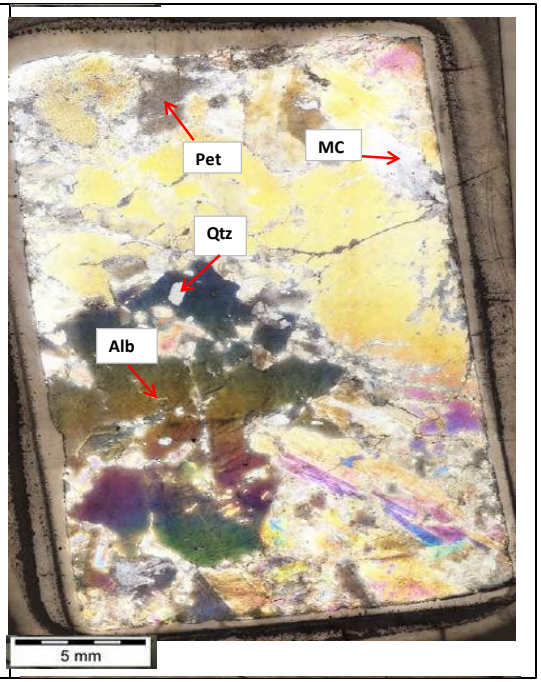

Sample S032- MP ZONE- PPL and XPL

Sample ID: **S034A- MP (Zone)** **MINERALOGY:** **Albite (Major)-0.5-4mm** **Quartz (Minor)- 0.5-2mm** **Microcline (Minor)->1.5mm** **Petalite (Accessory)->1mm**	**Albite is the dominant mineral, with minor quartz and microcline. Petalite is also present, but in accessory amounts.** **Albite twinning can also be identified.**		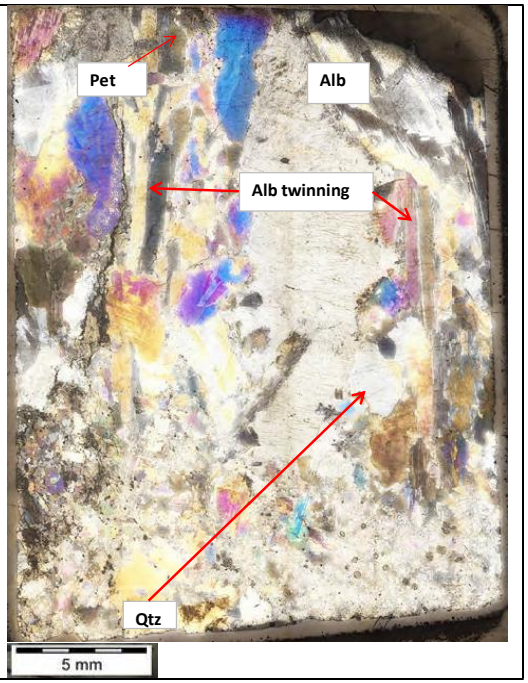

Sample S034A- MP ZONE- PPL and XPL

Sample ID: **S034B- MP (Zone)** **MINERALOGY:** **Albite (Major)-0.25- 4mm** **Quartz (Minor)- 0.25-1mm** **Microcline (Minor)- >1.5mm** **Petalite (Accessory)->1mm**	**Albite is the dominant mineral, with minor quartz and microcline. A graphic texure can be observed of quartz intergrown with ablite. Microcline appears to have inclusions of petalite albite and quartz.**		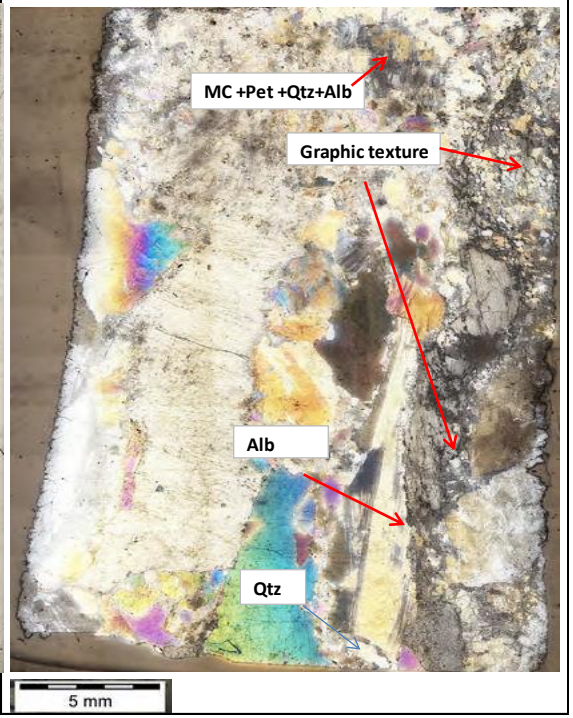

Sample S034B- MP ZONE- PPL and XPL

Sample ID: **S040-LMP (Zone)** **MINERALOGY:** **Petalite (Major)-> 11mm** **Quartz (Minor)- 0.5-3mm** **Albite (Minor)- 0.25- 4mm** **Spodumene (Minor)- 0.5- 1mm** **Garnet- (Accessory minerals)->0.5-1mm.** **Accessory minerals**	**Coarse- grained petalite is the dominant mineral in this section with its distinctive cleavage. It appers that there might be two versions of petalite in this section, of which one could be the primary unaltered version and the other one a secondary altered version. The altered petalite version appears to have distinctive cleavage planes.** **Spodumene intergrown with quartz (SQI), appears to be present as inclusions within the altering petalite. Albite and qaurtz also appear to be present around the bundaries of the primary petalite.Quartz ranges in grain size from coarse- grained to fine-grained qaurtz.** **Euhedral disseminated garnet crystals are also present within the qaurtz albite matrix.** **Greenish accessory minerals also present.**	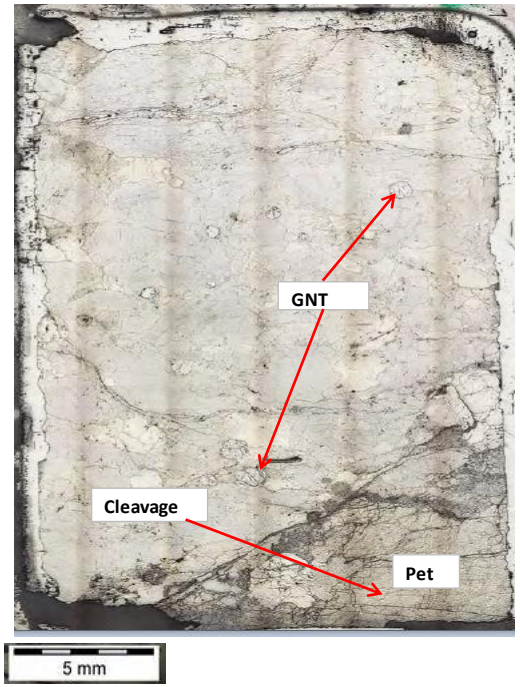	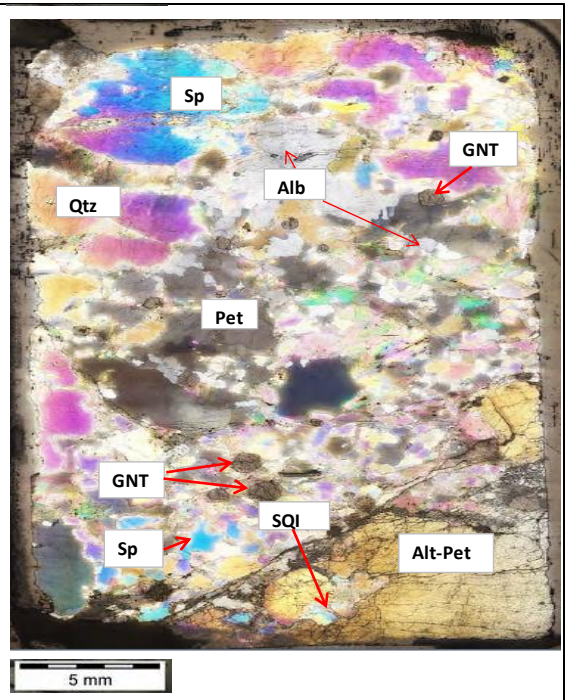

Sample S040- LMP ZONE- PPL and XPL

Sample ID: **S042- LMP (Zone)** **MINERALOGY:** **Albite (Major)- 0.25-1.5mm** **Quartz (Major)- 0.5-2.5mm** **Petalite (Accessory)->0.25mm** **Spodumene (Accessory)->0.5mm** **Accessory green minerals- 0.5-1.5mm**	**Albite and quartz are the dominant minerals in this section, with accessory amounts of petalite and spodumene within the matrix of albite and quartz. There is also a greenish accessory mineral which is medium to fine-grained**		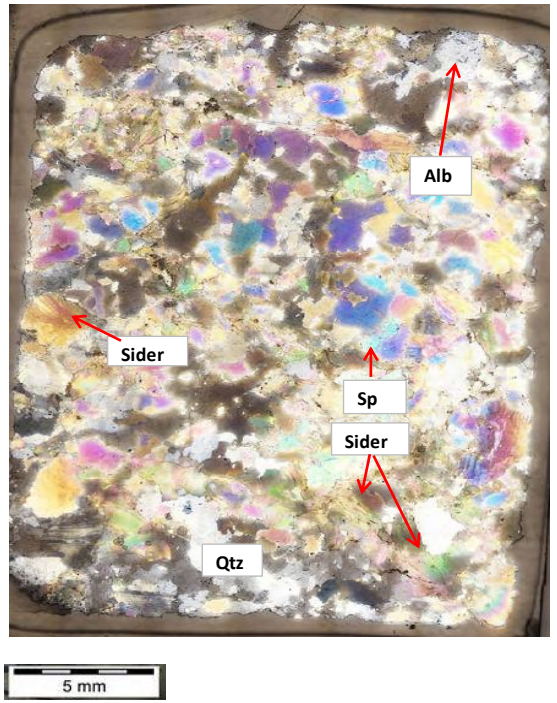

Sample S042- LMP ZONE- PPL and XPL

APPENDIX B

XRD RIETVELD RESULTS

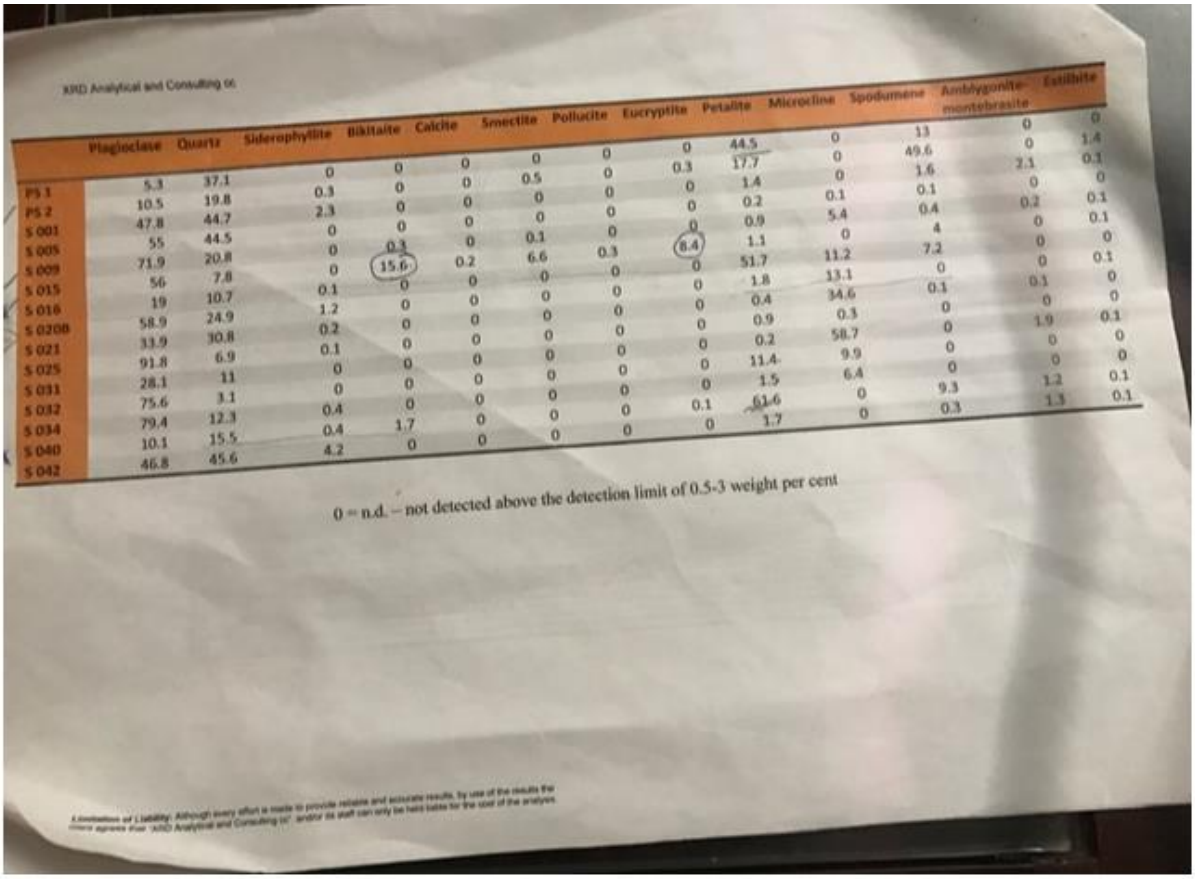

XRD Analytical and Consulting cc

	Plagioclase	Quartz	Siderophyllite	Bikitaite	Calcite	Smectite	Pollucite	Eucryptite	Petalite	Microcline	Spodumene	Amblygonite-montebrasite	Estilbite
PS 1	5.3	37.1	0	0	0	0	0	0	44.5	0	13	0	0
PS 2	10.5	19.8	0.3	0	0	0.5	0	0.3	17.7	0	49.6	0	1.4
S 001	47.8	44.7	2.3	0	0	0	0	0	1.4	0	1.6	2.1	0.1
S 005	55	44.5	0	0	0	0	0	0	0.2	0.1	0.1	0	0
S 009	71.9	20.8	0	0.3	0	0.1	0	0	0.9	5.4	0.4	0.2	0.1
S 015	56	7.8	0	15.6	0.2	6.6	0.3	8.4	1.1	0	4	0	0.1
S 016	19	10.7	0.1	0	0	0	0	0	51.7	11.2	7.2	0	0
S 020B	58.9	24.9	1.2	0	0	0	0	0	1.8	13.1	0	0	0.1
S 021	33.9	30.8	0.2	0	0	0	0	0	0.4	34.6	0.1	0.1	0
S 025	91.8	6.9	0.1	0	0	0	0	0	0.9	0.3	0	0	0
S 031	28.1	11	0	0	0	0	0	0	0.2	58.7	0	1.9	0.1
S 032	75.6	3.1	0	0	0	0	0	0	11.4	9.9	0	0	0
S 034	79.4	12.3	0.4	0	0	0	0	0	1.5	6.4	0	0	0
S 040	10.1	15.5	0.4	1.7	0	0	0	0.1	61.6	0	9.3	1.2	0
S 042	46.8	45.6	4.2	0	0	0	0	0	1.7	0	0.3	1.3	0.1

0 = n.d. – not detected above the detection limit of 0.5-3 weight per cent